NASA TECHNICAL NOTE




NASA TN D-6781

# MEASURED NOISE OF MODEL FAN-UNDER-WING AND FAN-ON-FLAP JET FLAP CONFIGURATIONS

*by John F. Groeneweg and Gene L. Minner*

*Lewis Research Center*
*Cleveland, Ohio 44135*

NATIONAL AERONAUTICS AND SPACE ADMINISTRATION • WASHINGTON, D. C. • MAY 1972

| | | |
|---|---|---|
| 1. Report No.<br>NASA TN D-6781 | 2. Government Accession No. | 3. Recipient's Catalog No. |
| 4. Title and Subtitle MEASURED NOISE OF MODEL FAN-UNDER-WING AND FAN-ON-FLAP JET FLAP CONFIGURATIONS | | 5. Report Date<br>May 1972<br>6. Performing Organization Code |
| 7. Author(s)<br>John F. Groeneweg and Gene L. Minner | | 8. Performing Organization Report No.<br>E-6739<br>10. Work Unit No.<br>132-80 |
| 9. Performing Organization Name and Address<br>Lewis Research Center<br>National Aeronautics and Space Administration<br>Cleveland, Ohio 44135 | | 11. Contract or Grant No.<br>13. Type of Report and Period Covered<br>Technical Note |
| 12. Sponsoring Agency Name and Address<br>National Aeronautics and Space Administration<br>Washington, D.C. 20546 | | 14. Sponsoring Agency Code |

15. Supplementary Notes

16. Abstract

Noise measurements were made on two jet flap systems proposed for STOL aircraft. In one case a 14.0-cm- (5.5-in.-) diameter fan was mounted under the wing such that the exhaust impinged on downwardly deflected flap segments. In the other case, the fan was located on the upper surface of the flap such that fan and flap moved as a unit, with no exhaust impingement. Results for takeoff and approach fan speeds and flap deflections were used to estimate STOL airplane perceived noise levels. Internally generated noise directivity corresponded with fan axis orientation for the fan-on-flap, but no consistent redirection of internal noise was observed with changes in flap angle for the fan-under-wing. With the fan-on-flap arrangement, the wing shielded some fan inlet noise from the ground. Since no impingement of the exhaust on solid surfaces occurred, the external noise was jet noise alone. In contrast, for the fan-under-wing, the jet/flap interaction noise dominated the external noise except at angles near the jet axis even with no flap deflection. If internal noise is reduced by fan design and acoustic treatment, the jet/flap interaction noise will dominate. Additional work is needed to establish a spectral correlation of interaction noise.

| | | |
|---|---|---|
| 17. Key Words (Suggested by Author(s))<br>Lift augmentation<br>Short Takeoff Aircraft (STOL)<br>Aerodynamic noise<br>Noise<br>Jet flap | 18. Distribution Statement<br>Unclassified - unlimited | |
| 19. Security Classif. (of this report)<br>Unclassified | 20. Security Classif. (of this page)<br>Unclassified | 21. No. of Pages<br>56 / 22. Price*<br>$3.00 |

* For sale by the National Technical Information Service, Springfield, Virginia 22151

# MEASURED NOISE OF MODEL FAN-UNDER-WING AND FAN-ON-FLAP JET FLAP CONFIGURATIONS

by John F. Groeneweg and Gene L. Minner

Lewis Research Center

## SUMMARY

Noise measurements were made on two models of jet flap systems proposed to provide lift augmentation for STOL aircraft. One configuration, called the fan-under-wing, had a 14.0-centimeter- (5.5-in.-) diameter fan mounted under a wing such that the exhaust impinged on downwardly deflected trailing edge flap segments. The other arrangement, called the fan-on-flap, had the fan located on the upper surfaces of the flap such that the fan and flap moved as a unit with no exhaust impingement. Noise data taken at conditions simulating takeoff and approach were separated into two types corresponding to internally generated fan and turbine noise and externally generated jet/flap interaction noise. The results were used to estimate STOL airplane perceived noise levels.

The directivity of internally generated noise for the fan-on-flap corresponded with fan axis orientation, and the wing shielded some inlet noise from the ground. Perceived noise estimates indicated that the shielding benefit would be realized at simulated takeoff attitude but not at approach. With no exhaust impingement, external noise was limited to jet noise alone; this is an important noise advantage compared to systems producing flap interaction noise.

For the fan-under-wing no consistent redirection of internal noise was observed below the wing in the flyover plane as the flaps were deflected. Strong jet/flap interaction noise dominated the external noise except at angles near the jet axis even with no flap deflection. The interaction noise increased with flap angle and peaked at microphone angles nearly normal to the final jet direction.

## INTRODUCTION

One method of augmenting the lift of aircraft to shorten takeoff and landing distances is to increase the circulation around the wing using a jet flap arrangement. The gas

stream from the engine exhaust is directed along an extended flap to form a jet sheet. Effects of the change in direction of the exhaust jet and the altered flow field around the wing combine to produce an increase in lift.

A primary consideration in the application of this lift augmentation system to short takeoff and landing (STOL) aircraft is the noise level produced on landing approach and takeoff. In addition to the engine noise similar to that associated with conventional aircraft, sources or directivity patterns peculiar to the jet flap geometry must be considered. For example, additional noise produced by exhaust jets interacting with wing and flap surfaces can be substantial, and directivity patterns depend on flap and engine orientations (refs. 1 and 2).

The model jet flap experiments reported here used a 14.0-centimeter- (5.5-in.-) diameter, 1.25 pressure ratio fan driven by a tip turbine. The fan was mounted on a model wing having a 165-centimeter (65-in.) span and a 66-centimeter (26-in.) chord. Noise levels associated with two forms of external flow control over the flap surfaces were investigated. One type was the fan-under-wing arrangement where the exhaust jet from the fan suspended under the wing was redirected by the lower surface of a downwardly deflected flap. The other type, called the fan-on-flap arrangement, had the fan positioned on the upper flap surface such that the fan and flap moved as an integral unit. This arrangement has been shown in wind tunnel tests to have favorable stall margin characteristics (ref. 3).

Far-field noise measurements were made for fan speeds and flap deflection angles corresponding to conditions representative of takeoff and landing: 100 percent speed with $30^{\circ}$ flap, and 76 percent speed with $60^{\circ}$ flap, respectively. Cases with no flap deflection at the same fan speeds were used as the basis of comparison for determining the noise characteristics attributable to flap orientation.

The noise data are separated into two types corresponding to internally generated fan and turbine noise and externally generated jet and jet/flap interaction noise. Directivity patterns are presented, and the results are used to estimate perceived noise levels for a full-scale STOL aircraft.

## APPARATUS AND PROCEDURE

### Model Description

A single fan and a semispan wing with replaceable flaps were used to model two jet flap systems. With the fan positioned beneath the wing and a two segment flap, an externally blown flap was modeled. This configuration is called the fan-under-wing. The other arrangement had the fan mounted on top of a single flap and is referred to as the fan-on-flap.

The tip driven fan is shown in cross section in figure 1. Cold gaseous nitrogen at pressures up to $2.76 \times 10^6$ newtons per square meter (400 lbf/in.$^2$) is supplied to the 15.2-centimeter- (6-in.-) diameter tip turbine which has 40 blades. The fan has 16 rotor blades and 21 stators. A fan pressure ratio of 1.25 is developed at 100-percent speed, which is 36 000 rpm. The ratio of fan air flow to turbine flow is 5 at full speed and the mass average exhaust velocity is 177 meters per second (580 ft/sec). While fan tip velocity is only 264 meters per second (865 ft/sec), the rotor-stator spacing is small at about 1/8 of a rotor chord, and so the fan is relatively noisy.

This fan was mounted on the wing segment shown in figure 2 where the fan is shown suspended under the wing. The wing has a span of 165 centimeters (65 in.) and a chord of 66 centimeters (26 in.). For the fan-under-wing case the two flap segments shown can be deflected to intercept and turn the fan exhaust. Figure 3 shows the $30^\circ$ and $60^\circ$ deflections which were tested. All flap angles are measured with respect to the wing undersurface.

For the fan-on-flap configuration, the two flap segments were replaced by a single flap with the fan located on top at the same spanwise position. The $0^\circ$, $30^\circ$, and $60^\circ$ deflections for this arrangement are illustrated in figure 4. Note that the fan and flap move as an integral unit, that the fan exhaust does not impinge on any flap or wing-surfaces, and that the $0^\circ$ flap refers to a case where the fan axis is actually at $17^\circ$ to the wing undersurface.

These cross-sectional views of the configurations given in figures 2 to 4 are used to identify data sets in figures throughout this report.

Table I summarizes the configurations tested and shows that the same fan speeds and flap deflections were used for the two jet flap systems. One hundred percent fan speed with $30^\circ$ flaps simulated a takeoff condition, while 76 percent and $60^\circ$ flaps simulated approach. The same speed conditions with no flap deflection were used to isolate flap effects.

## Noise Measurements

Far field noise measurements were made by 1.27-centimeter- (1/2-in.-) diameter microphones located in two mutually perpendicular planes through the fan axis (fig. 5). The bulk of the data were taken in the plane perpendicular to the wing - called the flyover plane. Eighteen microphones were located at $10^\circ$ increments on a 4.57-meter (15-ft) radius in the horizontal plane of the fan axis at a height of 1.90 meters (6.25 ft) above the concrete surface of the test site. For each flap setting a space was left in the microphone array to allow the exhaust stream to pass through. Angles $\theta$ in the flyover plane are measured with respect to the wing undersurface with $0^\circ$ in the forward direc-

tion. A limited number of measurements were made in the sideline plane - parallel to the wing undersurface - for the fan-under-wing configuration. A single microphone suspended from a boom at a constant height of 4.57 meters (15 ft) above the fan axis was moved through a series of angles $\alpha$ ranging from $40^{\circ}$ to $140^{\circ}$ as measured from the fan axis in the sideline plane. One-third octave analyses with an averaging time of about 1.5 seconds were performed on three noise data samples at each condition. These data were corrected to standard day conditions of $15^{\circ}$ C ($59^{\circ}$ F) and 70-percent relative humidity. Narrow band analyses were also performed on data from selected microphones.

The measured sound pressure levels are affected by reflection from the hard ground plane. Successive reinforcements and cancellations between direct and reflected signals occur at half wavelength intervals. Ideal corrections to the 1/3-octave spectra were calculated from equation (23) of reference 4 and are shown in figure 6 for the two measurement planes. The calculation assumes that the source is a point source which emits white noise above a hard, specularly reflecting plane. Alternate positive and negative corrections are indicated at low frequencies where the 1/3-octave bandwidths are narrow enough to resolve cancellations and reinforcements. As frequency is increased, the number of maxima and minima in each 1/3-octave band increases so that the correction tends to a constant determined by the square of the ratio of direct to reflected path lengths. This is because the reflected wave is weaker by the amount of extra inverse square law attenuation experienced in comparison to the direct wave which traveled a shorter distance. Corrections for the data measured in the sideline plane at $\alpha = 90^{\circ}$ are substantially less than in the flyover plane for the frequency range of interest because of the greater path difference associated with the boom microphone. The calculated correction curves of figure 6 indicate the frequencies most affected and the sign of the correction necessary. However, the magnitudes are questionable because of real effects such as the finite source size, and thus these corrections were not applied to the experimental spectra.

The noise data were used to estimate perceived noise levels for takeoff and approach of a 45 360-kilogram (100 000-lbm) gross weight aircraft with four engines operating under the conditions listed in table II. Takeoff conditions are a total thrust of 266 900 newtons (600 000 lbf) at 100-percent speed and a fan pressure ratio of 1.25. The flap angle is $30^{\circ}$ and the wing undersurface is at $20^{\circ}$ to the horizontal corresponding to the sum of climb angle and angle of attack (e.g., $12^{\circ}$ climb and $8^{\circ}$ angle of attack). On approach, thrust is 154 400 newtons (37 400 lbf) at 76-percent speed and a pressure ratio of 1.14. Flap deflection is $60^{\circ}$ and the wing undersurface is at $0^{\circ}$ to the horizontal corresponding to the sum of a glide slope and angle of attack which cancel each other. The diagram with table II illustrates these configurations and shows that the perceived noise levels were calculated at the different flyover angles $\gamma$ of the ground observer with respect to the horizontal plane through the aircraft at an altitude of 152.4 meters (500 ft).

Fan aerodynamic measurements were not made during the noise tests; therefore, the pressure ratios and exhaust velocities tabulated are those made in wind tunnel tests at the same fan speeds. For all perceived noise decibel (PNdB) estimates the sound pressure levels were scaled by the thrust ratio between full scale and model; 266 900 to 493 newtons (60 000 to 110 lbf) at 100-percent speed or 10 log 545 = 27.4 decibels. With the condition that the full-scale engine fan pressure ratios and exhaust velocities are the same as those for the model, the thrust scaling is equivalent to scaling by the ratio of fan flow areas. The procedures for frequency scaling are discussed for the separate cases of internal and external noise in the respective results sections. It should be emphasized that the scaled PNdB values apply only for the conditions specified in table II.

## RESULTS AND DISCUSSION

The jet flap noise data are separated on a spectral basis into two types for discussion purposes. Internal noise refers to that noise generated inside the fan including the tip turbine contribution. External noise refers to noise generated outside the fan by the interaction of the exhaust jet with the surrounding air (jet noise) and with wing and flap surfaces (jet-flap interaction noise). The data were examined to determine how internal noise directivity was affected by flap orientation and how the external interaction noise depended on flap deflection for the fan-under-wing. A complete set of 1/3-octave sound pressure level plots are included in the appendix.

### Internal Noise

A 1/3-octave spectrum illustrating the character of the internal noise produced by the fan is shown in figure 7. For the fan-on-flap configuration illustrated, which has the fan exit located at the flap trailing edge, the sound pressure levels at aft angles are not influenced by wing surface and approach those attributable to the fan alone. No clear evidence of jet noise in the form of a broad hump in the spectrum between 100 and 1000 hertz is present. The internal noise is dominated by the fan blade passage tone at 7310 hertz occurring in the 8-kilohertz band, its second harmonic at 14 600 hertz occurring in the 16-kilohertz band and the turbine blade passage frequency at 18 300 hertz occurring in the 20-kilohertz band. The peak occurring in the 400- and 500-hertz bands is the 1/3-octave resolution of the first of the combination tones occurring at multiples of the shaft rotation frequency, in this case 460 hertz. The source of these combination tones is unexplained, particularly in view of the low fan tip speed of 200 meters per second (657 ft/sec).

These features are clarified by the corresponding narrow band spectra shown in figure 8. Figure 8(a), which covers the range from 1 to 20 kilohertz, shows the blade passage frequencies and combination tones mentioned. Figure 9(b), which covers the range from 100 to 1000 hertz, shows the strong first combination tone apparent in the 1/3-octave analysis and the absence of any broadband jet noise hump.

Directivity of the internal noise in the flyover plane for the fan-on-flap is influenced by two factors. The fan inlet is shielded from the ground by the wing, and the flap deflections involve a rotation of the fan axis. This latter point suggested that, provided the noise under the wing comes mainly from the rear, the directivity may be invariant if angles are always referenced to the fan axis. Figure 9 confirms the notion for the 1/3-octaves containing the blade passage frequencies. The sound pressure level variation with angle is the same relative to the fan axis for deflected and undeflected flaps at each speed. Note also that the levels are lower at forward angles where the wing surface is interposed between the inlet and the microphones. For wavelengths shorter than a few centimeters, such as those associated with the blade passage tones, the roughly 50.8-centimeter (20-in.) wing segment ahead of the fan can be an effective reflector.

The directivity of the blade passage frequency for the fan-under-wing is shown in figure 10 where levels are plotted as functions of angle in the flyover plane. At 100-percent speed (fig. 10(a)) the tone is much more constant with angle than for the fan-on-flap since the inlet is not shielded from the microphone. Deflecting the flap to $30^{\circ}$ produced no significant change. At 76-percent speed (fig. 10(b)) the results are the same at aft angles, but lowering the flap to $60^{\circ}$ lowered the blade passage tone at forward angles. This result is unexplained. Aerodynamic measurements made on the fan in a wind tunnel showed no apparent change in the fan performance introduced by the $60^{\circ}$ flap.

Estimates of perceived noise levels for internal noise were made for a 45 360-kilogram (100 000-lbm) gross weight aircraft operating under the conditions of table II. The levels were scaled by thrust ratio as described in the previous section. All frequencies were divided by 4. This frequency scaling placed the blade passage frequency in the 2000- and 2500-hertz bands for 76- and 100-percent speeds, respectively. These frequencies are reasonable for fans of about 66 725-newton (15 000-lbf) thrust; four of these fans are considered to supply the total 266 900-newton (60 000-lbf) thrust. Although the scaled turbine frequency of 4570 hertz at 76 percent may be lower than is typical of a full-scale turbine, the uniform frequency scaling by 4 was used for simplicity. Perceived noise levels were estimated both with and without the turbine tone at the approach conditions. In all cases perceived noise computations were terminated with the 1/3-octave band which contained the actual 20 000-hertz data scaled to 5000 hertz, except for the turbine tone removal where the maximum band of the scaled data was 4000 hertz. External noise did not affect the estimates because the scaled spectra were dominated by blade passage frequencies with the external noise appearing at the low frequency extreme where its contribution to perceived noise was negligible.

The resulting estimated perceived noise levels produced by internal noise are shown in figure 11 as functions of angle relative to the horizontal $\gamma$. Fan-under-wing and fan-on-flap arrangements are compared for the same flap configuration in each of four cases. Figures 11(a) and (b) are for takeoff conditions with $0^{\circ}$ and $30^{\circ}$ flap deflections, respectively, while figures 11(c) and (d) are for approach conditions with $0^{\circ}$ and $60^{\circ}$ flap deflections, respectively. Although cases of no flap deflection are not realistic takeoff and approach STOL configurations, they are included to separate aircraft attitude effects from flap orientation effects which were discussed in connection with figures 9 and 10. The maximum perceived noise levels of around 120 PNdB are representative of those produced by fans which incorporate no noise reducing design features or acoustic treatment.

Figure 11(a) illustrates the inlet shielding advantage of the fan-on-flap as compared to the fan-under-wing. At angles less than $70^{\circ}$ the fan-on-flap is substantially less noisy. At aft angles the slightly higher levels of the fan-under-wing may indicate some downward reflection of internal noise by the wing and flap surfaces. With $30^{\circ}$ flap deflection for takeoff, the estimates of figure 11(b) show that the inlet shielding advantage of the fan-on-flap is retained. Rotating the axis of the fan-on-flap to the $30^{\circ}$ position placed the maximum aft noise at $80^{\circ}$ relative to the horizontal.

Reduced noise levels in the forward quadrant are again shown in figure 11(c) for the fan-on-flap relative to the fan-under-wing at approach attitude but with no flap deflection, similar to the takeoff condition shown in figure 11(a). The solid points include the scaled turbine noise whereas the open circles were obtained by truncating the last scaled 1/3-octave band which contained the turbine fundamental. Only at angles of $130^{\circ}$ and beyond is the turbine contribution significant for the fan-under-wing. Turbine noise for the fan-on-flap is greatest at $110^{\circ}$.

The actual approach conditions with flap deflections of $60^{\circ}$ produce the perceived noise directivity patterns shown in figure 11(d). Most of the forward shielding advantage of the fan-on-flap is no longer present because at the $60^{\circ}$ flap angle the exit of the fan radiates more directly to the ground. In contrast to figures 11(a) to (c) the fan-on-flap noise is greater than the fan-under-wing noise in the angle range from $60^{\circ}$ to $90^{\circ}$. Inclusion of the turbine noise increases perceived noise levels for both flap systems by about 3 PNdB at angles from $70^{\circ}$ to $110^{\circ}$.

Estimates of internally generated noise on a 152.4-meter (500-ft) sideline were calculated from data taken in the sideline plane for the fan-under-wing. Levels for the same four conditions given for the flyover plane in figure 11 are shown for the sideline plane in figure 12. In general, the noise levels in the sideline plane are lower than in the flyover plane. At takeoff, figure 12(a) shows no consistent differences in directivity between $0^{\circ}$ and $30^{\circ}$ flap angles over the range of microphone angles considered. Comparison of the approach conditions in figure 12(b) shows that lowering the flap to $60^{\circ}$ lowers the aft radiated noise, which indicates some shielding of internal noise from the

aft angles where the deflected flap interrupts the direct path between the fan and microphone. Turbine noise contributions over the range of sideline angles shown are negligible except for $130^{\circ}$ and $140^{\circ}$ with $0^{\circ}$ flap.

It is noteworthy that, for the fan-on-flap configuration, there are aerodynamic and mechanical reasons which favor an arrangement with a larger number of smaller engines than the four-engine aircraft discussed previously. Such an arrangement was discussed in reference 3. From a noise point of view, small engines would probably have higher rotative speeds and perhaps higher frequency internal noise than large engines. Therefore, the previous frequency scaling of the internally generated noise would require reconsideration for such an arrangement.

The important feature of internally generated noise is that it is amenable to reduction by acoustic treatment. Practical STOL fans must employ a combination of low noise fan design features with acoustically treated nacelles to reduce internal noise by at least 25 to 30 PNdB below the levels estimated by scaling of the model data as previously reported. If such reductions are accomplished, external noise becomes dominant.

## External Noise

In the case of the fan-on-flap configuration, externally generated noise is limited to jet noise since no impingement of the exhaust jet on solid surfaces occurs. Also, the exhaust velocities are relatively low (less than 177 m/sec, 580 ft/sec), and internal noise is high; therefore, jet noise is not clearly distinguishable in the spectrum at most angles. This was the case for figure 7, and inspection of the fan-on-flap spectra in the appendix shows similar behavior except at a few aft angles. Thus, the type of external noise emphasized here is the jet/flap interaction noise produced by exhaust stream impingement on solid surfaces occurring with the fan-under-wing arrangement.

The clearest examples of interaction noise were observed in the sideline plane where the ground reflection effects were small and the sensitivity to flap angle was greater, although the magnitudes of the interaction noise were less than in the flyover plane. Figure 13 compares 1/3-octave spectra for $0^{\circ}$ and $60^{\circ}$ flap settings at an angle of $130^{\circ}$ in the sideline plane. The $0^{\circ}$ case shows only internal noise with features similar to figure 7. However, when the flap is lowered into the flow at a $60^{\circ}$ angle an extensive interaction noise hump emerges in the range from 160 to 2000 hertz. Clearly, if the internal fan noise were reduced, the external interaction noise would dominate the spectrum. Note that the internal noise above 3150 hertz is lower for the $60^{\circ}$ flap, supporting the observation made in connection with figure 12 that toward the rear in the sideline plane the flap reflects internal noise.

Narrow band analyses for the conditions of figure 13 are shown in figure 14. The frequency range from 250 to 5000 hertz is covered in figure 14(a) with a 16-hertz bandwidth while figure 14(b) covers the range from 100 to 1000 hertz with a 3.2-hertz bandwidth. Broadband interaction noise produced by deflecting the flap to $60^{\circ}$ is clearly shown at frequencies less than about 2000 hertz. The first combination tone at 460 hertz still can be distinguished with interaction noise present as shown in figure 14(b). Figure 14(a) also shows the crossover of the spectra at about 2000 hertz and the lower levels at higher frequencies for the $60^{\circ}$ flap which are associated with redirection of internal noise by the deflected flap.

While the most striking changes in the spectra were observed in the sideline plane as the flap was lowered, the bulk of the data and perceived noise estimates were for the flyover plane where the maximum levels were observed. Figure 15 shows the 1/3-octave interaction noise spectra in the flyover plane at $70^{\circ}$ for the same fan-under-wing configuration just discussed. The narrow band counterparts are given in the frequency range from 100 to 1000 hertz in figure 16. In contrast to the data for the sideline plane, the $0^{\circ}$ fan-under-wing case clearly shows broadband interaction noise. In general, although the jet scrubbing along the undeflected wing undersurface produced little discernable interaction noise in the sideline plane, it produced substantial interaction noise in the flyover plane. The $0^{\circ}$ fan-on-flap data are included in figures 15 and 16 as a reference case approximating the fan alone, where mainly internal noise is present with only a hint of broad band noise that could be associated with jet noise. Interaction noise effects arising at 100-percent fan speed (36 000 rpm) were qualitatively similar to those at the lower speed shown.

In order to calculate overall sound pressure levels and perceived noise levels for external noise, it was necessary to develop methods of removing internally generated noise from the 1/3-octave spectra. The methods used can be understood by referring to figure 15. At frequencies less than about 1000 hertz the main internal noise influences on the spectra are the combination tones. The first combination tone was removed by linearly interpolating from the levels in the bands adjacent to those influenced by the tone (e.g., 400 and 500 Hz at 76-percent speed with interpolations indicated by the short dashed lines). At frequencies greater than 1000 hertz, broadband internal noise along with combination tones become stronger relative to the external noise and must be removed along with the higher frequency blade passage tones. The procedure used was to linearly extrapolate the interaction noise levels to higher frequencies using a constant rate of decrease in decibel level per decade beginning with the first data point on the high frequency side of the band containing the first combination tone. This procedure is illustrated by the long dashed lines for the fan-under-wing data in figure 15. A slope of -17 decibels per decade was used which is also the high frequency slope of the SAE ground spectrum for jet noise (ref. 5). An examination of fan-under-wing spectra which do show an extended high frequency decay in interaction noise indicate this decay rate to

be a reasonable average. The particular spectra referred to are those where internal noise is reflected away from a microphone by flap or wing surfaces. This occurs at aft angles in the sideline plane as discussed in connection with figure 12 and is further illustrated in figure 33(c) in the appendix. The prominent decay is also evident in the flyover plane at rear angles where a deflected flap shielded the microphone from internal noise, as shown for example in figures 28(d), 29(d), and 29(e) in the appendix. The particular slope used does not affect overall sound pressure levels for the interaction noise since they are determined by levels in the vicinity of the peak. Calculations showed that varying the slope from -15 to -20 decibels per decade resulted in less than 1 PNdB change in maximum perceived noise levels. The maximum frequency used in all external noise PNdB calculations was 4000 hertz. In this respect calculations showed that continuing the -17 decibel per decade extrapolation to 10 000 hertz increased the maximum perceived noise levels by less than 1.5 PNdB in all cases.

Most of the fan-on-flap spectra, particularly at 76-percent speed, showed no low frequency jet noise peak. Only at a few angles near the jet was it possible to estimate jet noise by fairing the SAE ground spectrum (ref. 5) through the data at low frequencies.

The angular variation of overall sound pressure level of external noise produced by the model in the flyover plane is shown in figure 17. Figure 17(a), for 100-percent fan speed, includes single point estimates of jet noise for the fan-on-flap configurations with the dashed curves through the points indicating typical jet noise directivity as reported in reference 6. The $0^{\circ}$ fan-under-wing noise is comparable to the jet noise near the jet axis but differs greatly at forward angles. Thus, the interaction noise associated with the jet flow along the wing undersurface is higher than jet noise alone and has a more uniform directivity pattern. Lowering the flap $30^{\circ}$ increases the interaction noise and shifts the noise in the inlet quadrant farther forward.

In order to compare the interaction noise directivities, the data of figure 17 were replotted in figure 18 with angles measured relative to the final jet direction, that is, the direction at which the jet leaves the trailing edge of the flap. Referencing the angles in this manner shows a remarkable similarity in the directivities for undeflected and deflected flap cases, respectively. For the deflected flap cases the exhaust velocity change associated with the two speeds (76 and 100 percent) balances the change in the strength of the interaction associated with the two flap deflections ($30^{\circ}$ and $60^{\circ}$) to produce the same noise levels. This is fortuitous. However, shape similarity indicates that for the deflected flap cases the most intense interaction noise is radiated in a direction nearly normal to the final jet direction.

The overall sound pressure levels in the sideline plane are shown in figure 19 for those cases where external noise was indentifiable in the spectra. A two lobed directivity pattern is indicated by the $60^{\circ}$ flap, 76-percent data with a minimum at $90^{\circ}$. The

levels are generally lower than in the flyover plane and increase as the angle is increased from $90^{\circ}$ to larger values toward the rear in agreement with data in reference 1.

Estimates of aircraft perceived noise levels considering only externally generated noise are shown for simulated takeoff and approach conditions in figures 20(a) and (b), respectively. Zero degree flap cases are included for comparison with the corresponding deflected flap configurations actually representative of STOL takeoff and approach. As before the conditions for which these estimates apply are listed in table II. The data were not adjusted for any aircraft forward velocity effects, on the assumption that noise generated at the wing and flap surfaces depends only on the jet velocity relative to the surfaces.

No frequency scaling was used because a spectral correlation of interaction noise as a function of jet and impingement geometry was lacking. For the present fan-under-wing geometry with the annular fan exhaust which is nearly tangent to the wing under surface, the appropriate geometric variable to use in a Strouhal number for spectral correlation has not been determined. The effects on perceived noise levels of frequency shifts with scale were treated separately on a general basis for these data without explicitly specifying a characteristic dimension and will be discussed in terms of required adjustments to figure 20.

In general, the perceived noise angular distributions in figure 20 resemble the overall sound pressure level distributions of figure 17, and the fan-on-flap points representing jet noise alone are substantially below the fan-under-wing curves determined by jet flap interaction noise. Maximum perceived noise levels for the fan-under-wing fall in the range from 97 to 101 PNdB for approach and takeoff. These values are somewhat above the often mentioned STOL noise goal of 95 PNdB at 152.4 meters (500 ft). Since the levels in figure 20 are estimates obtained by scaling and are subject to some uncertainty, the intention here is not to emphasize exact decibel levels. However, the results do indicate that a fan-under-wing arrangement of this type must operate in the neighborhood of the relatively low pressure ratios and associated exhaust velocities reported here (see table II) if interaction noise is to be limited to levels less than 100 PNdB at 152.4 meters (500 ft). This conclusion is in agreement with the estimates made in reference 2. It must be emphasized again that the assumption throughout this discussion of external noise levels is that internal noise has been reduced to low enough levels that it need not be considered.

The levels of figure 20 must be adjusted to account for any frequency shifts in the interaction noise spectrum associated with changes in scale in going from the model to a full-size STOL aircraft. In order to examine the effects of frequency scaling on the perceived noise estimates, the interaction noise spectra at angles where the perceived noise level was a maximum were translated downward in frequency by various amounts and new perceived noise levels were calculated. In this way adjustments to the levels

in figure 20 associated with frequency scaling were determined and are plotted as the ordinate in figure 21. The abscissa is the ratio of the scaled frequency to experimental frequency. For example, if interaction noise frequencies were shifted downward by a factor of 4 ($f/f_o = 0.25$) associated with increased engine size, the maximum noise levels in figure 20 would be lowered as much as 5 decibels.

## SUMMARY OF RESULTS

Noise measurements were made on two jet flap lift augmentation systems: a fan-under-wing configuration and a fan-on-flap arrangement. Examination of the internally and externally generated noise characteristics lead to the following conclusions:

1. Internal noise from the fan inlet was partially shielded from the ground by the wing for the fan-on-flap arrangement. Perceived noise estimates indicated that this benefit would be realized on takeoff but not at the approach attitude and flap deflection.

2. The internal noise of the fan-under-wing was lowered by a shielding action of the deflected flap surfaces at aft angles in the sideline plane and at rear angles above the flap in the flyover plane. However, no consistent redirection of internal noise was observed at angles below the wing in the flyover plane of the fan-under-wing configuration as the flap was deflected from $0^o$ to $60^o$.

3. The external noise for the fan-under-wing arrangements was dominated by jet/flap interaction noise. Even with no flap deflection the interaction noise was substantially greater than jet noise alone. For deflected flap cases the interaction noise increased with flap angle and peaked at microphone angles around $90^o$ to the final jet direction.

4. Since the external noise associated with the fan-on-flap configuration is jet noise alone, that arrangement has an important noise advantage over the fan-under-wing system with its more intense interaction noise.

Lewis Research Center,
National Aeronautics and Space Administration,
Cleveland, Ohio, February 14, 1972,
132-80.

# APPENDIX - ONE-THIRD-OCTAVE SOUND PRESSURE LEVEL DATA

This appendix presents the complete set of 1/3-octave sound pressure level spectra measured in the testing of the jet flap configurations (figs. 22 to 33). The data are corrected to standard day conditions of $15^{\circ}$ C ($59^{\circ}$ F) and 70-percent relative humidity. The organization of these figures is as follows: fan-on-flap configurations, flyover plane; fan-under-wing, flyover plane; and fan-under-wing, sideline plane. Each figure contains spectra at several adjacent angles. These angles are measured relative to a line along the undersurface of the wing with $0^{\circ}$ in the forward direction (see fig. 5). The data taken in the sideline plane have been adjusted to a 4.57 meter (15 ft) radius.

## REFERENCES


1. Maglieri, Domenic J.; and Hubbard, Harvey H.: Preliminary Measurements of the Noise Characteristics of Some Jet-Augmented Flap Configurations. NASA Memo 12-4-58L, 1959.

2. Dorsch, R. G.; Krejsa, E. A.; and Olsen, W. A.: Blown Flap Noise Research. Paper 71-745, AIAA, June 1971.

3. Sanders, Newell D.; Diedrich, James H.; Hassell, James L., Jr.; Hickey, David H.; Luidens, Roger W.; and Stewart, Warner L.: V/STOL Propulsion. Aircraft Propulsion. NASA SP-259, 1971, pp. 135-168.

4. Howes, Walton L.: Ground Reflection of Jet Noise. NASA TR R-35, 1959.

5. Anon.: Jet Noise Prediction. Aerospace Information Report 876, SAE, July 1965.

6. Minner, Gene L.; and Feiler, Charles E.: Low-Speed Jet Noise from a 1.83-Meter (6-ft) Fan for Turbofan Engines. Paper 71-586, AIAA, June 1971.

TABLE I. - BLOWN FLAP CONFIGURATIONS

| Condition (measurement plane) | Configuration | Fan speed, percent (a) | Flap angle, deg |
|---|---|---|---|
| Fan-on-flap (flyover plane) | 1 | 100 | 0 |
| | 1 | 76 | 0 |
| | 2 | 100 | 30 |
| | 3 | 76 | 60 |
| Fan-under-wing (flyover and sideline planes) | 4 | 100 | 0 |
| | 4 | 76 | 0 |
| | 5 | 100 | 30 |
| | 6 | 76 | 60 |

[a] 100 percent = 36 000 rpm.

TABLE II. - CONDITIONS FOR PNdB ESTIMATES AT 152.4 METERS (500 FT)

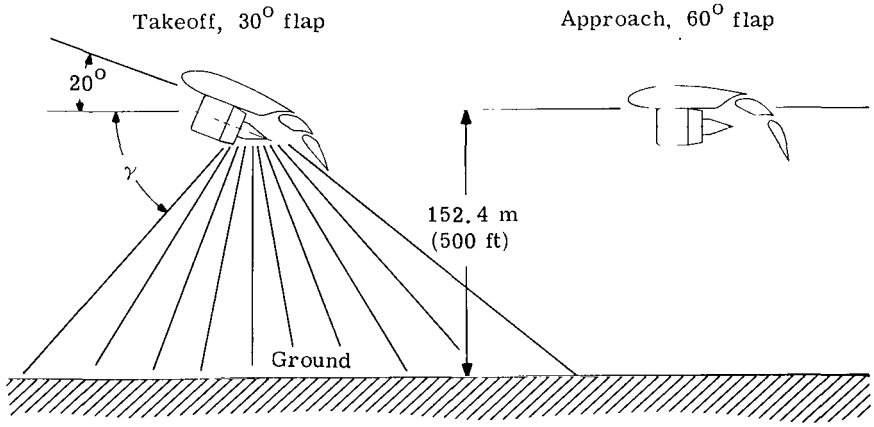


| Simulated condition | Thrust, N (lb) | Engine speed, percent | Fan pressure ratio | Fan exhaust velocity, m/sec (ft/sec) | Angle of wing under surface with respect to horizontal, deg | Flap angle, deg |
|---|---|---|---|---|---|---|
| Takeoff | $2.669\times10^5$ (60 000) | 100 | 1.25 | 177 (580) | 20 | 30 |
| Approach | $1.544\times10^5$ (34 700) | 76 | 1.14 | 137 (450) | 0 | 60 |

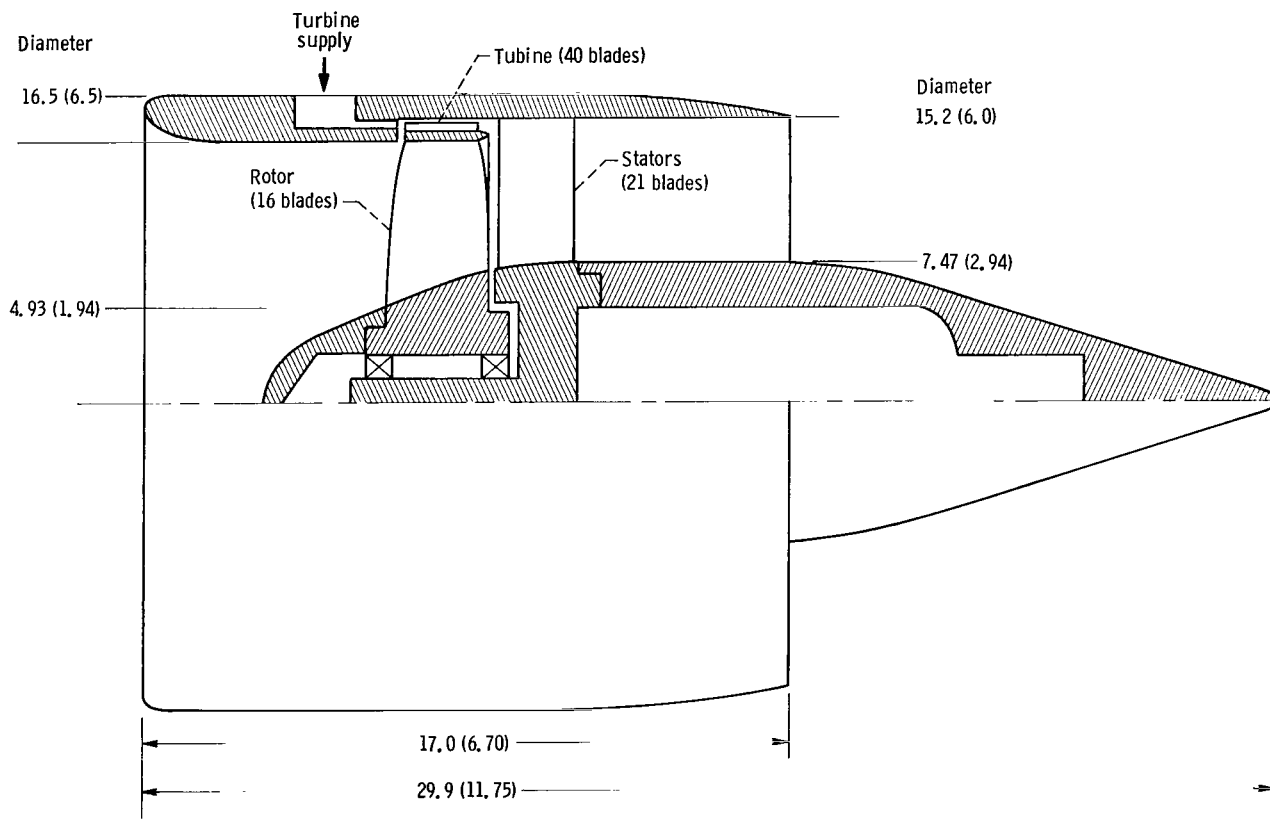


Figure 1. - Model fan. Dimensions are in centimeters (in.).

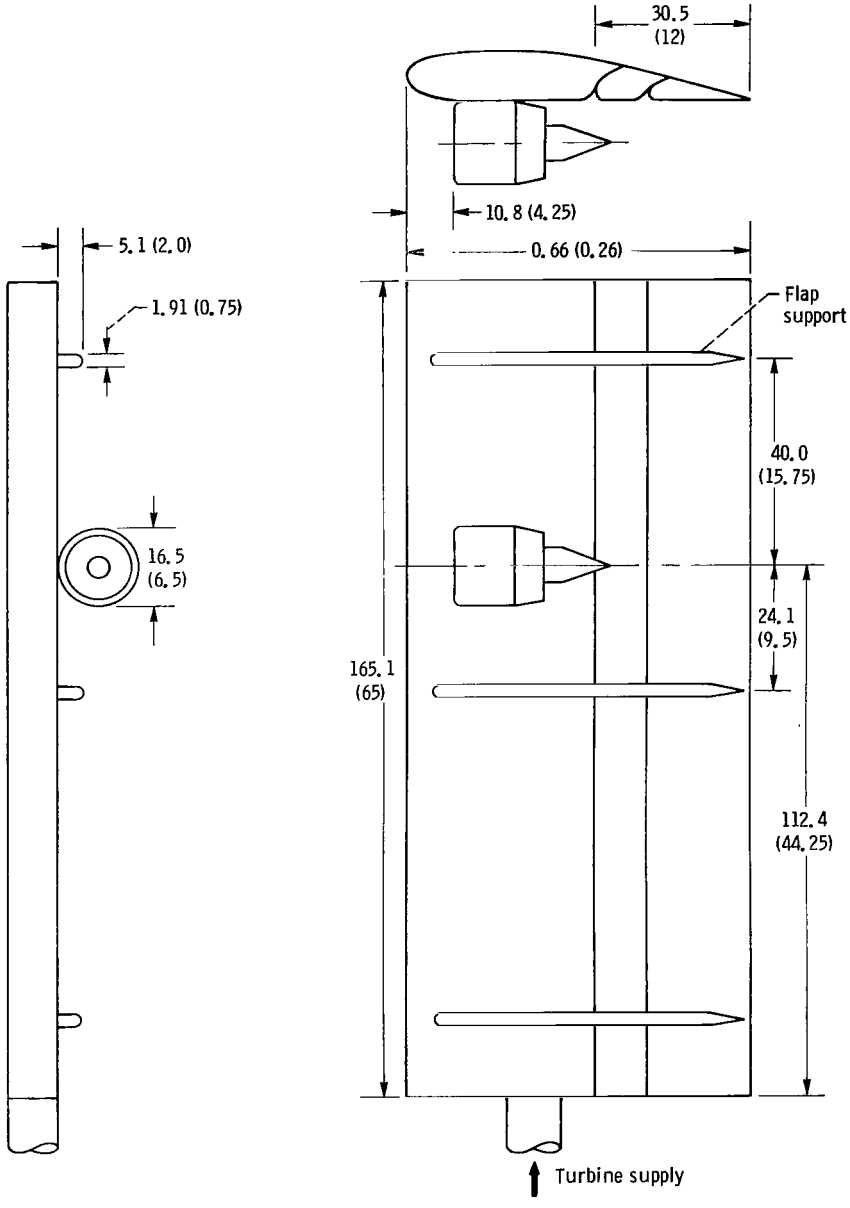


Figure 2. - Model wing shown with $0^{0}$ flap and fan under wing. Dimensions are in centimeters (in.).

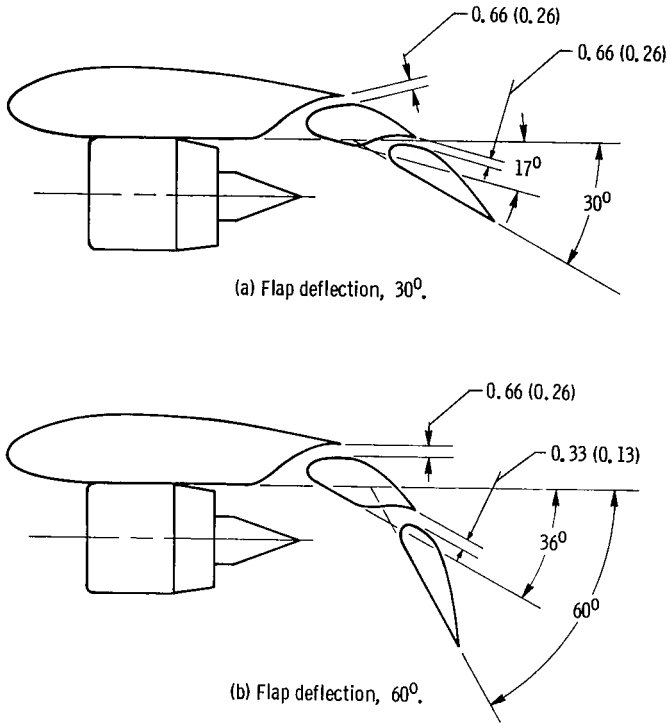


Figure 3. - Fan-under-wing geometry. Dimensions are in centimeters (in.).

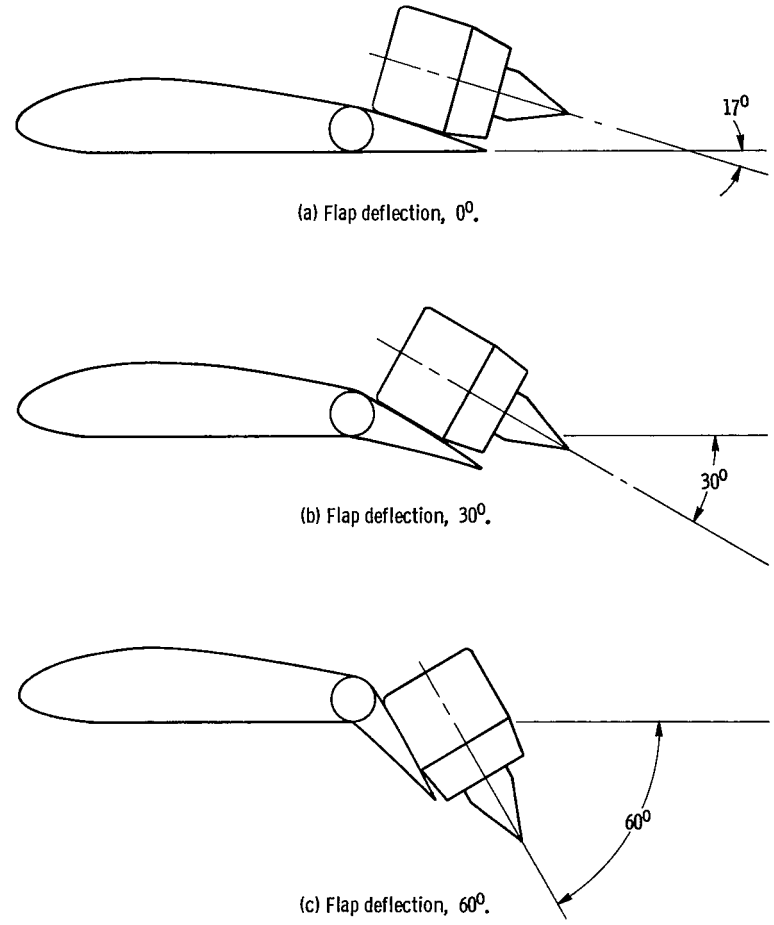


Figure 4. - Fan-on-flap geometry.

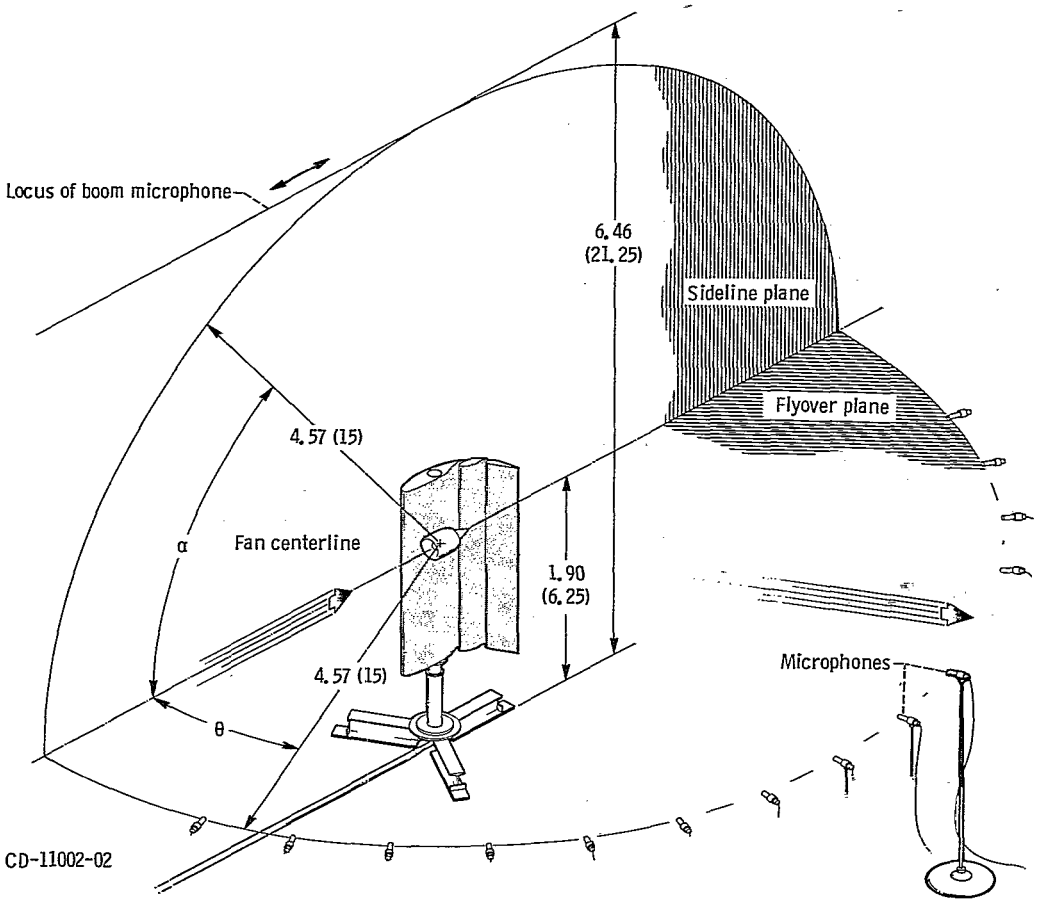


Figure 5. - Measurement geometry. Dimensions are in meters (ft).

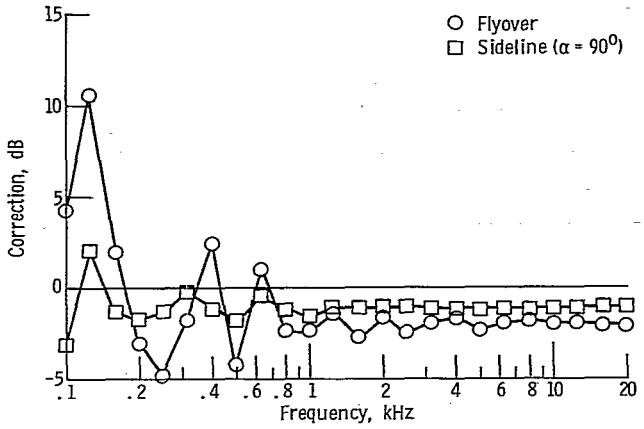


Figure 6. - Theoretical 1/3-octave sound pressure level ground reflection corrections.

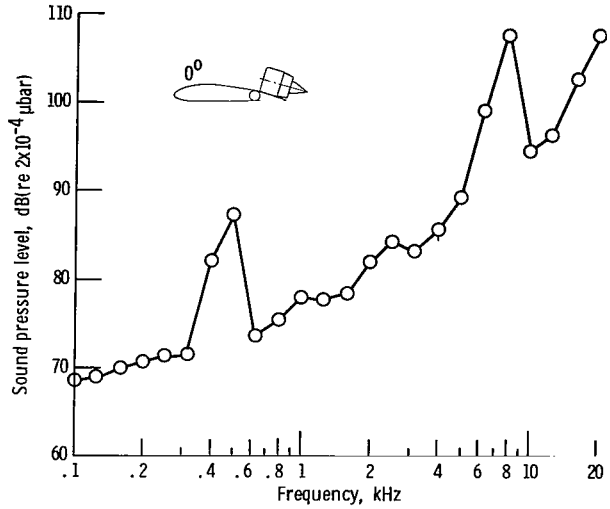


Figure 7. - One-third-octave spectrum illustrating internal noise for fan-on-flap. Fan speed, 76 percent; flap deflection, 0°, radius, 4.57 meters; angle in flyover plane, θ = 130°.

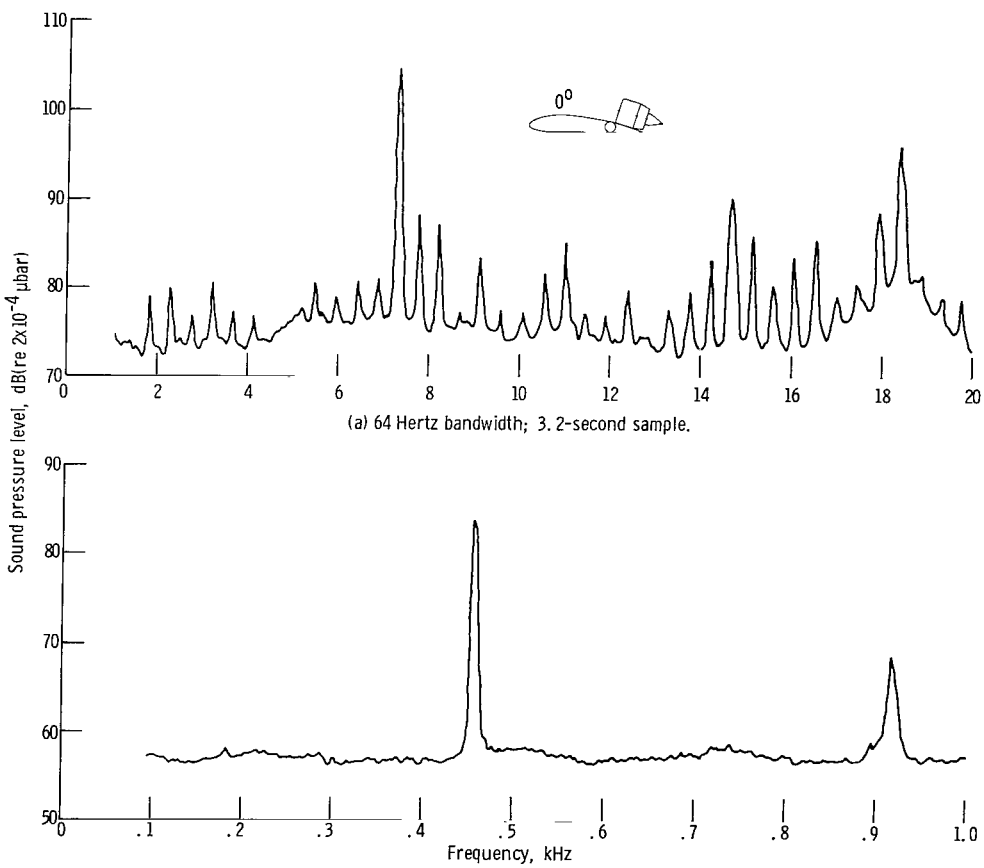


(a) 64 Hertz bandwidth; 3.2-second sample.

(b) 3.2 Hertz bandwidth; 64-second sample.

Figure 8. - Narrow band spectra illustrating internal noise for fan-on-flap. Fan speed, 76 percent; flap deflection, 0°; radius, 4.57 meters; angle in flyover plane, θ = 130°.

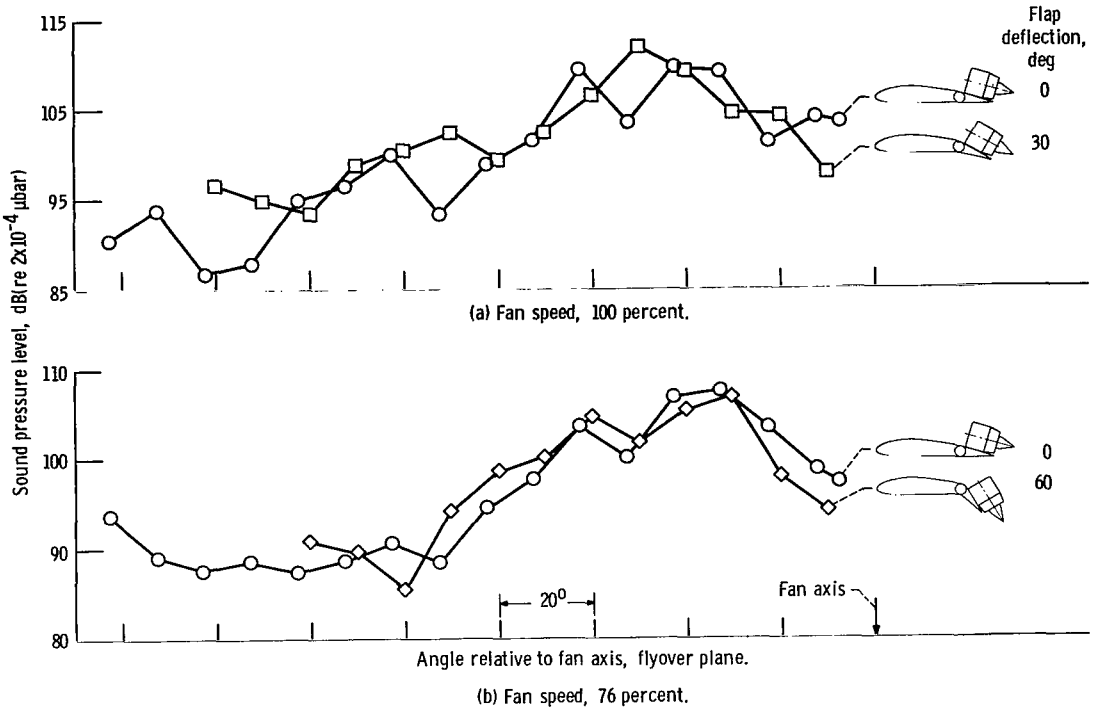


Figure 9. - Sound pressure levels in 1/3-octave band containing blade passage frequency for fan-on-flap. Radius, 4.57 meters.

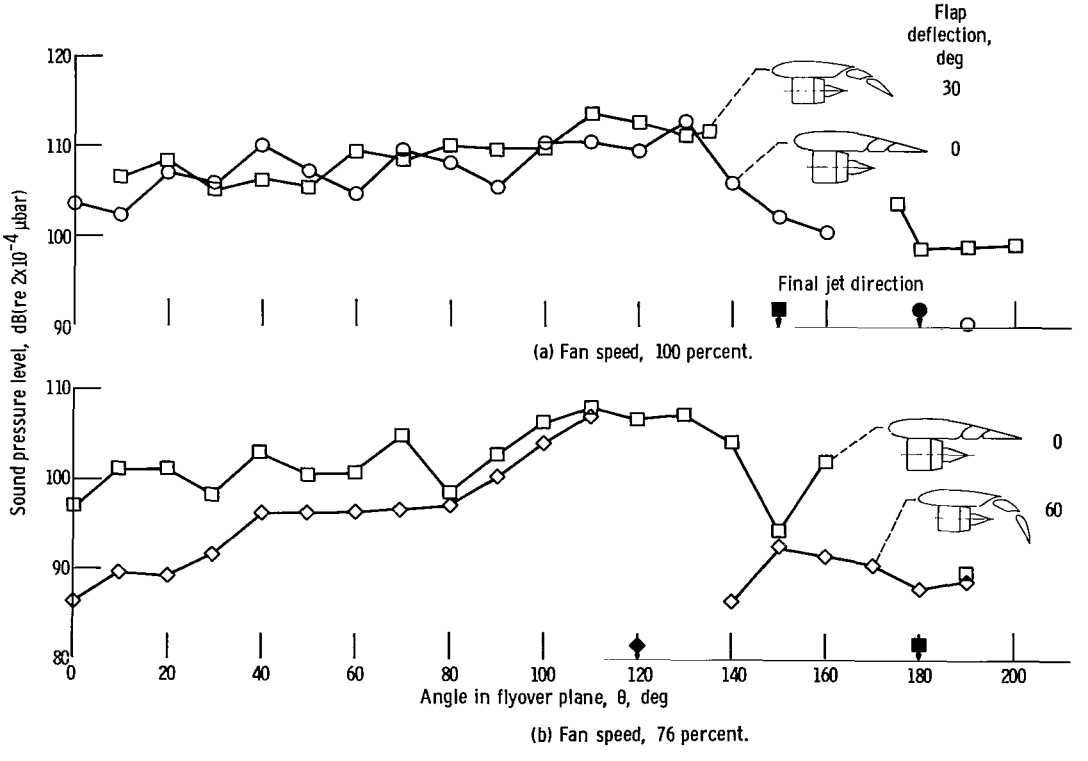


Figure 10. - Sound pressure levels in 1/3-octave band containing blade passage frequency. Radius, 4.57 meters.

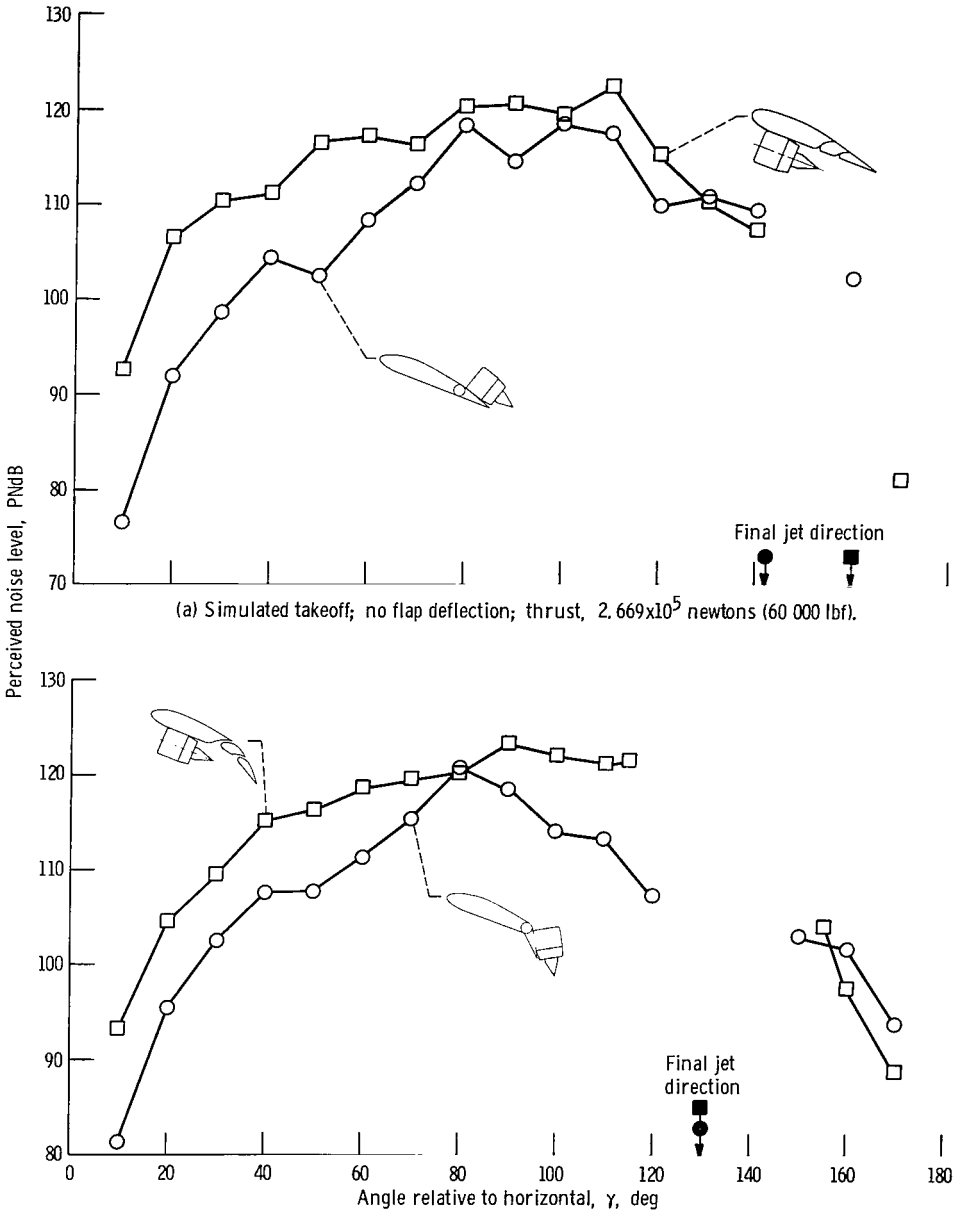


(a) Simulated takeoff; no flap deflection; thrust, $2.669 \times 10^5$ newtons (60 000 lbf).

(b) Simulated takeoff; flap deflection, $30^0$; thrust, $2.669 \times 10^5$ newtons (60 000 lbf).

Figure 11. - Estimated perceived noise levels of internally generated noise at 152.4-meter (500-ft) flyover. Frequencies scaled down by 4; aircraft gross weight, 45 360 kilograms (100 000 lbm).

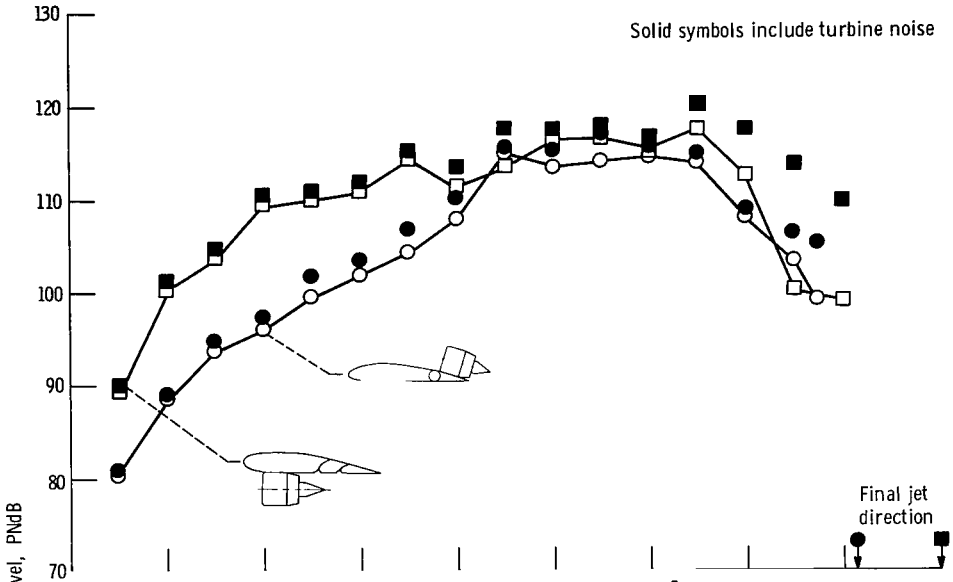


(c) Simulated approach; no flap deflection; thrust, $1.544 \times 10^5$ newtons (34 700 lbf).

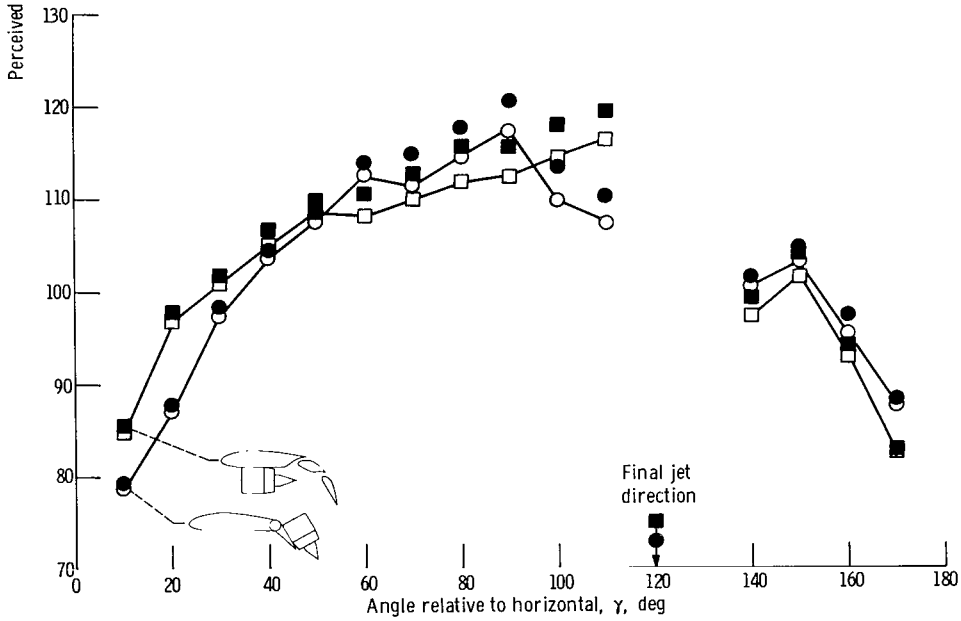


(d) Simulated approach; flap deflection, $60^0$; thrust, $1.544 \times 10^5$ newtons (34 700 lbf).

Figure 11. - Concluded.

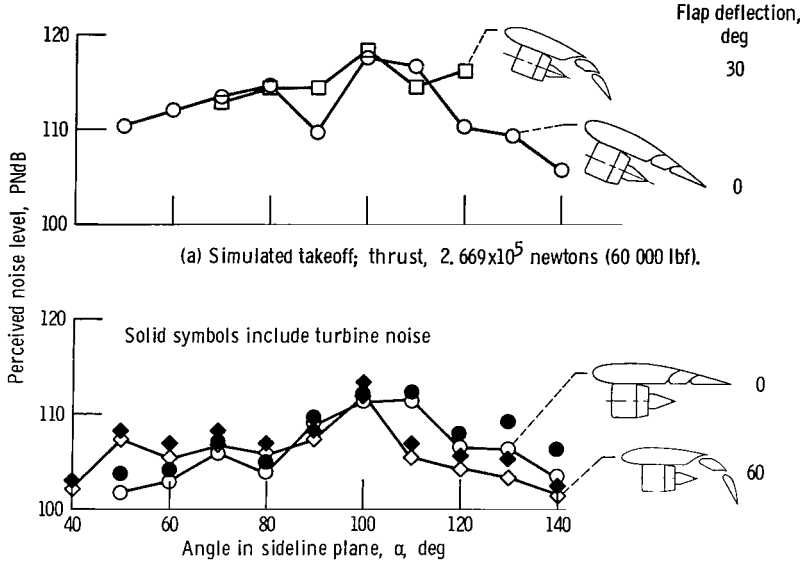


Figure 12. - Estimated perceived noise levels of internally generated noise on 152.4-meter (500-ft) sideline. Frequency scaled down by 4; aircraft gross weight, 45 360 kilograms (100 000 lbm).

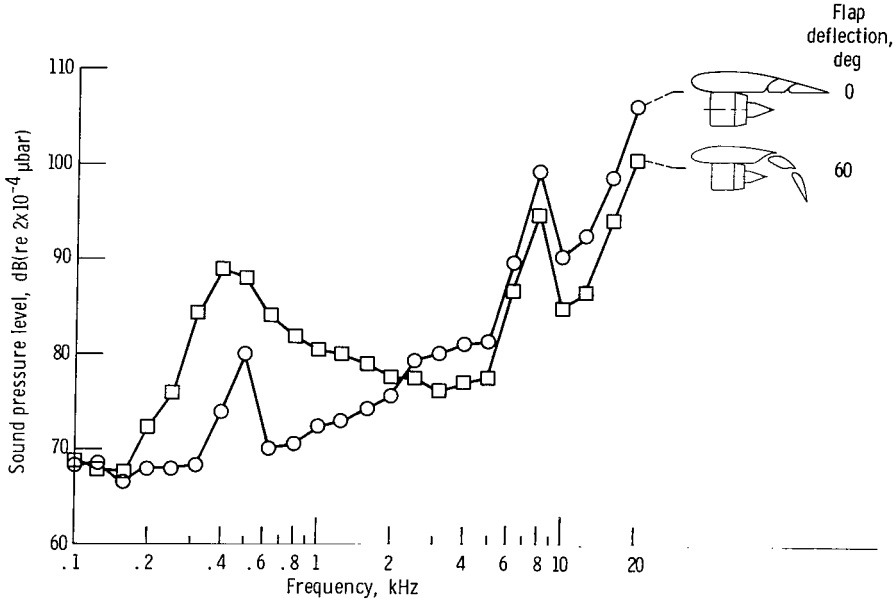


Figure 13. - One-third-octave spectra illustrating external interaction noise in sideline plane for fan-under-wing. Fan speed, 76 percent; radius, 4.57 meters; angle in sideline plane, $\alpha = 130^{\circ}$.

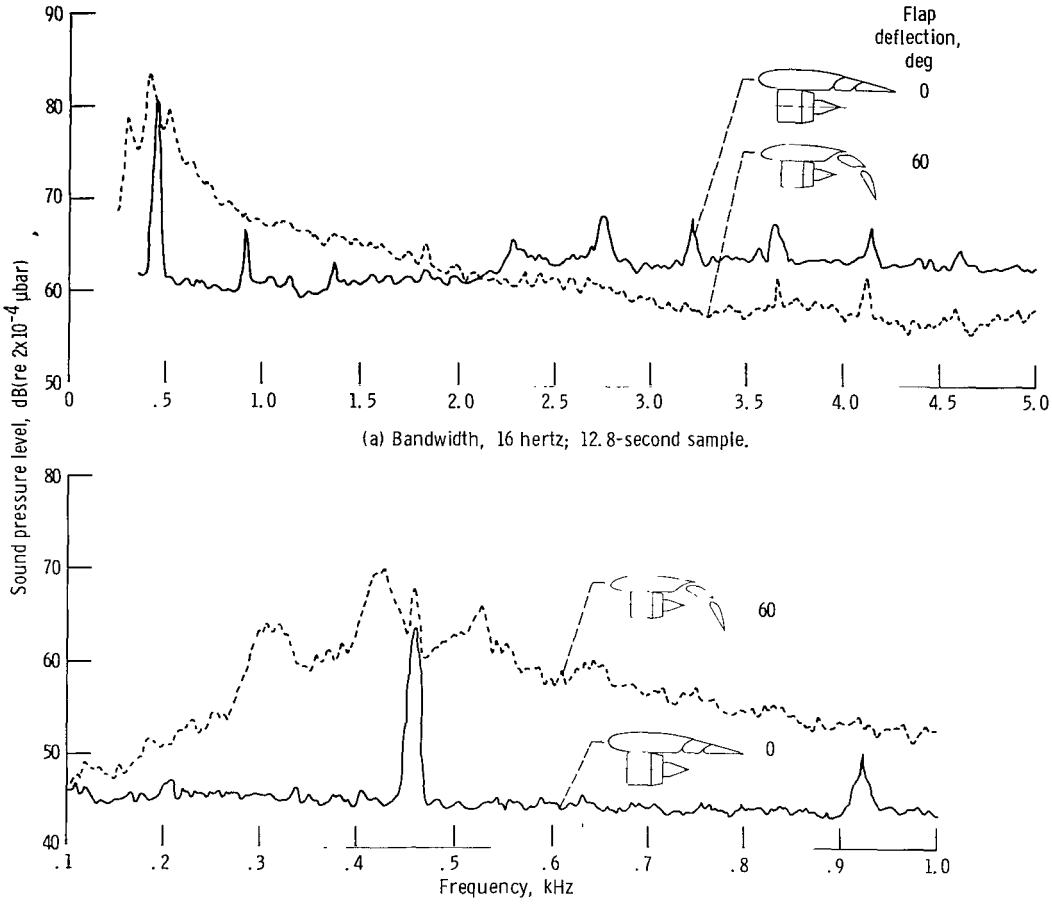


(a) Bandwidth, 16 hertz; 12.8-second sample.

(b) Bandwidth, 3.2 hertz; 32-second sample.

Figure 14. - Narrow band spectra illustrating external interaction noise in sideline plane for fan-under-wing. Fan speed, 76 percent; radius, 4.57 meters; angle in sideline plane, $\alpha = 130^{0}$.

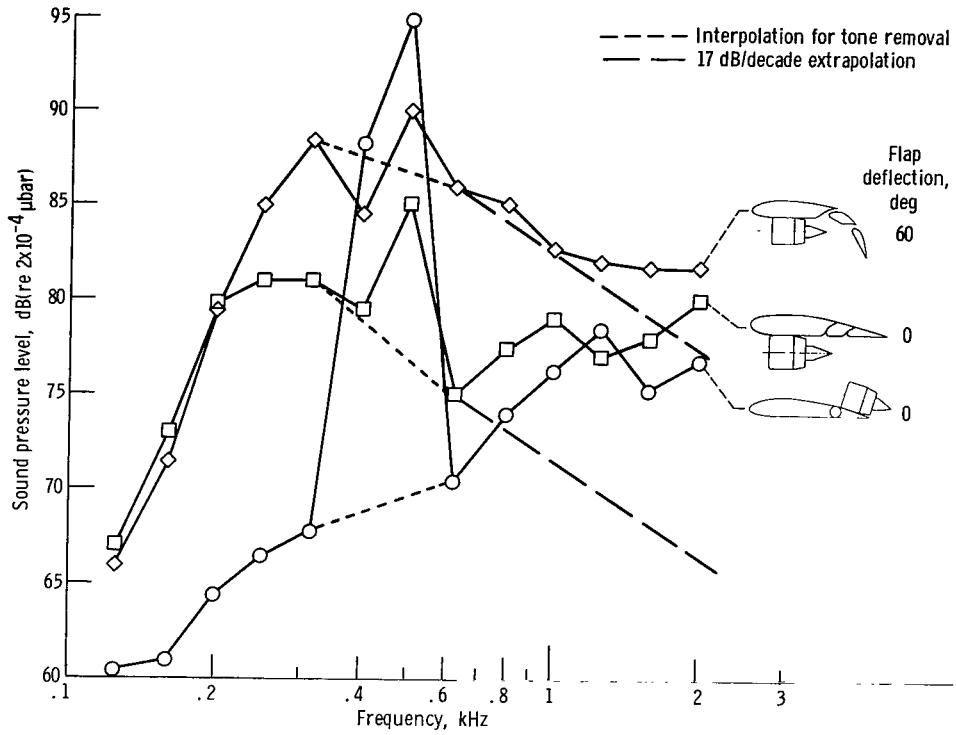


Figure 15. - One-third-octave spectra of jet/flap interaction noise in flyover plane. Fan speed, 76 percent; radius, 4.57 meters; angle in flyover plane, $\theta = 70^{o}$.

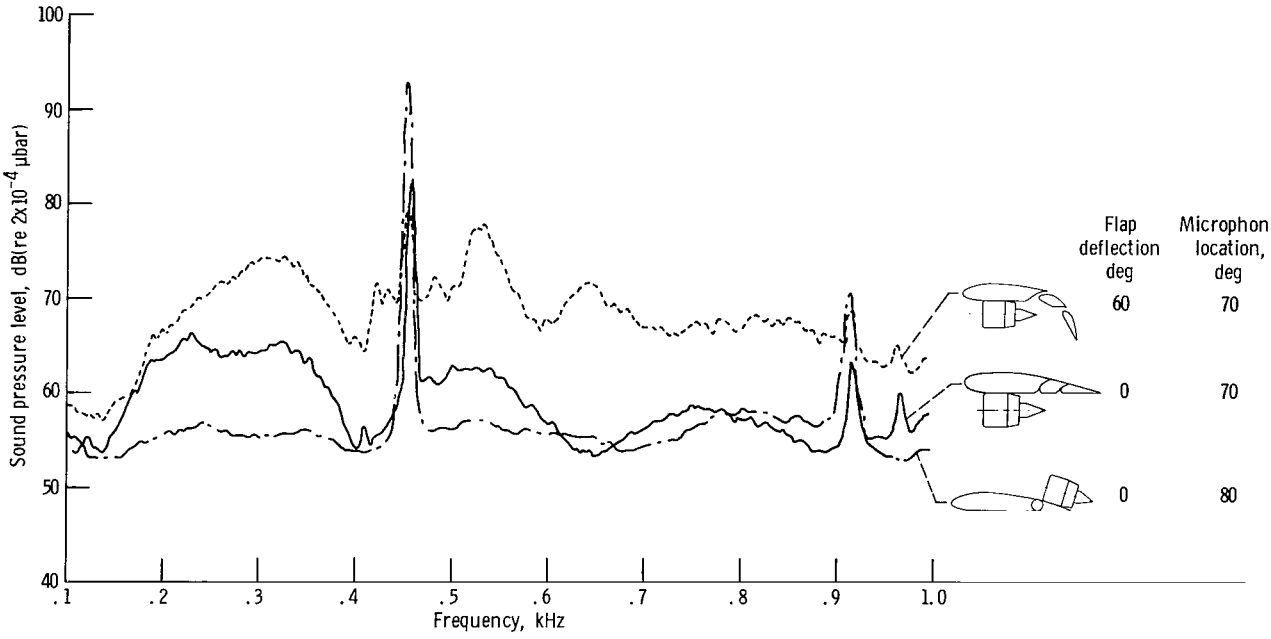


Figure 16. - Narrow band spectra of jet/flap interaction noise in flyover plane. Fan speed, 76 percent; radius, 4.57 meters; bandwidth, 3.2 hertz; 32-second sample.

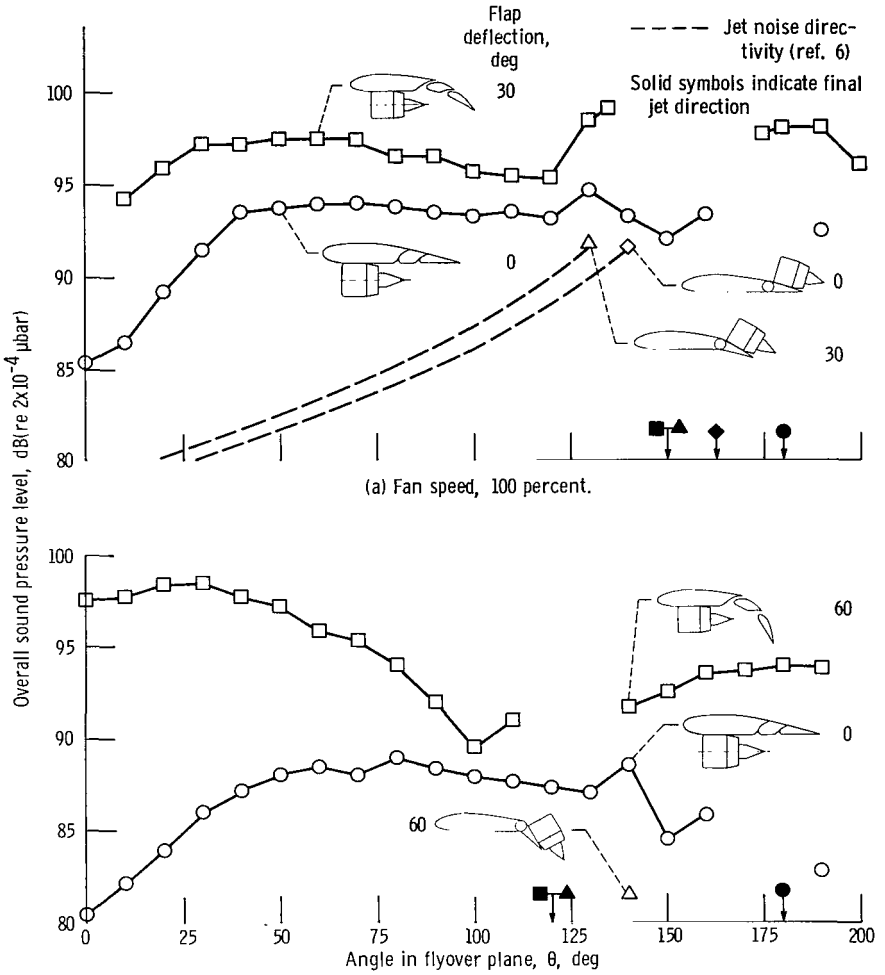


(a) Fan speed, 100 percent.

(b) Fan speed, 76 percent.

Figure 17. - Overall sound pressure level of external noise as function of angle in flyover plane. Radius, 4.57 meters.

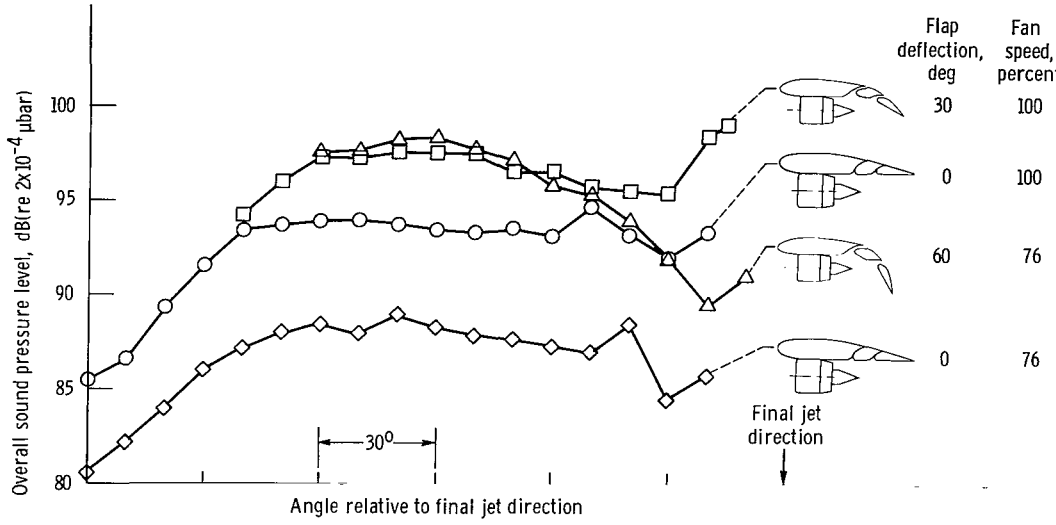


Figure 18. - Overall sound pressure level of external noise as function of angle relative to final jet direction in fly-over plane. Radius, 4.57 meters.

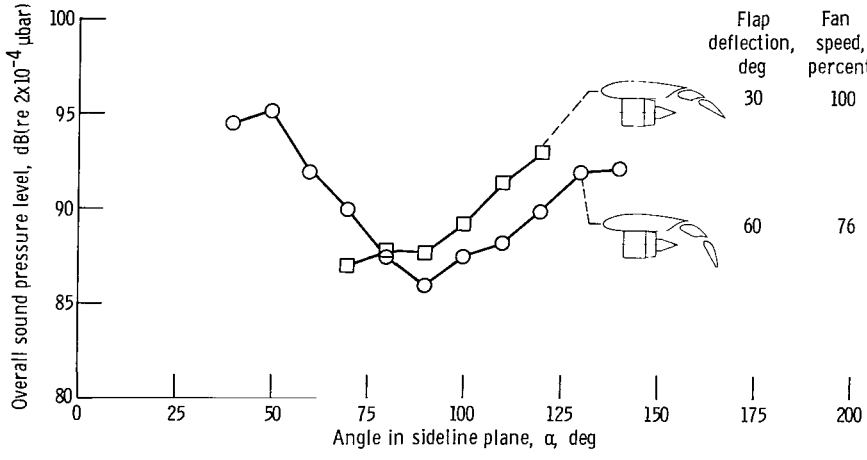


Figure 19. - External noise overall sound pressure level as function of angle in sideline plane. Radius, 4.57 meters.

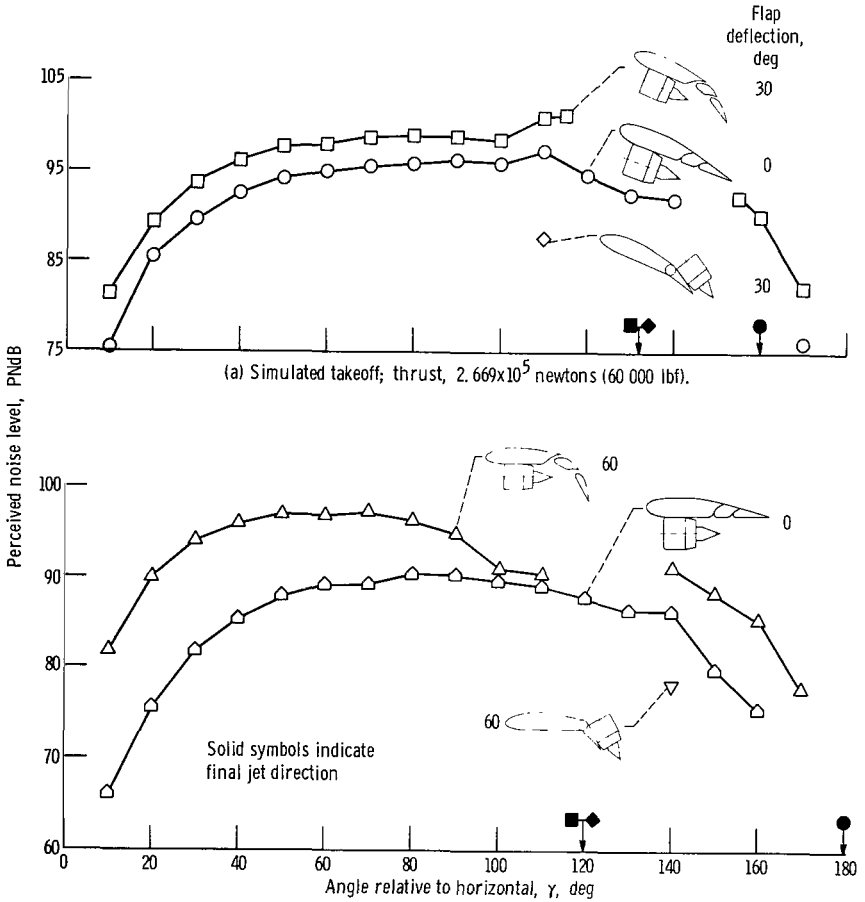


(b) Simulated approach; thrust, 1.544x10^5 newtons (34 700 lbf).

Figure 20. - Estimated perceived noise levels of externally generated noise due to jet and jet/flap interaction at 152.4 meters (500 ft). Frequencies not scaled. Aircraft gross weight, 45 360 kilograms (100 000 lbm).

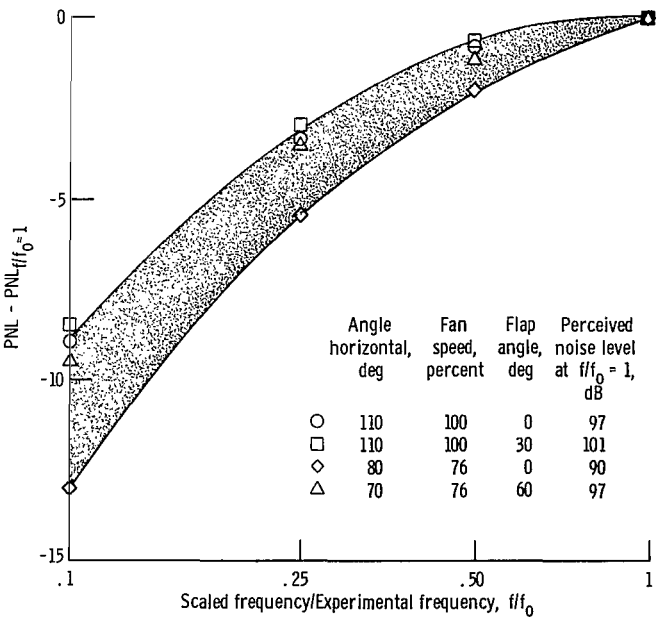


Figure 21. - Effect of frequency scaling on estimated maximum perceived noise levels of external noise for fan-under-wing.

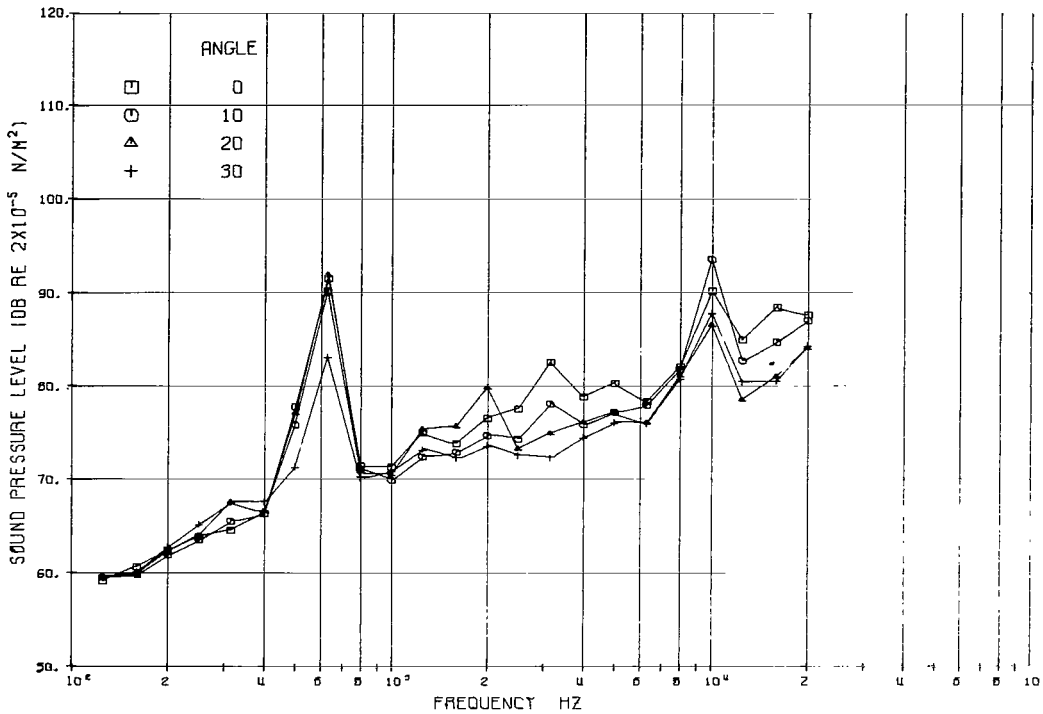


(a) Microphone angles, $0^0$, $10^0$, $20^0$, and $30^0$.

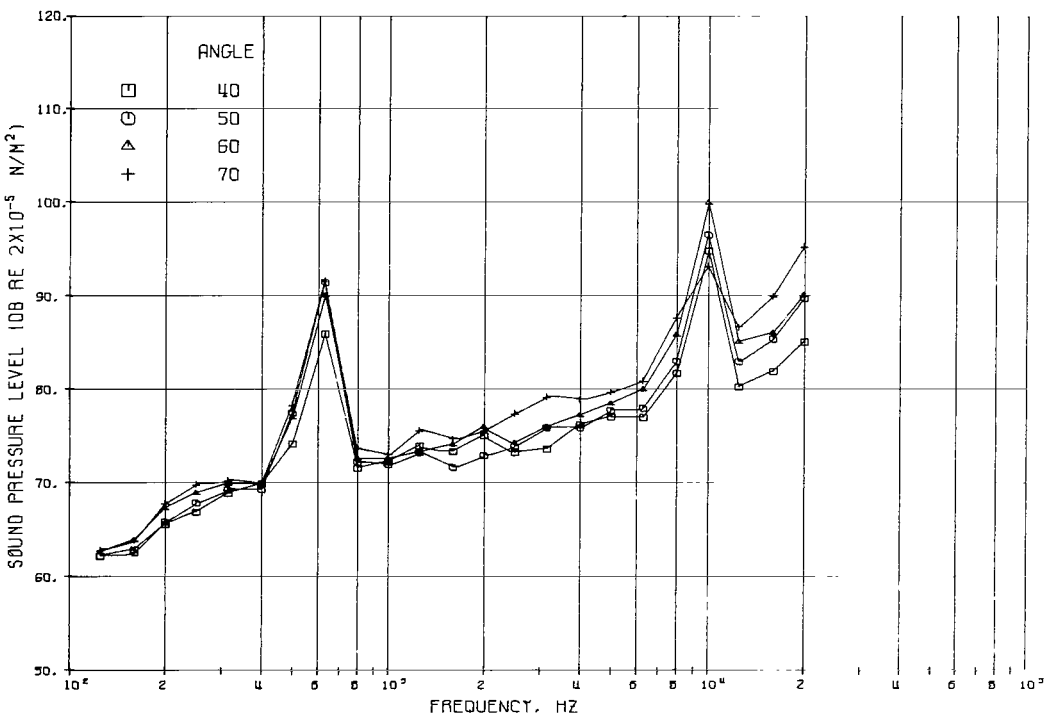


(b) Microphone angles, $40^0$, $50^0$, $60^0$, and $70^0$.

Figure 22. - Sound pressure level of jet flap noise on 4.57-meter radius in flyover plane. Configuration 1: fan-on-flap; flap deflection, $0^0$; fan speed, 100 percent.

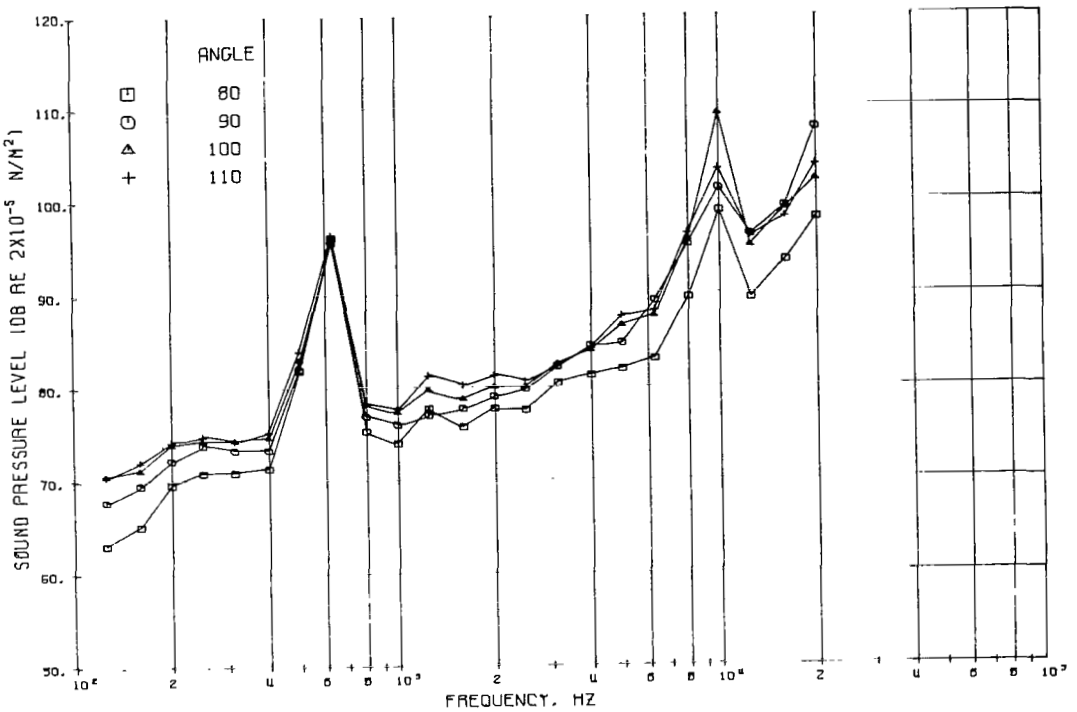


(c) Microphone angles, 80°, 90°, 100°, and 110°.

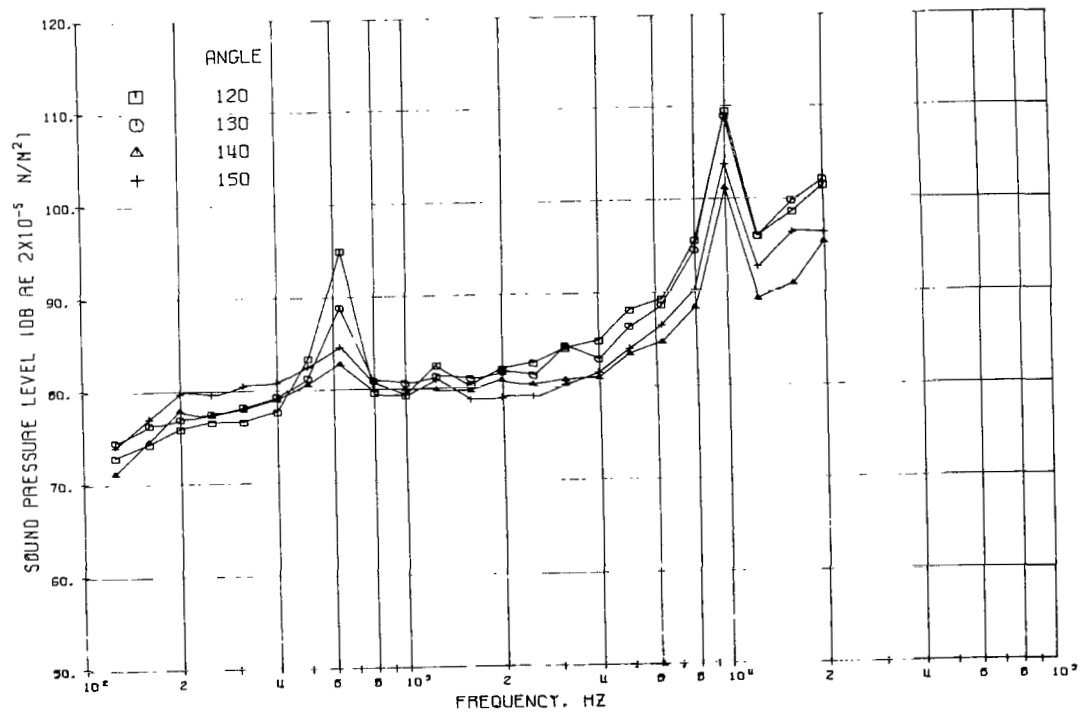


(d) Microphone angles, 120°, 130°, 140°, and 150°.

Figure 22. - Continued.

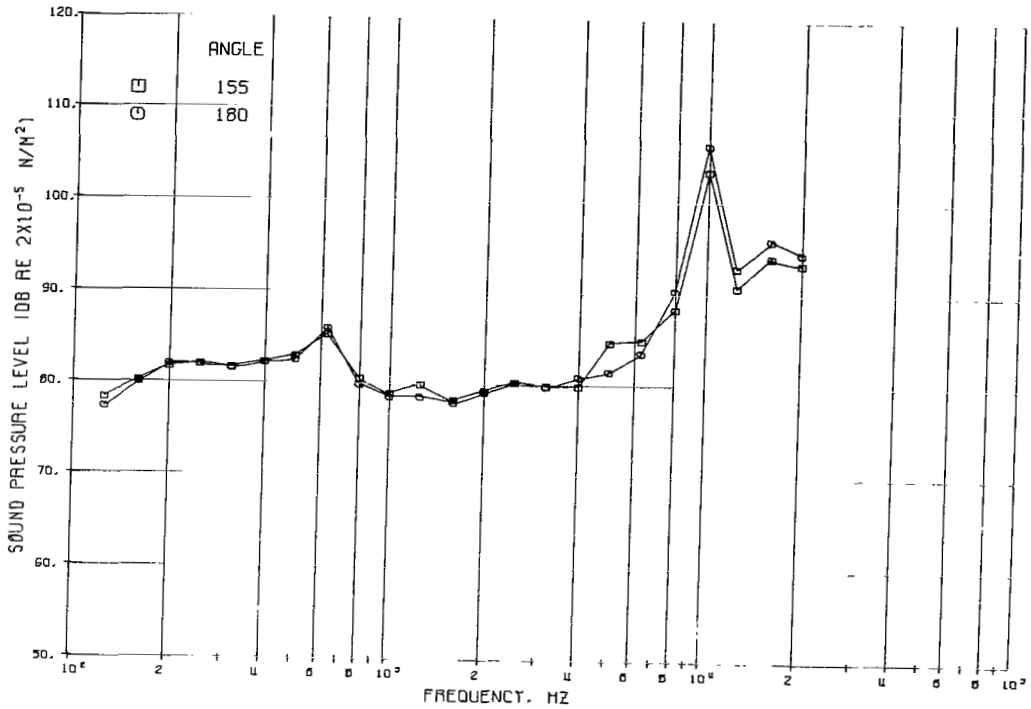


(e) Microphone angles, 155° and 180°.

Figure 22. - Concluded.

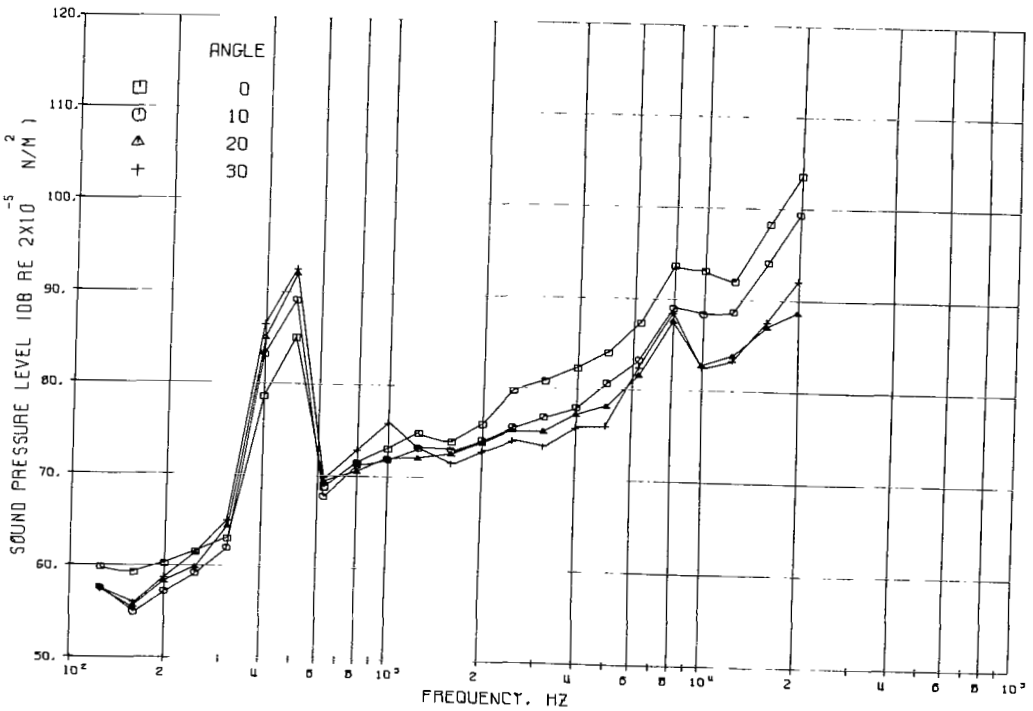


(a) Microphone angles, 0°, 10°, 20°, and 30°.

Figure 23. - Sound pressure level of jet flap noise on 4.57-meter radius in flyover plane. Configuration 1: fan-on-flap; flap deflection, 0°; fan speed, 76 percent.

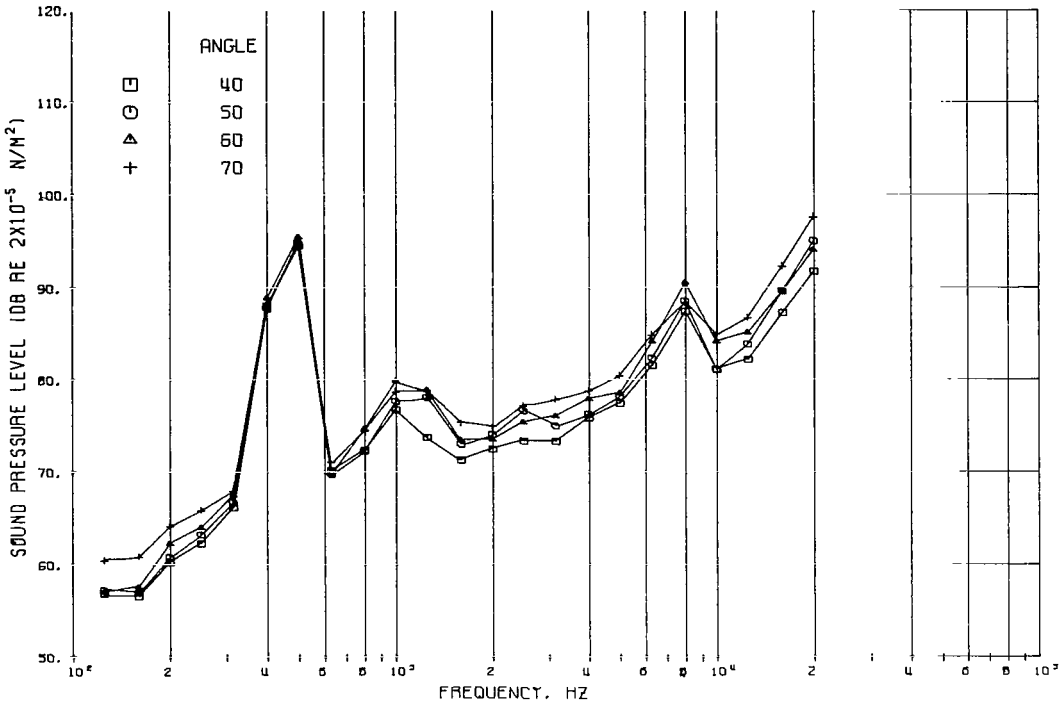


(b) Microphone angles, 40°, 50°, 60°, and 70°.

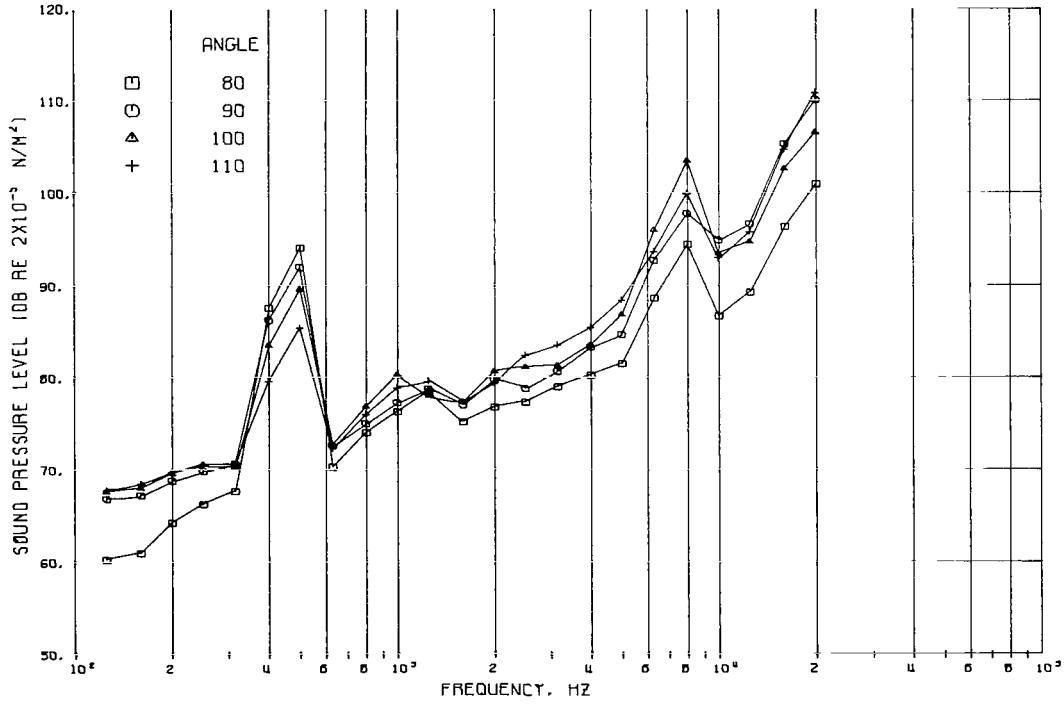


(c) Microphone angles, 80°, 90°, 100°, and 110°.

Figure 23. - Continued.

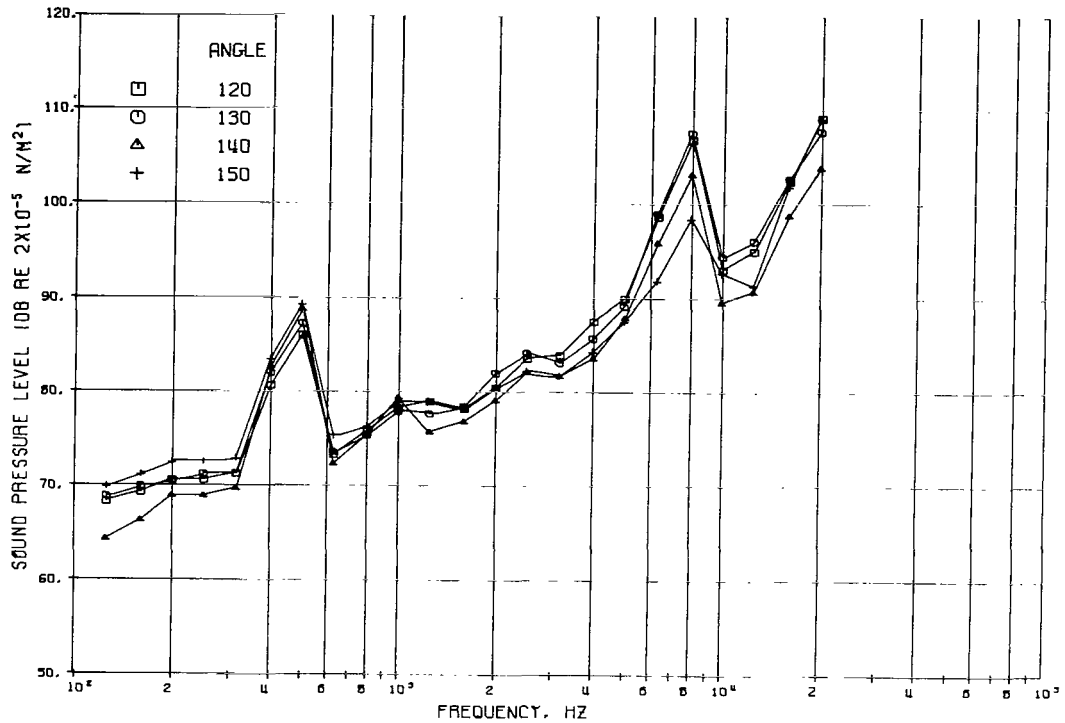


(d) Microphone angle, 120°, 130°, 140°, and 150°.

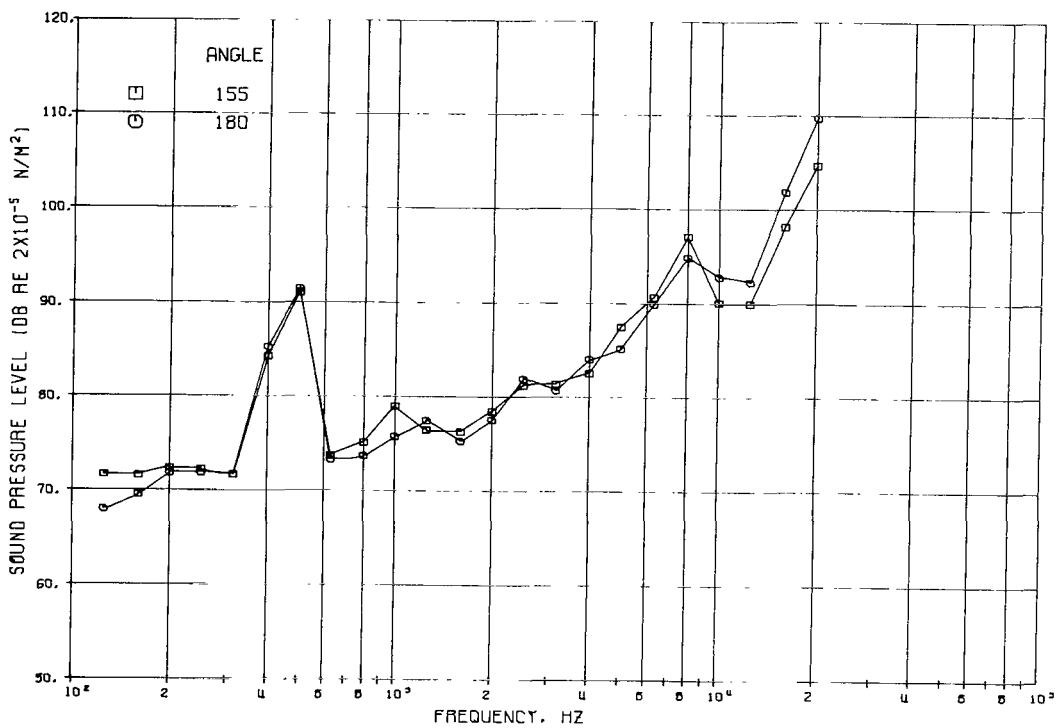


(e) Microphone angles, 155° and 180°.

Figure 23. - Concluded.

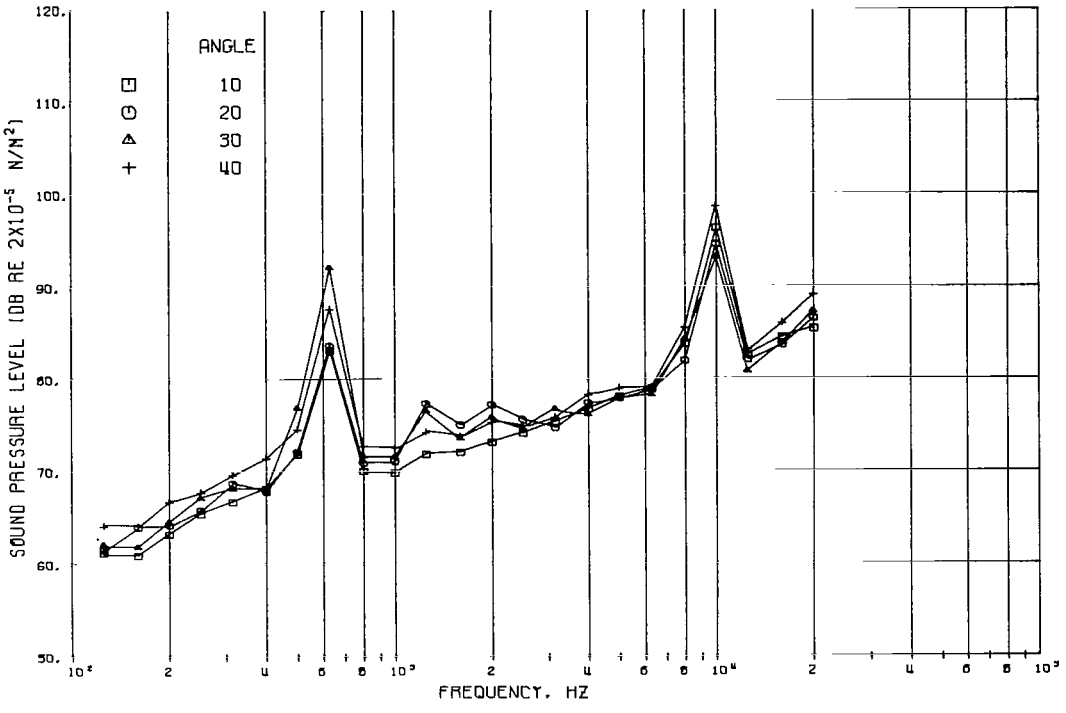


(a) Microphone angles, $10^0$, $20^0$, $30^0$, and $40^0$.

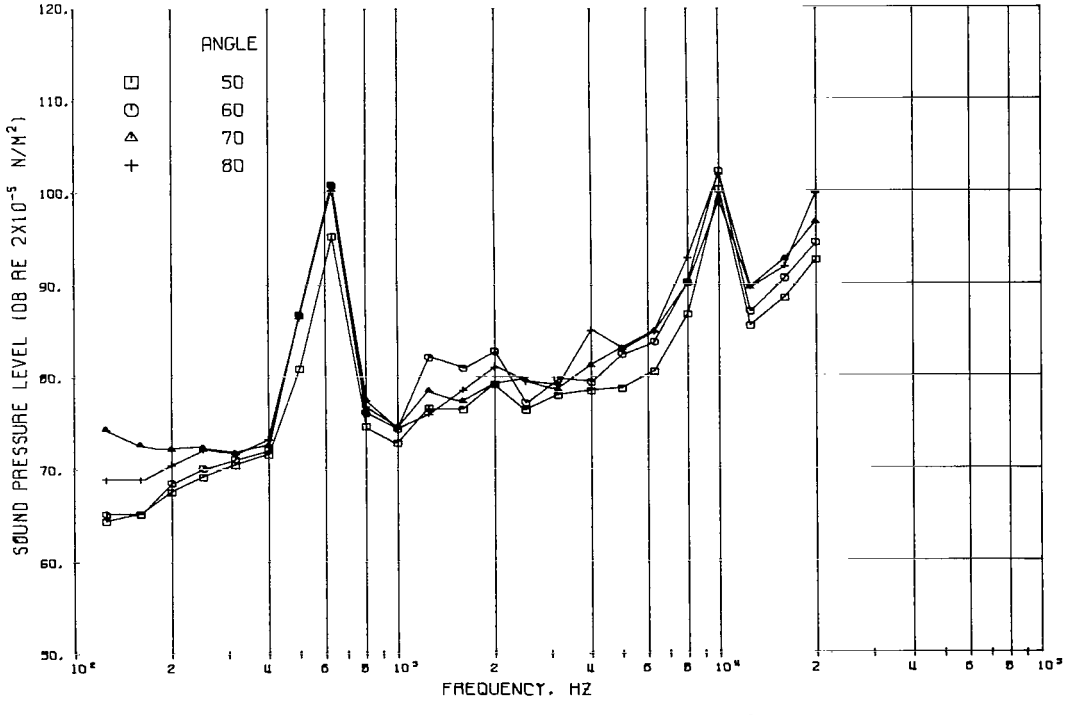


(b) Microphone angles, $50^0$, $60^0$, $70^0$, and $80^0$.

Figure 24. - Sound pressure level of jet flap noise on 4.57-meter radius in flyover plane. Configuration 2: fan-on-flap; flap deflection, $30^0$; fan speed, 100 percent.

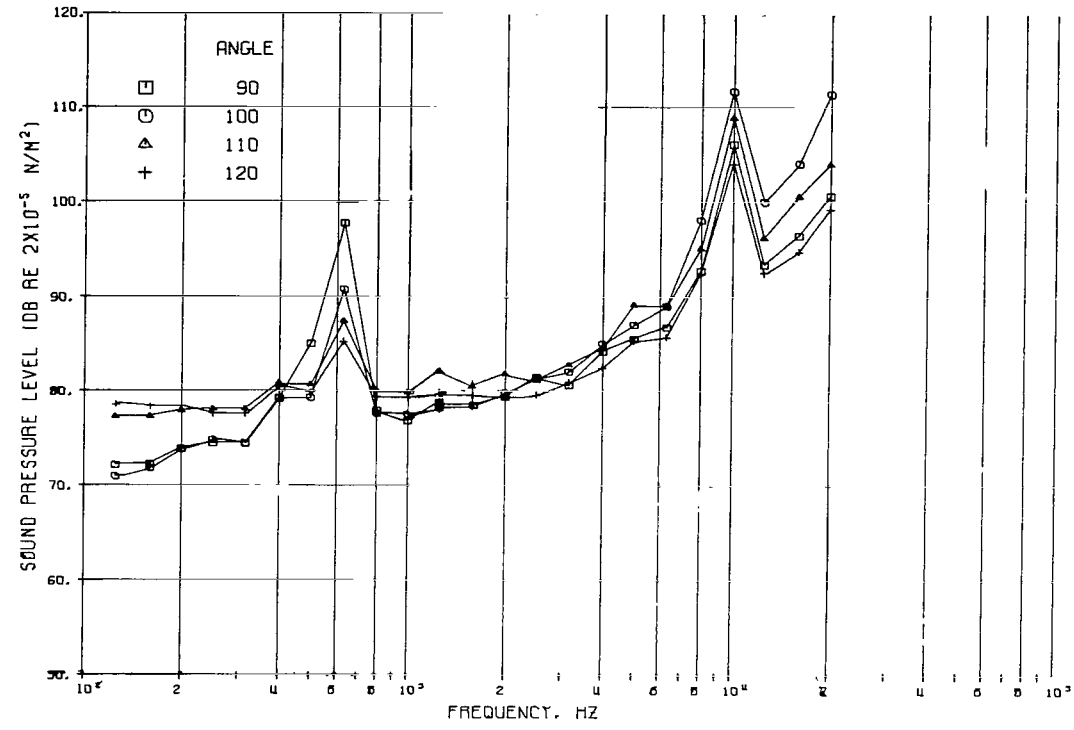


(c) Microphone angles, 90°, 100°, 110°, and 120°.

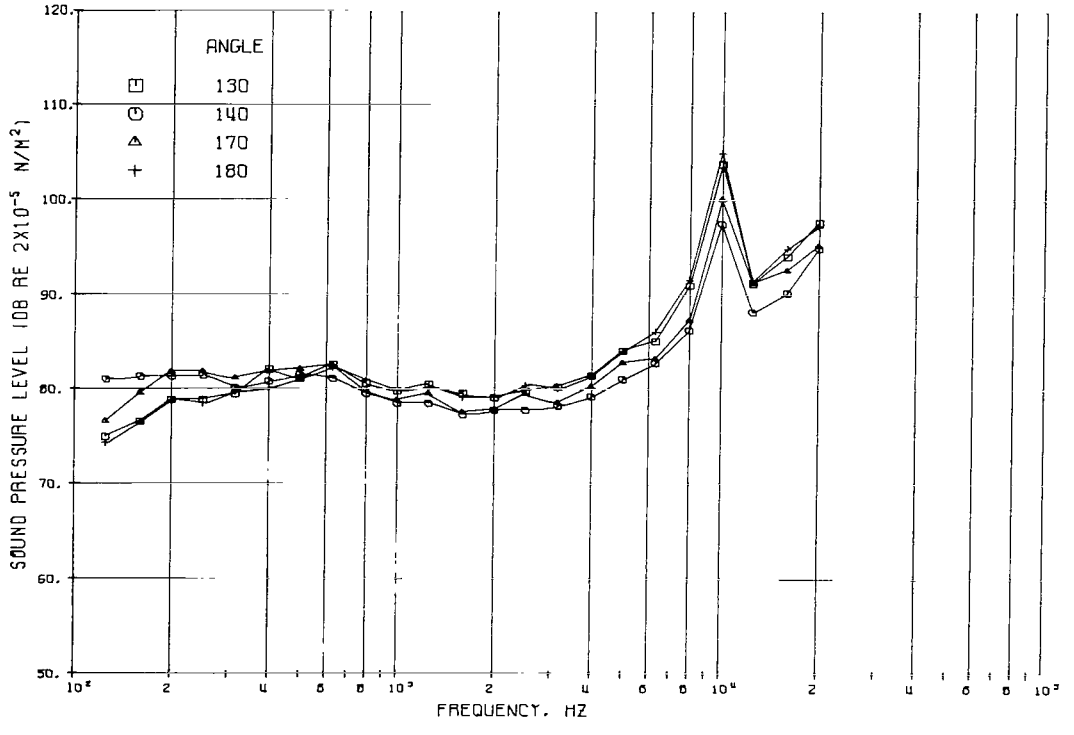


(d) Microphone angles, 130°, 140°, 170°, and 180°.

Figure 24. - Continued.

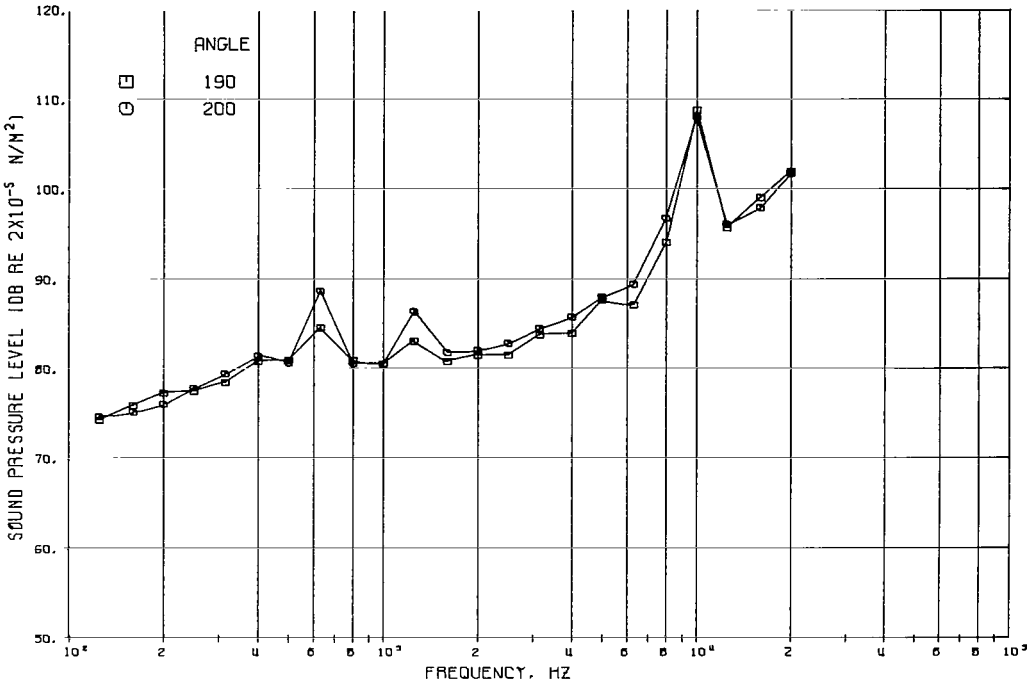


(e) Microphone angles, $190^0$ and $200^0$.

Figure 24. - Concluded.

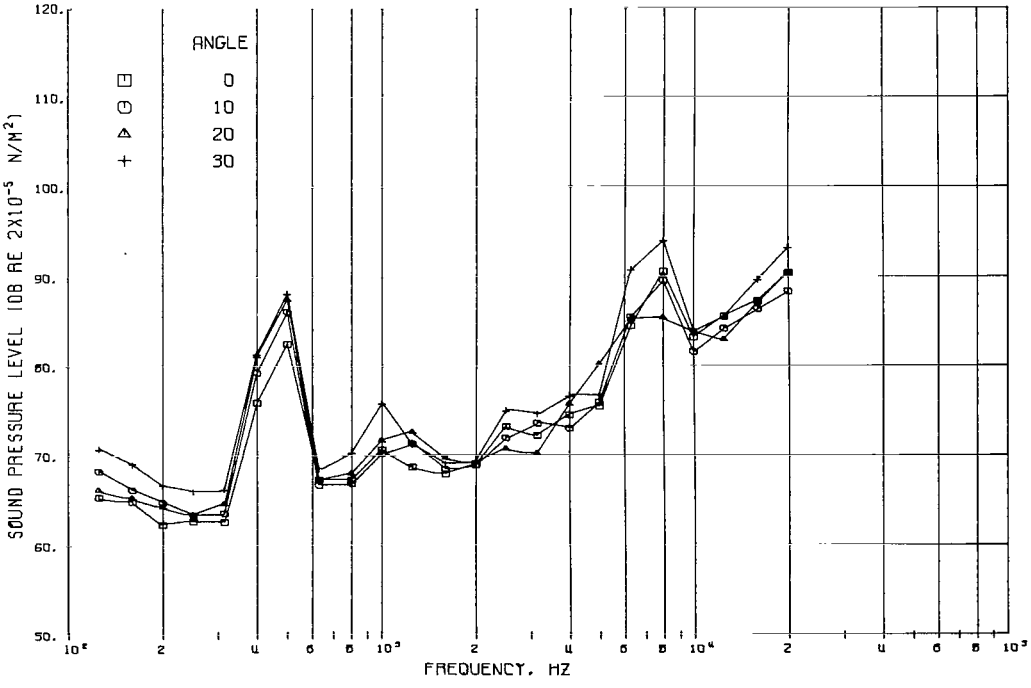


(a) Microphone angles, $0^0$, $10^0$, $20^0$, and $30^0$.

Figure 25. - Sound pressure level of jet flap noise on 4.57-meter radius in flyover plane. Configuration 3: fan-on-flap; flap deflection, $60^0$; fan speed, 76 percent.

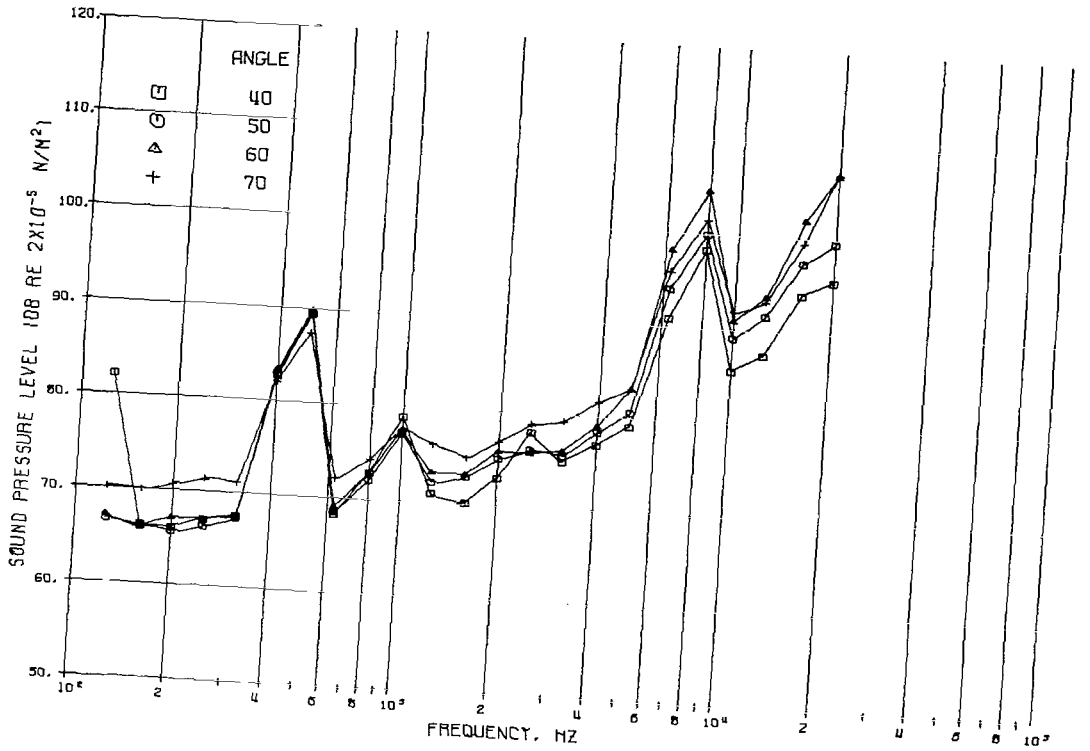


(b) Microphone angles, 40°, 50°, 60°, and 70°.

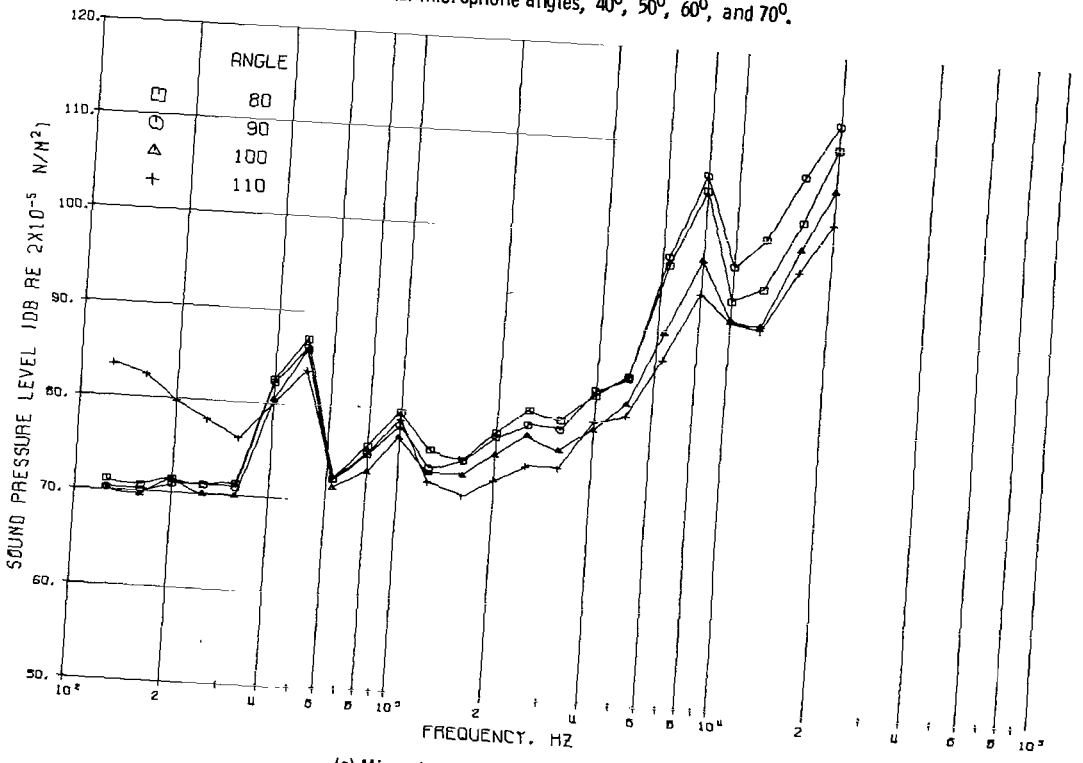


(c) Microphone angles, 80°, 90°, 100°, and 110°.

Figure 25. - Continued.

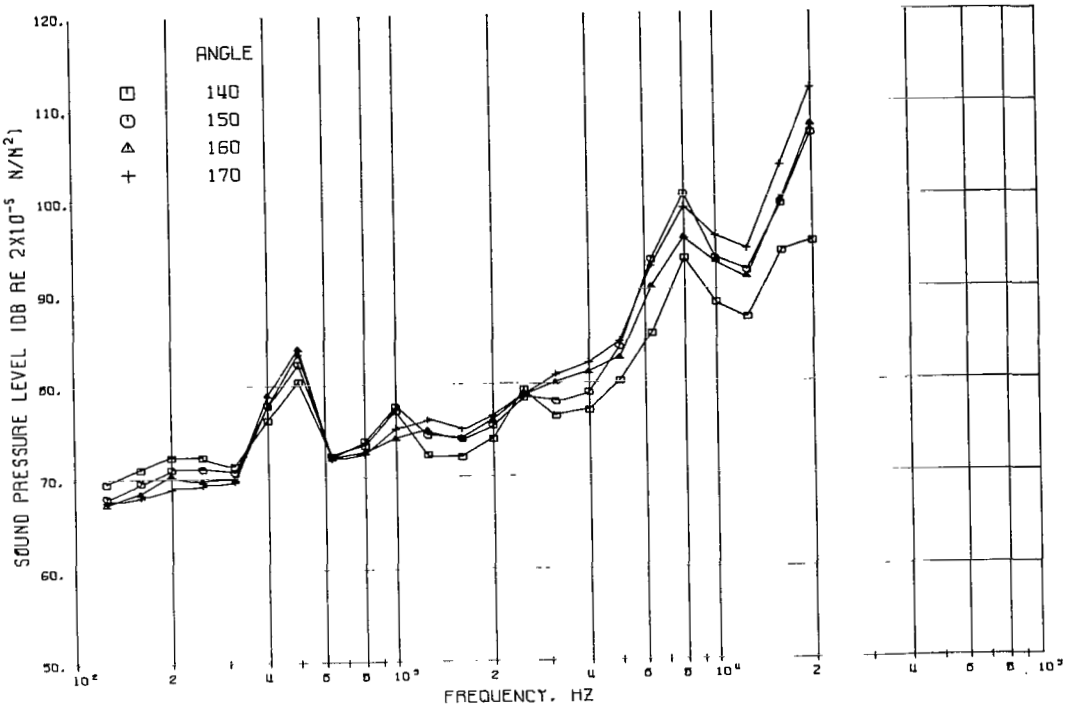


(d) Microphone angles, 140°, 150°, 160°, and 170°.

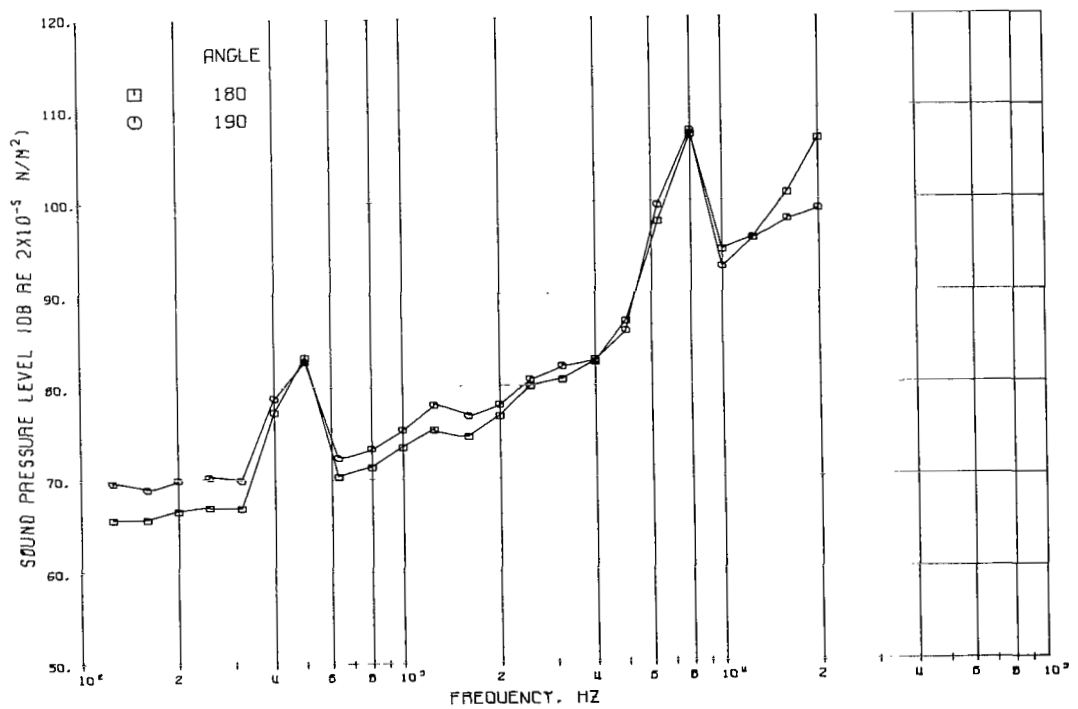


(e) Microphone angles, 180° and 190°.

Figure 25. - Concluded.

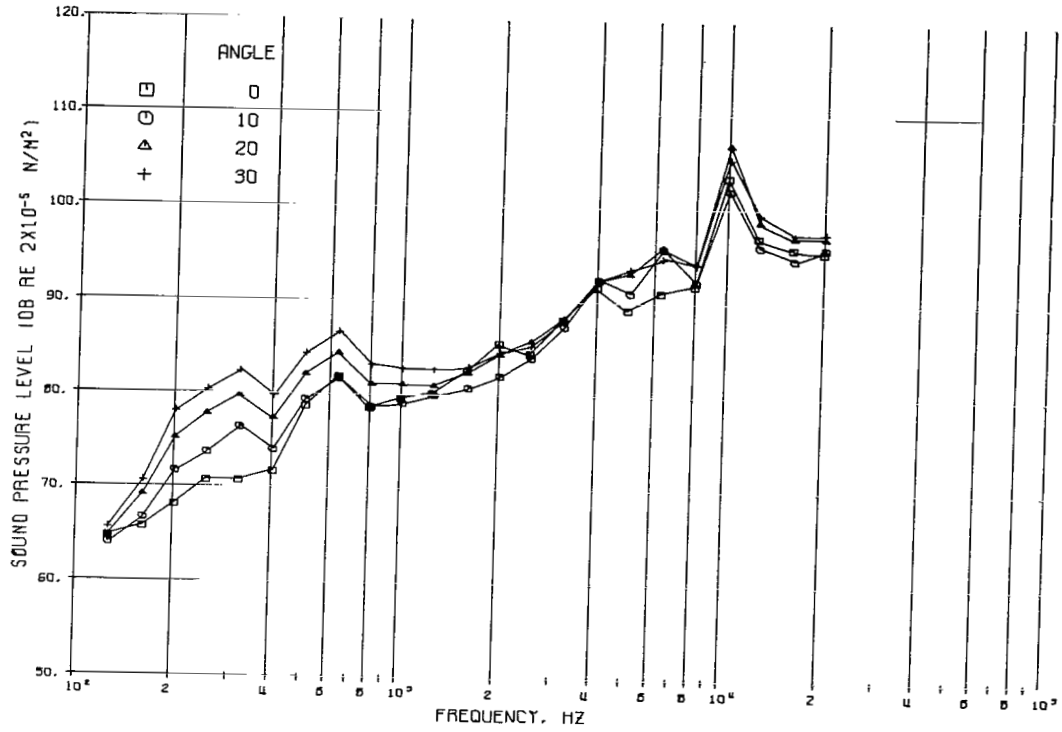


(a) Microphone angles, $0^0$, $10^0$, $20^0$, and $30^0$.

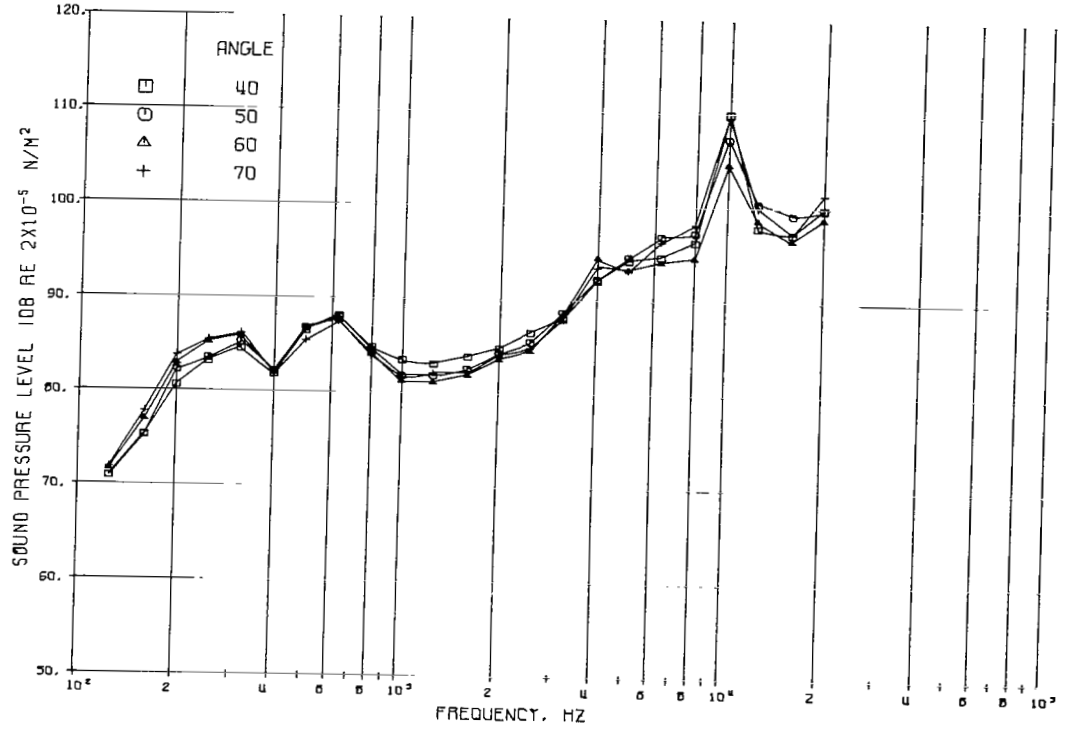


(b) Microphone angle, $40^0$, $50^0$, $60^0$, and $70^0$.

Figure 26. - Sound pressure level of jet flap noise on 4.57-meter radius in flyover plane. Configurature 4: fan-under-wing; flap deflection, $0^0$; fan speed, 100 percent.

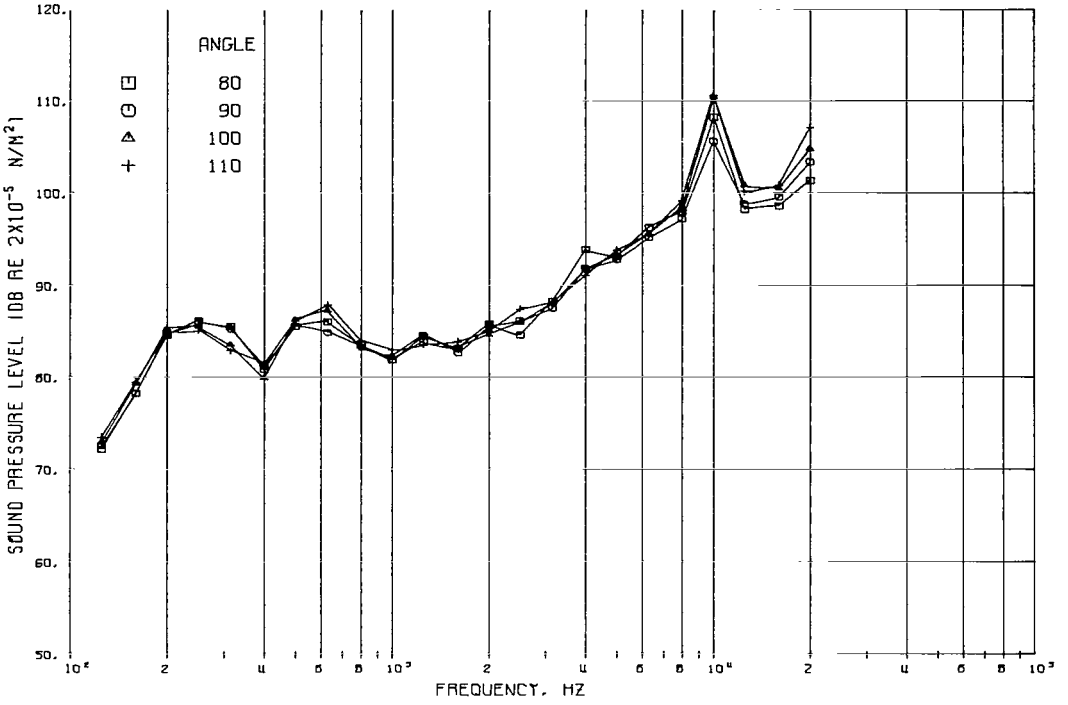


(c) Microphone angle, 80°, 90°, 100°, and 110°.

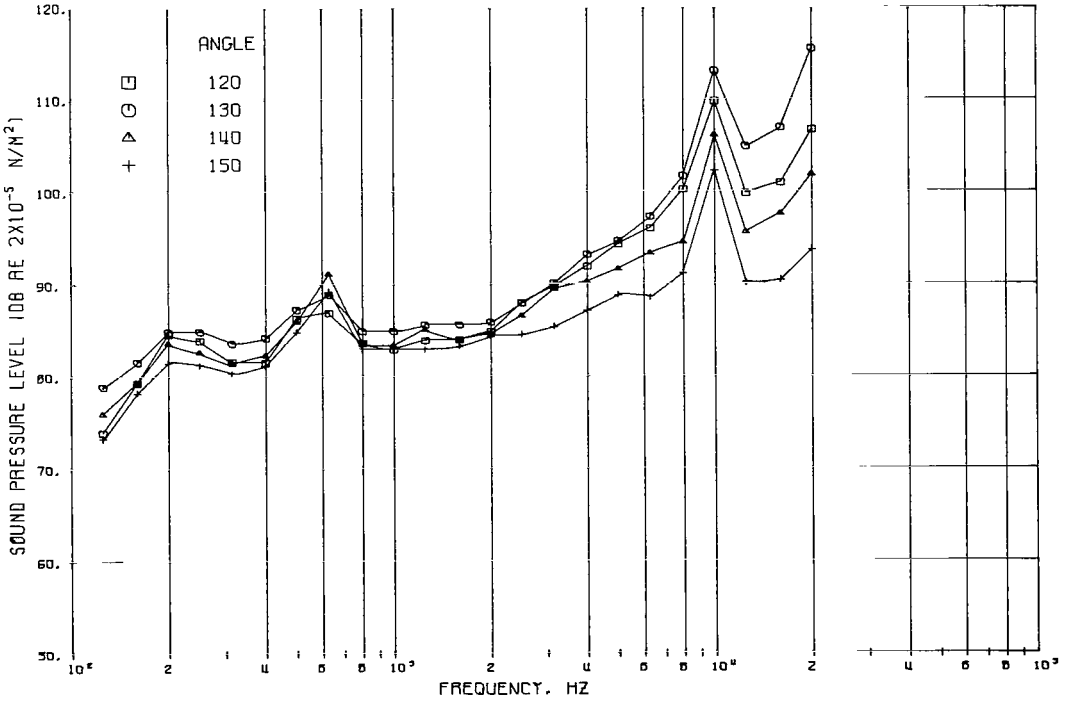


(d) Microphone angle, 120°, 130°, 140°, and 150°.

Figure 26. - Continued.

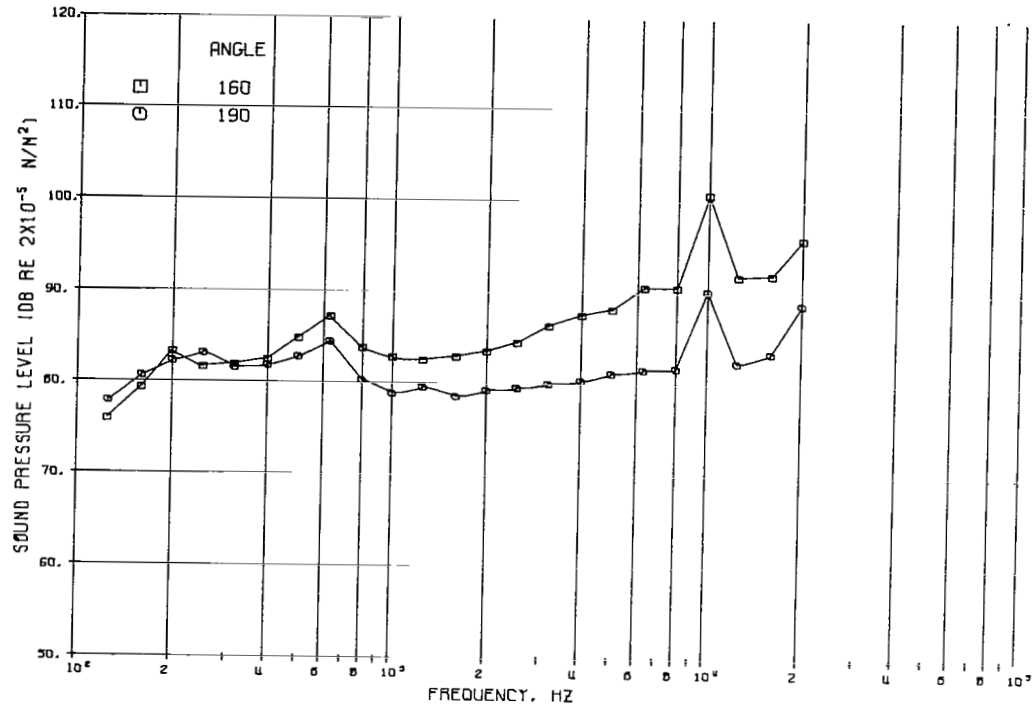


(e) Microphone angles, $160^0$ and $190^0$.

Figure 26. - Concluded.

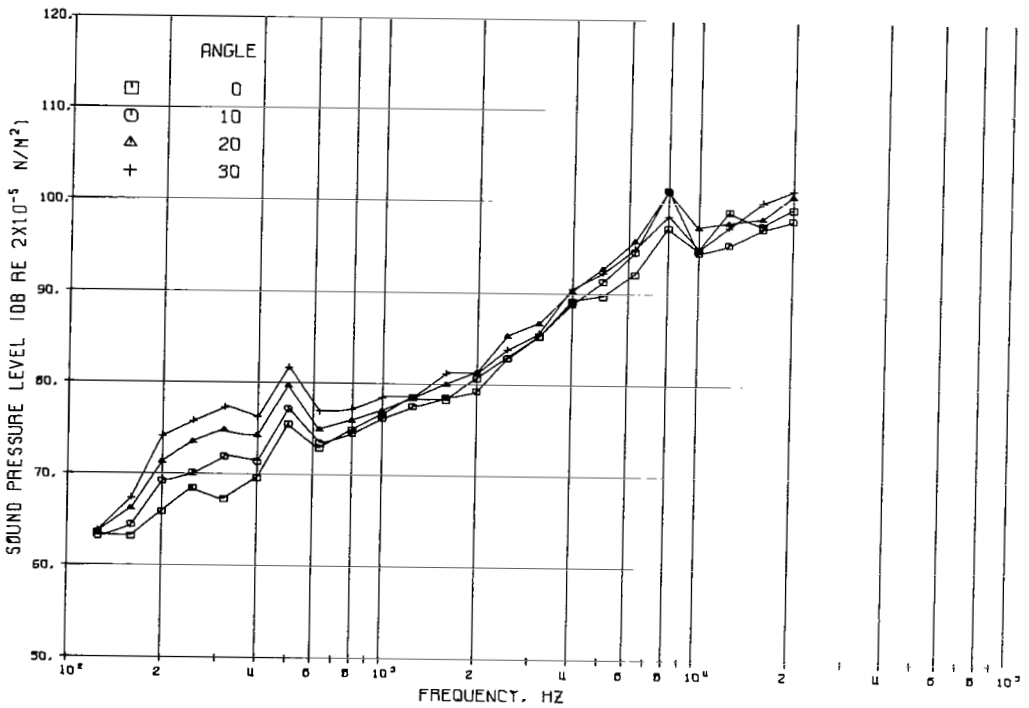


(a) Microphone angles, $0^0$, $10^0$, $20^0$, and $30^0$.

Figure 27. - Sound pressure level of jet flap noise on 4.57-meter radius in flyover plane. Configuration 4: fan-under-wing; flap deflection, $0^0$; fan speed, 76 percent.

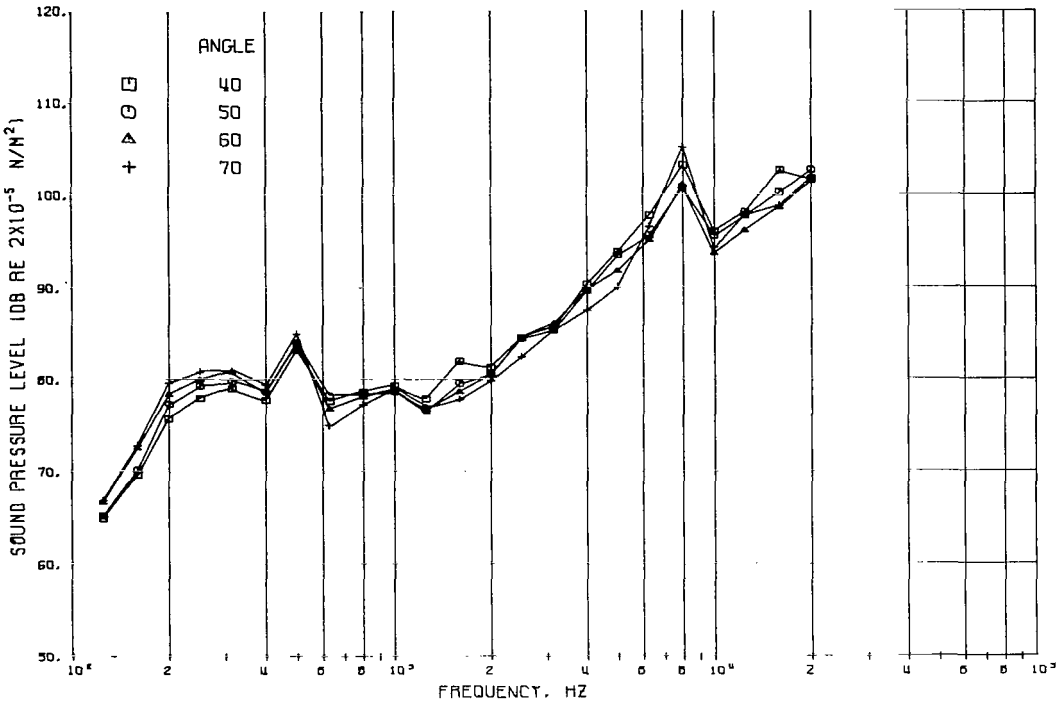


(b) Microphone angles, 40°, 50°, 60°, and 70°.

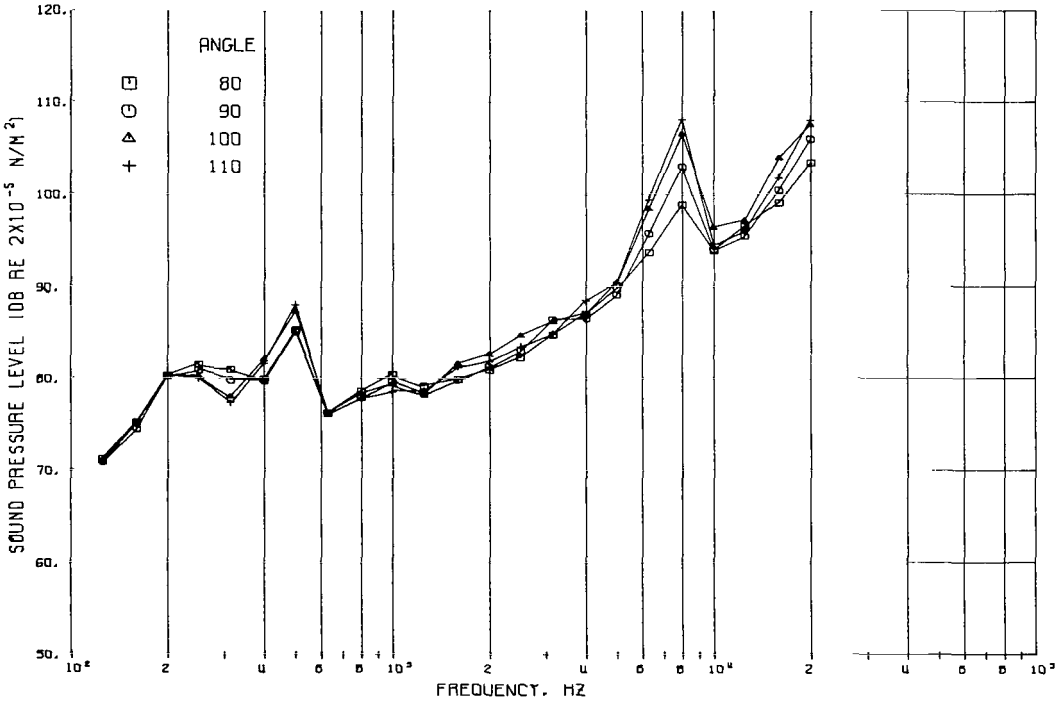


(c) Microphone angles, 80°, 90°, 100°, and 110°.

Figure 27. - Continued.

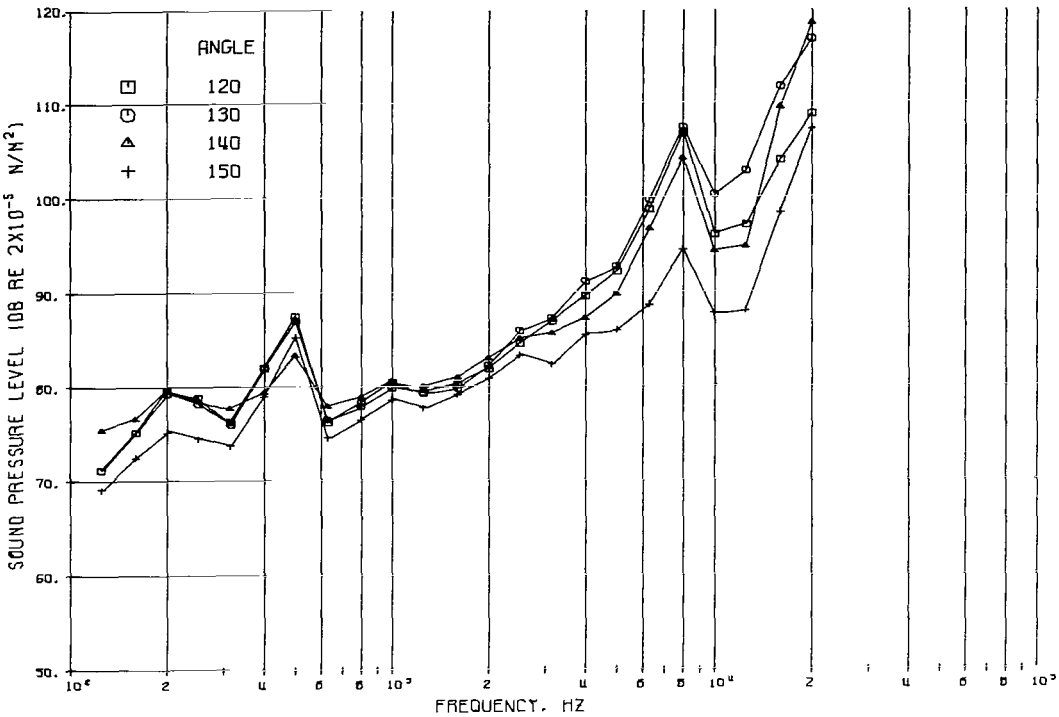


(d) Microphone angles, 120°, 130°, 140°, and 150°.

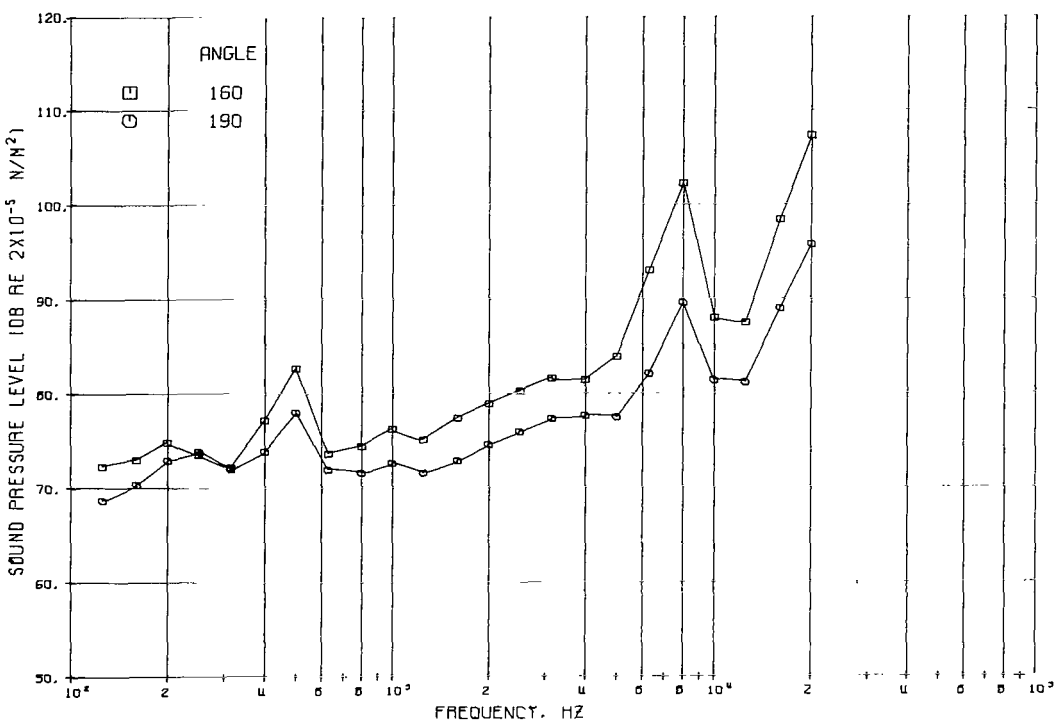


(e) Microphone angles, 160° and 190°.

Figure 27. - Concluded.

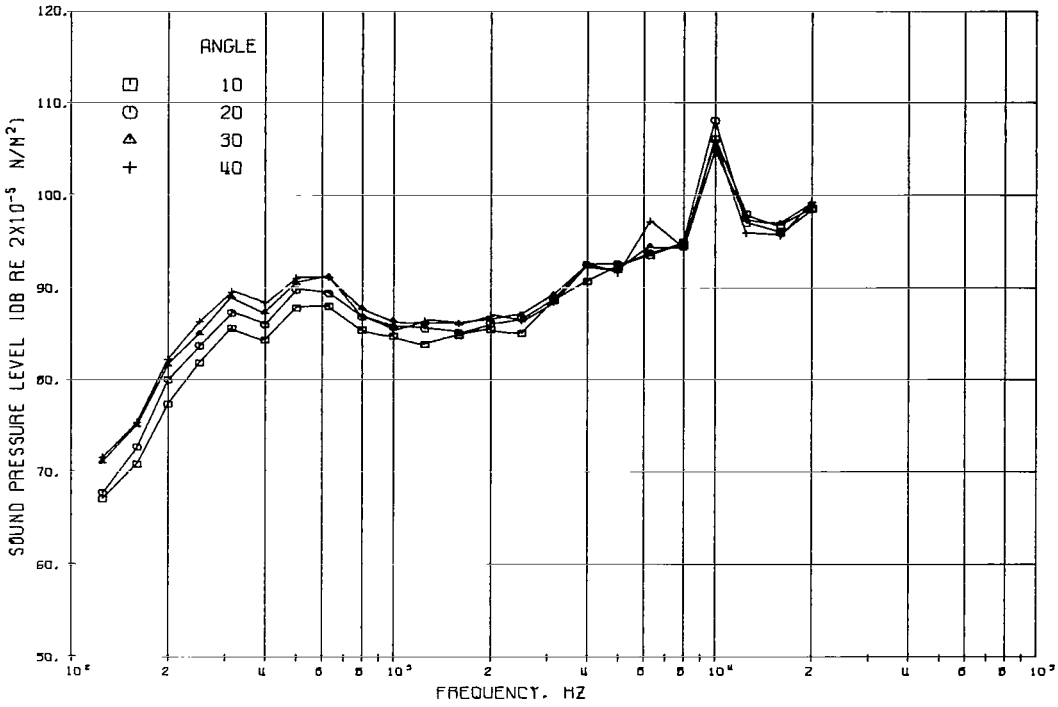


(a) Microphone angles, $10^0$, $20^0$, $30^0$, and $40^0$.

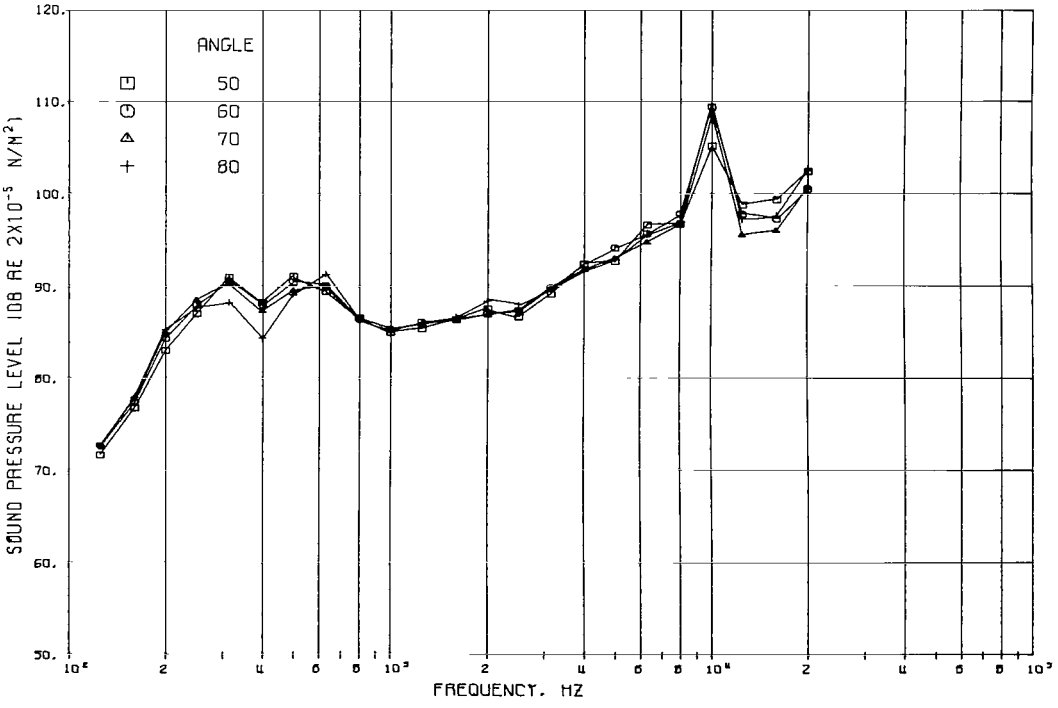


(b) Microphone angles, $50^0$, $60^0$, $70^0$, and $80^0$.

Figure 28. - Sound pressure level of jet flap noise on 4.57-meter radius in flyover plane. Configuration 5: fan-under-wing; flap deflection, $30^0$; fan speed, 100 percent.

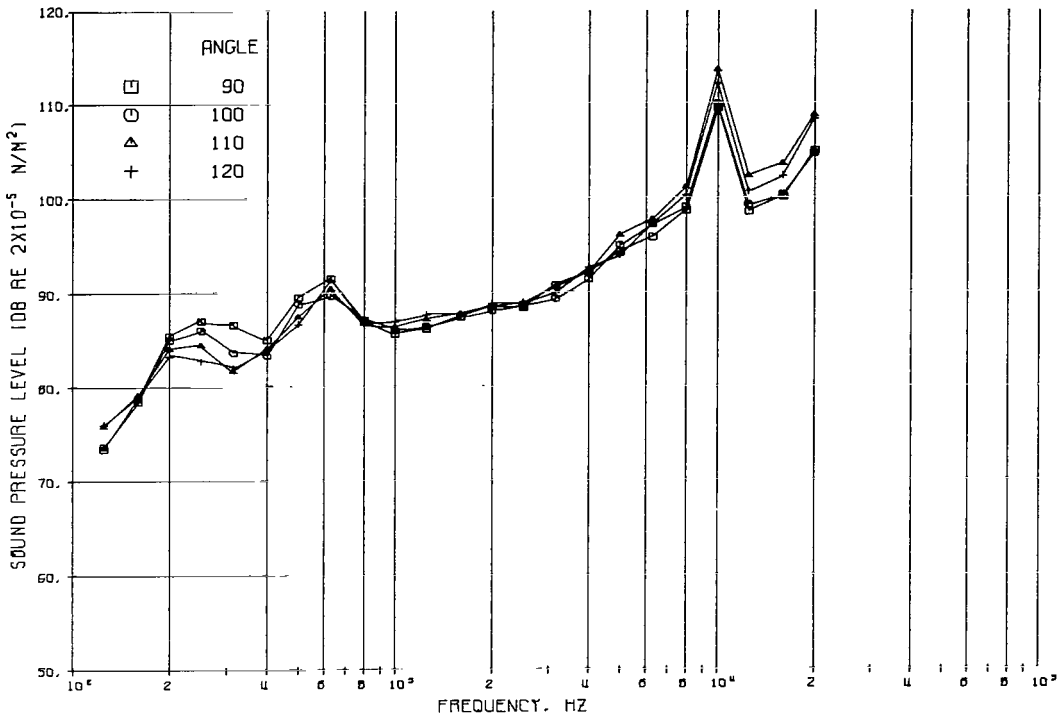


(c) Microphone angles, 90°, 100°, 110°, and 120°.

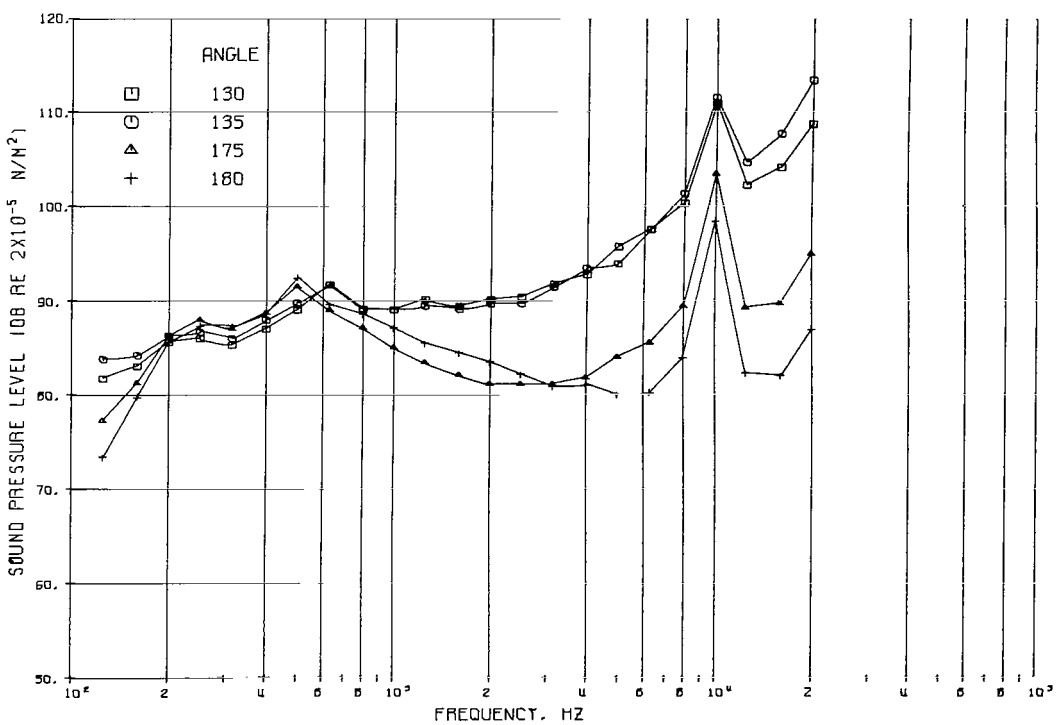


(d) Microphone angles, 130°, 135°, 175°, and 180°.

Figure 28. - Continued.

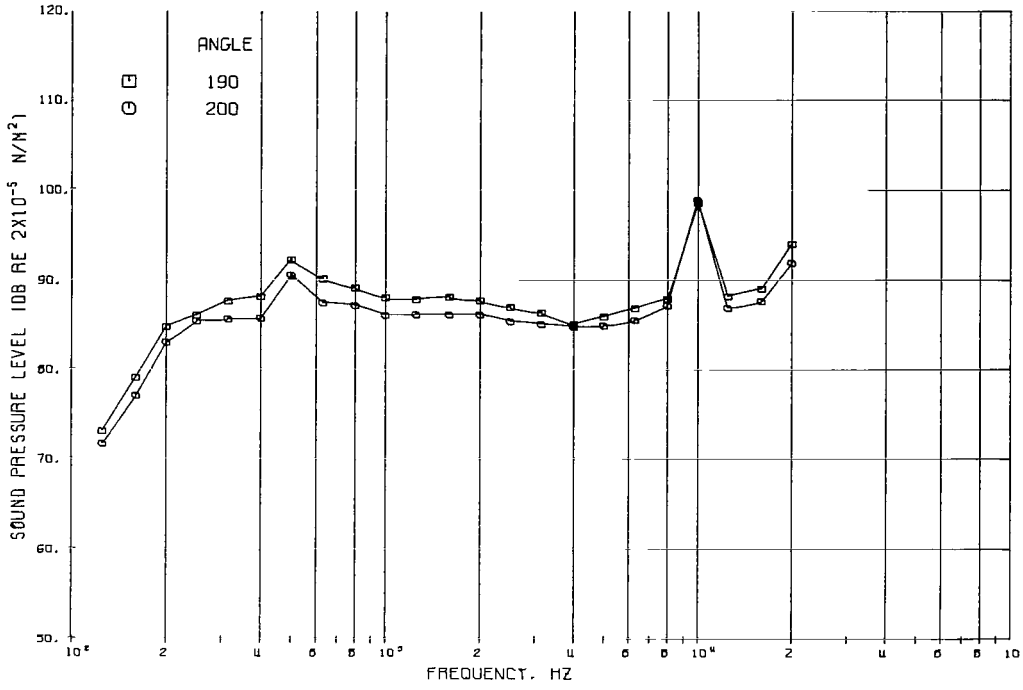


(e) Microphone angles, $190^0$ and $200^0$.

Figure 28. - Concluded.

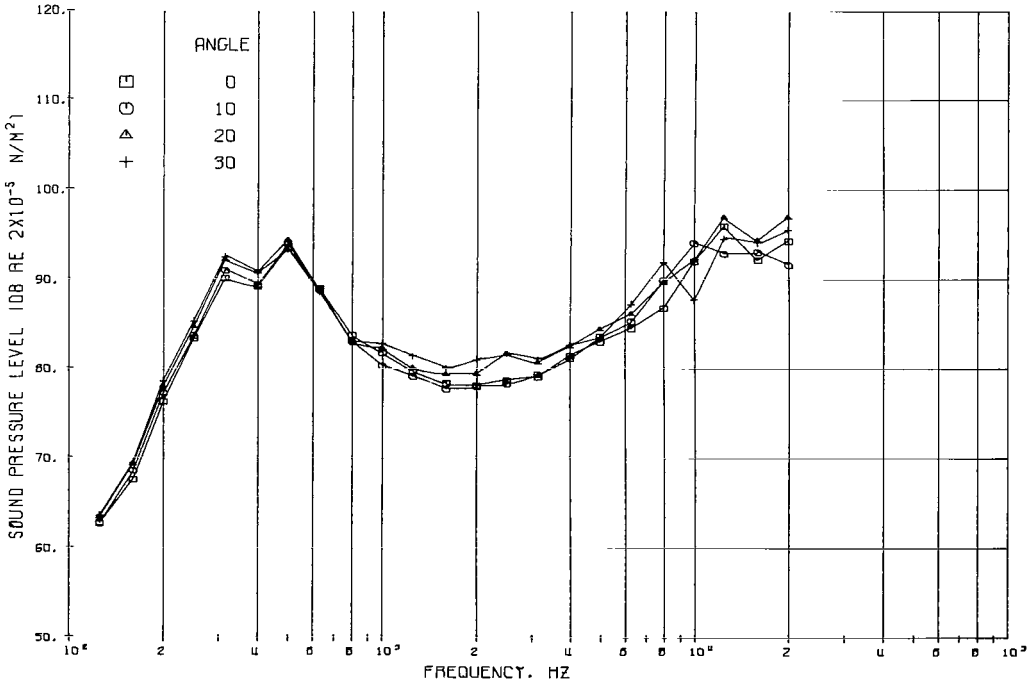


(a) Microphone angles, $0^0$, $10^0$, $20^0$, and $30^0$.

Figure 29. - Sound pressure level of jet flap noise on 4.57-meter radius in flyover plane. Configuration 6: fan-under-wing; flap deflection, $60^0$; fan speed, 76 percent.

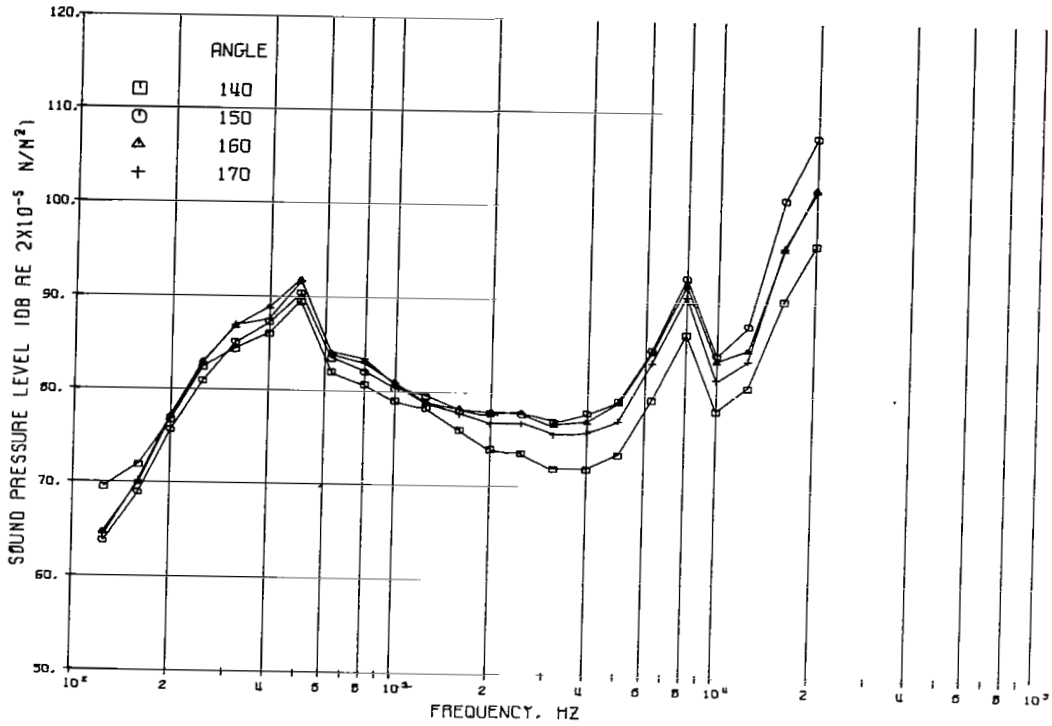


(d) Microphone angles, 140°, 150°, 160°, and 170°.

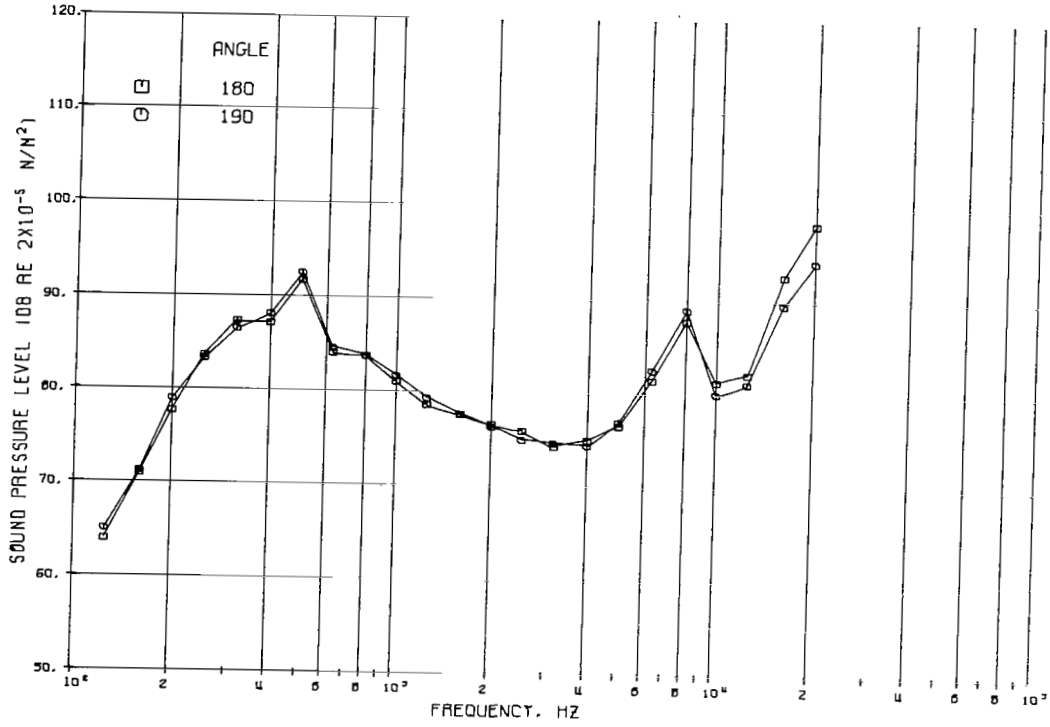


(e) Microphone angles, 180° and 190°.

Figure 29. - Concluded.

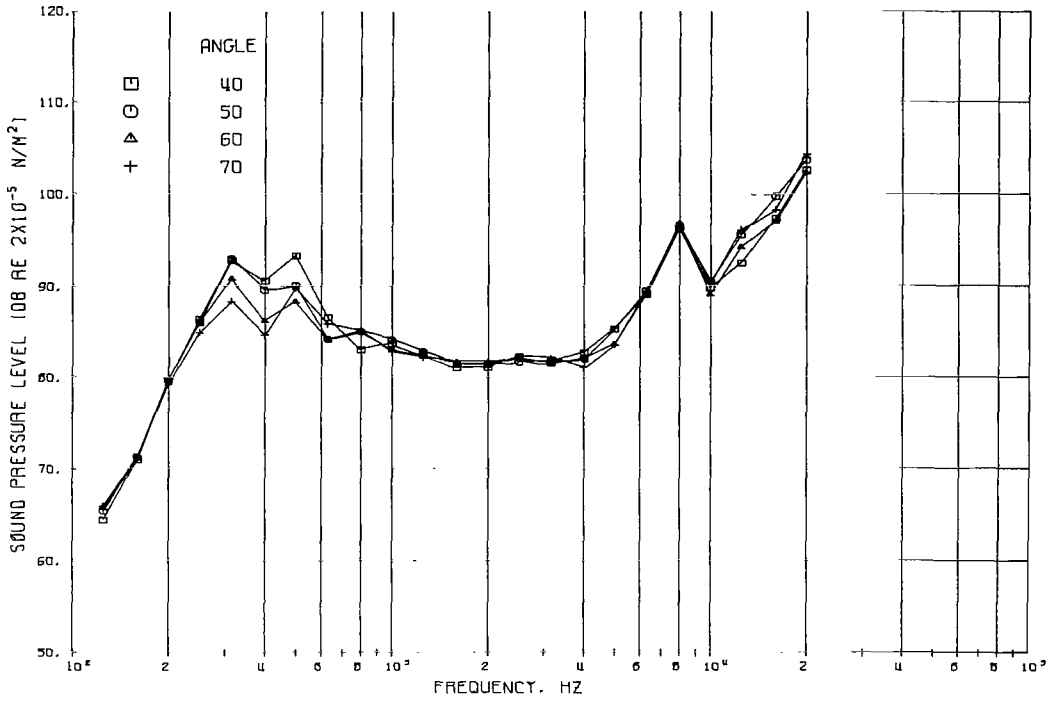


(b) Microphone angles, 40°, 50°, 60°, and 70°.

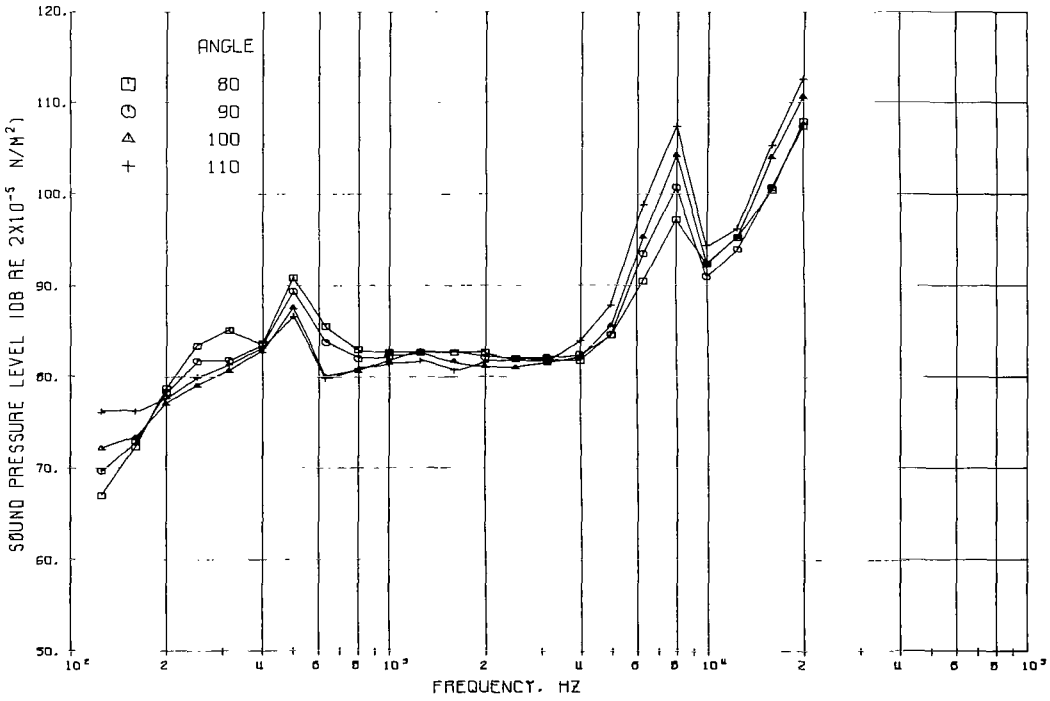


(c) Microphone angles, 80°, 90°, 100°, and 110°.

Figure 29. - Continued.

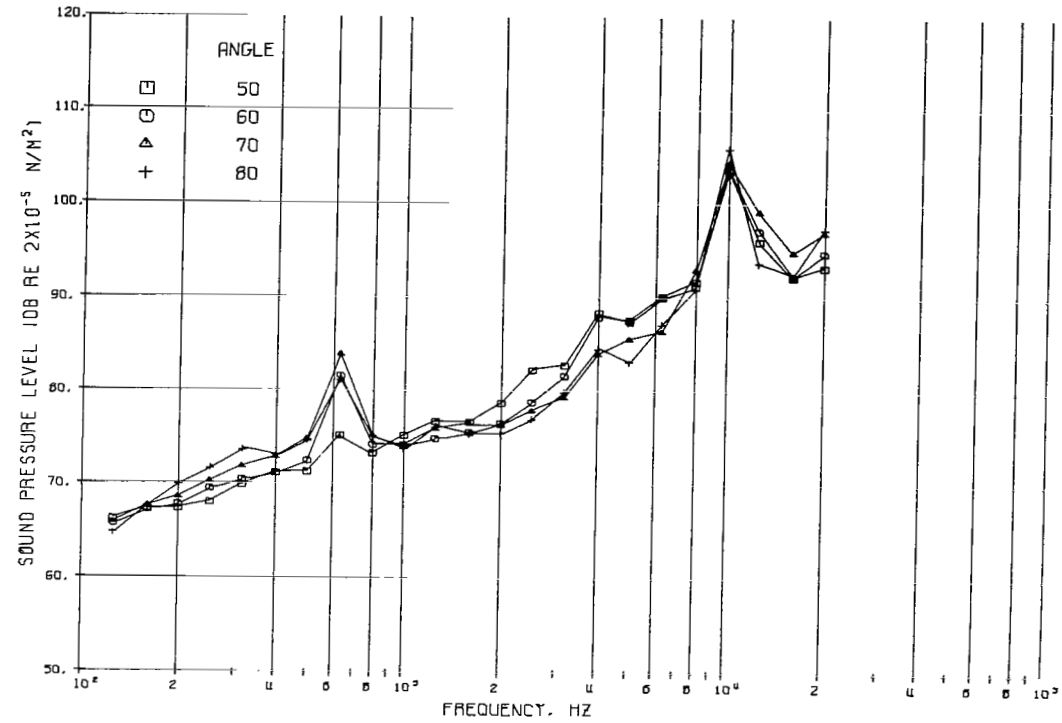


(a) Microphone angles, 50°, 60°, 70°, and 80°.

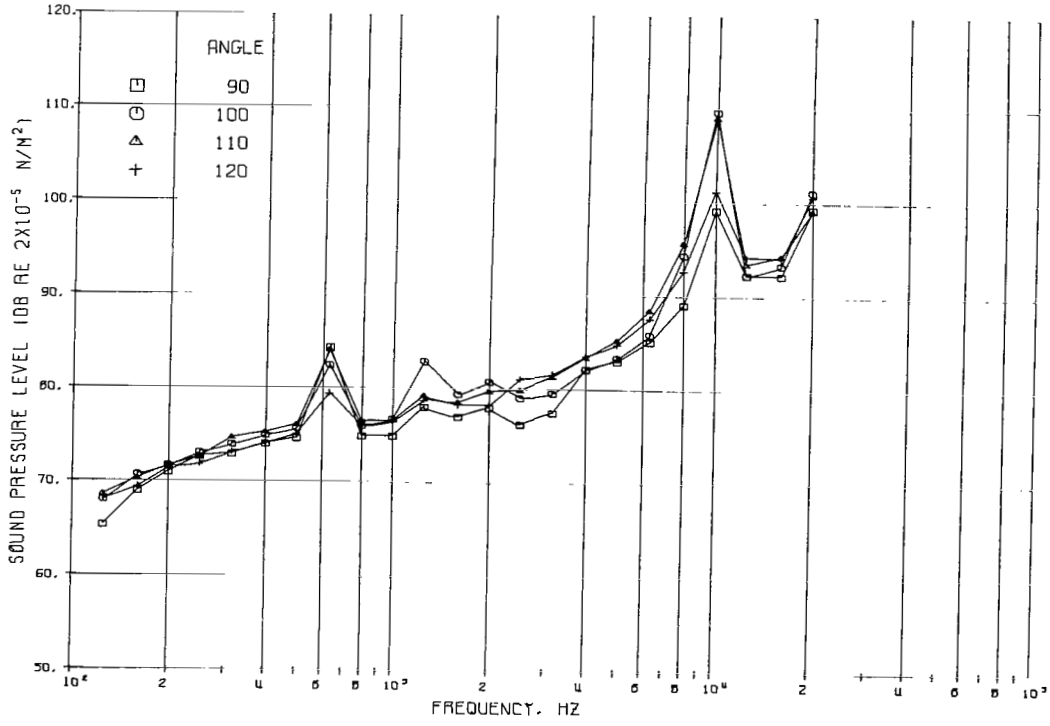


(b) Microphone angles, 90°, 100°, 110°, and 120°.

Figure 30. - Sound pressure level of jet flap noise on 4.57-meter radius in sideline plane. Configuration 4; fan-under-wing; flap deflection, 0°; fan speed, 100 percent.

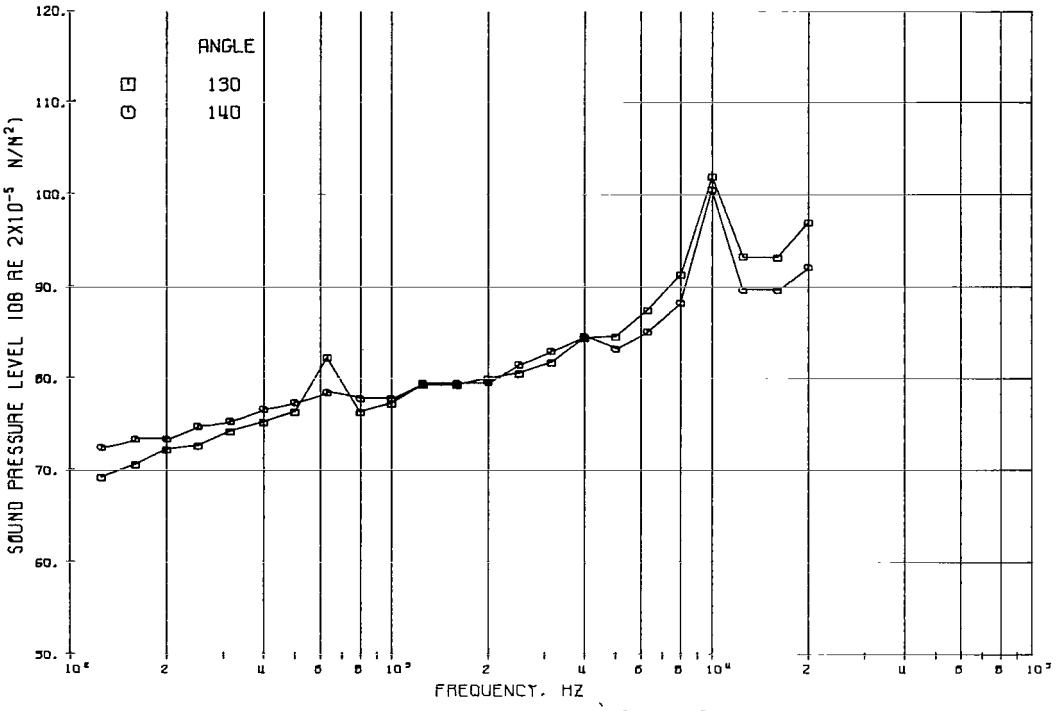


(c) Microphone angles, 130° and 140°.

Figure 30. - Concluded.

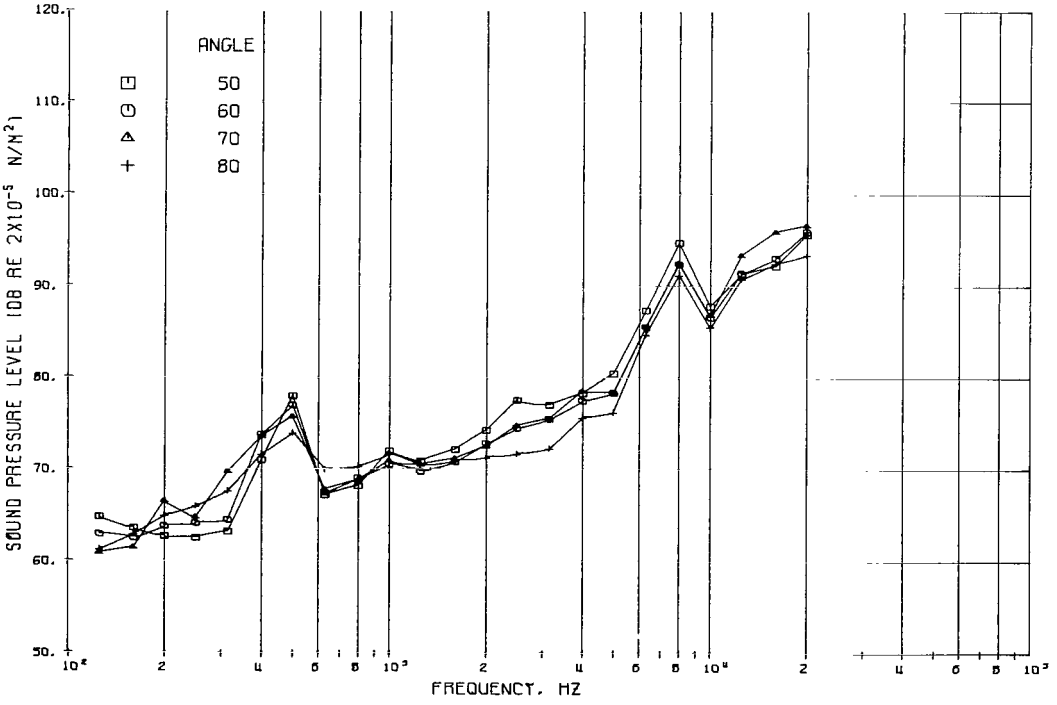


(a) Microphone angles, 50°, 60°, 70°, and 80°.

Figure 31. - Sound pressure level of jet flap noise on 4.57-meter radius in sideline plane. Configuration 4: fan-under-wing; flap deflection, 60°; fan speed, 76 percent.

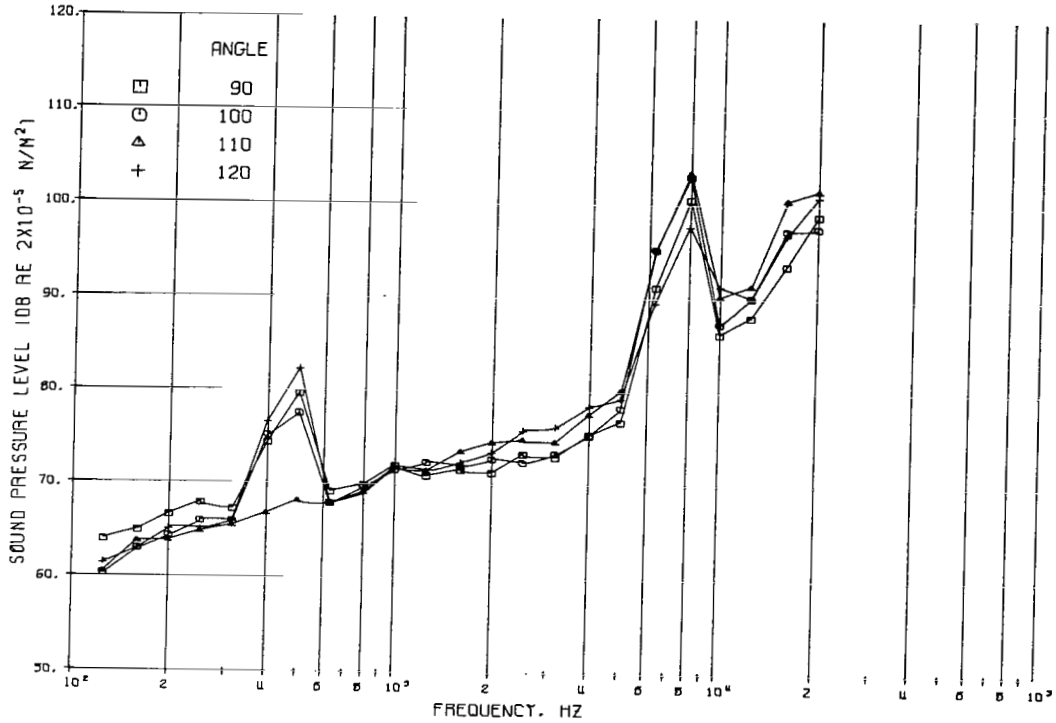


(b) Microphone angles, 90°, 100°, 110°, and 120°.

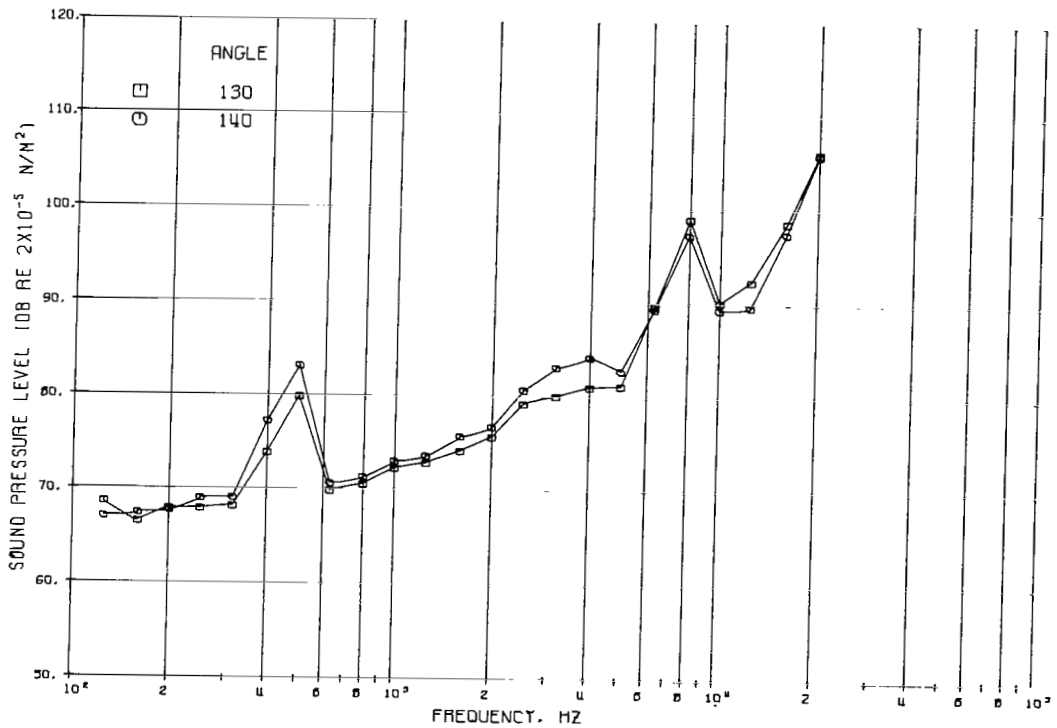


(c) Microphone angles, 130° and 140°.

Figure 31. - Concluded.

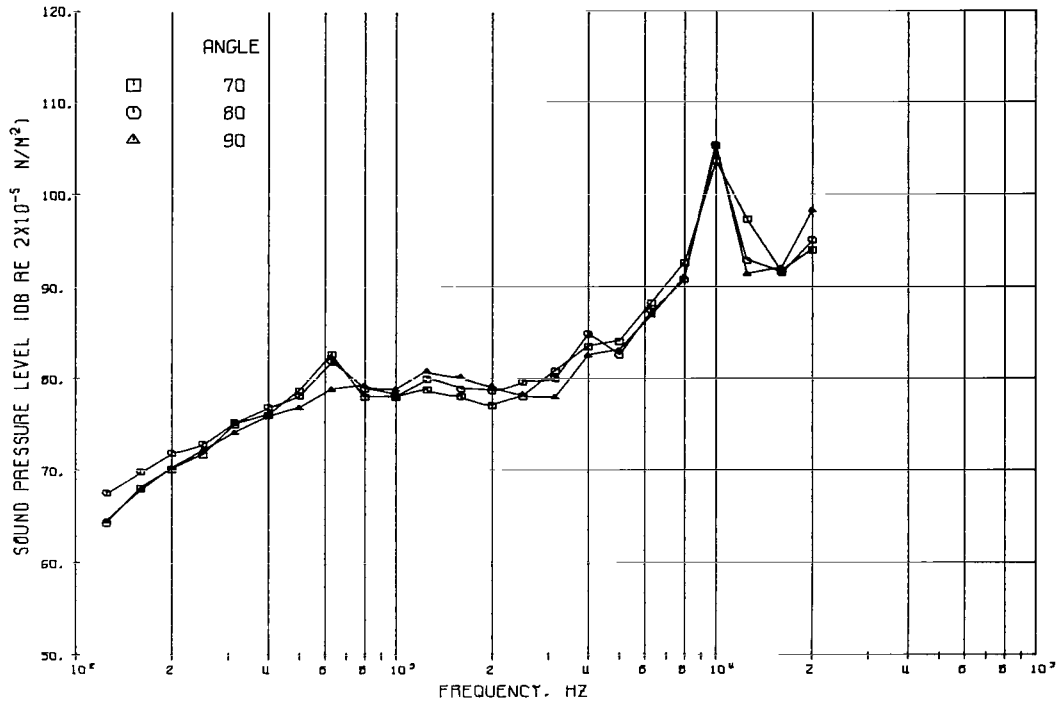


(a) Microphone angles, 70°, 80°, and 90°.

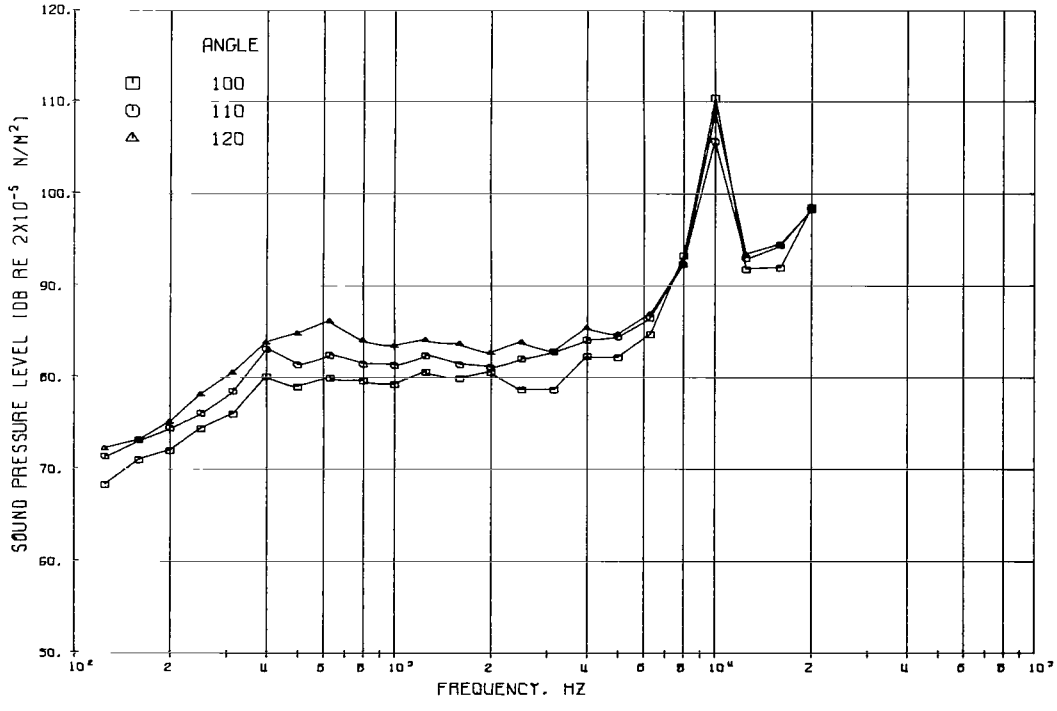


(b) Microphone angles, 100°, 110°, and 120°.

Figure 32. - Sound pressure level of jet flap noise on 4.57-meter radius in sideline plane. Configuration 5: fan-under-wing; flap deflection, 30°; fan speed, 100 percent.

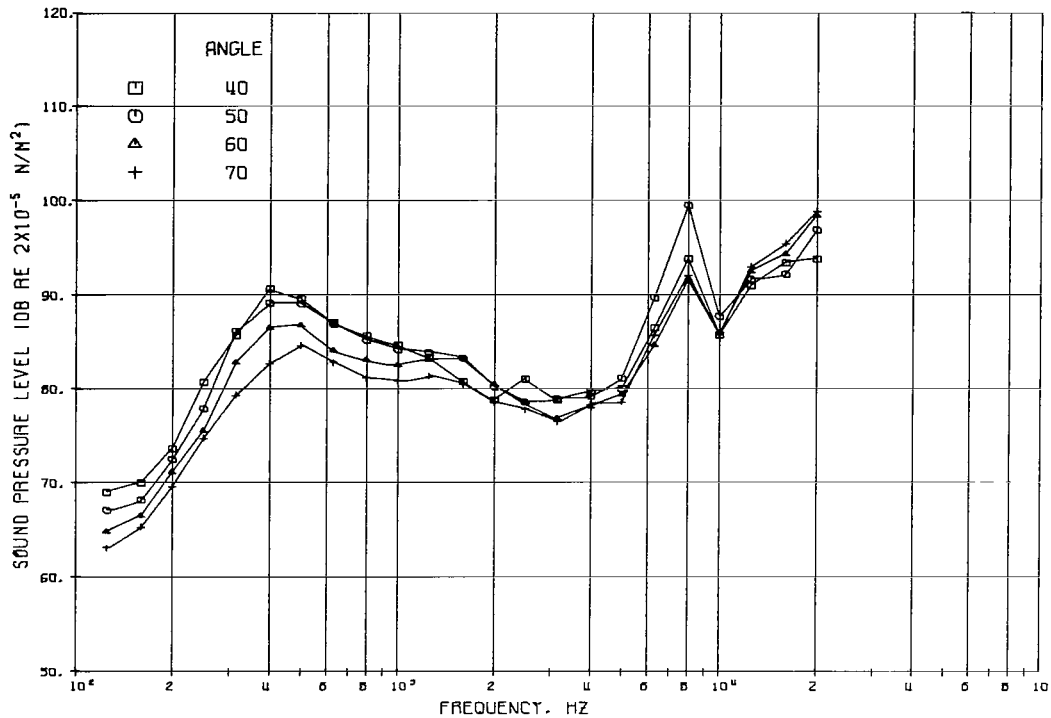


(a) Microphone angles, 40°, 50°, 60°, and 70°.

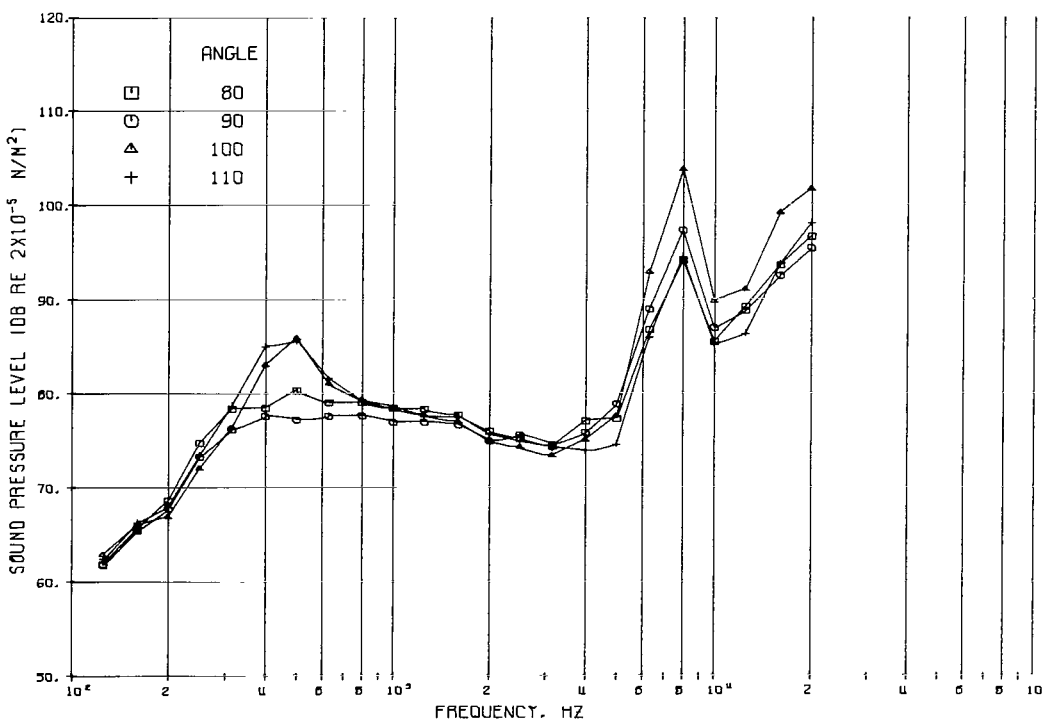


(b) Microphone angles, 80°, 90°, 100°, and 110°.

Figure 33. - Sound pressure level of jet flat noise on 4.57-meter radius in sideline plane. Configuration 6: fan-under-wing; flap deflection, 60°; fan speed, 76 percent.

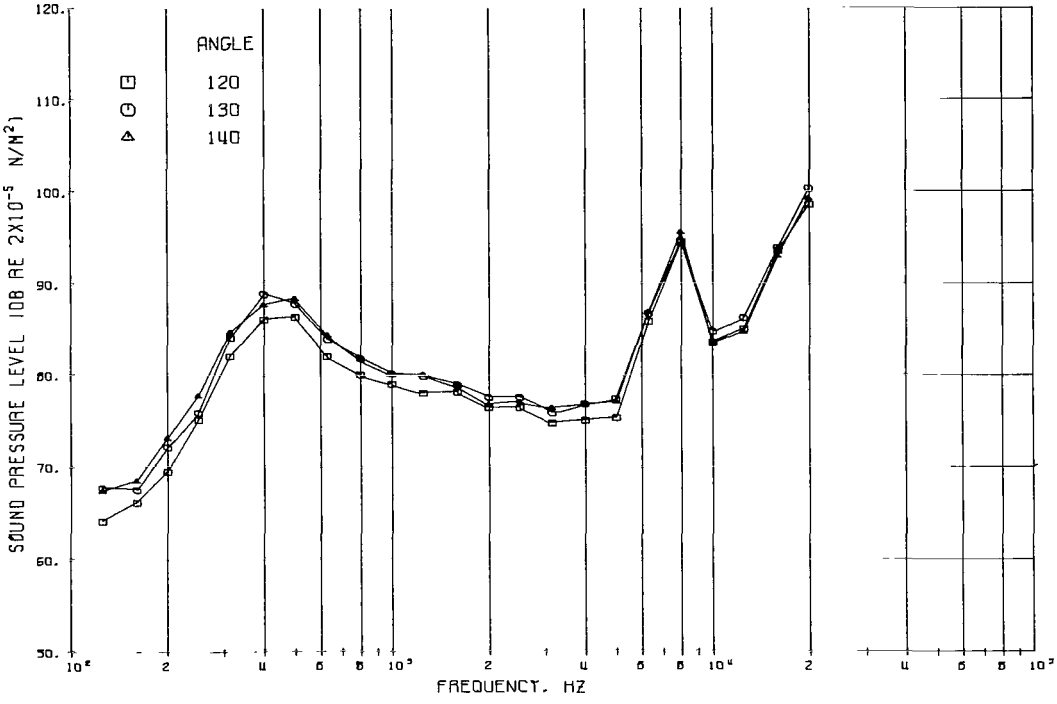


(c) Microphone angles, $120^0$, $130^0$, and $140^0$.

Figure 33. - Concluded.

*"The aeronautical and space activities of the United States shall be conducted so as to contribute . . . to the expansion of human knowledge of phenomena in the atmosphere and space. The Administration shall provide for the widest practicable and appropriate dissemination of information concerning its activities and the results thereof."*

—NATIONAL AERONAUTICS AND SPACE ACT OF 1958

# NASA SCIENTIFIC AND TECHNICAL PUBLICATIONS

TECHNICAL REPORTS: Scientific and technical information considered important, complete, and a lasting contribution to existing knowledge.

TECHNICAL NOTES: Information less broad in scope but nevertheless of importance as a contribution to existing knowledge.

TECHNICAL MEMORANDUMS: Information receiving limited distribution because of preliminary data, security classification, or other reasons.

CONTRACTOR REPORTS: Scientific and technical information generated under a NASA contract or grant and considered an important contribution to existing knowledge.

TECHNICAL TRANSLATIONS: Information published in a foreign language considered to merit NASA distribution in English.

SPECIAL PUBLICATIONS: Information derived from or of value to NASA activities. Publications include conference proceedings, monographs, data compilations, handbooks, sourcebooks, and special bibliographies.

TECHNOLOGY UTILIZATION PUBLICATIONS: Information on technology used by NASA that may be of particular interest in commercial and other non-aerospace applications. Publications include Tech Briefs, Technology Utilization Reports and Technology Surveys.

*Details on the availability of these publications may be obtained from:*

**SCIENTIFIC AND TECHNICAL INFORMATION OFFICE**

**NATIONAL AERONAUTICS AND SPACE ADMINISTRATION**

**Washington, D.C. 20546**